A COMPUTATIONAL STUDY OF THE STRUCTURE, BONDING, AND THERMOCHEMICAL PROPERTIES OF PRIMARY OZONIDES DERIVED FROM SUBSTITUTED PHENOL AND THIOPHENOL

MASTER OF SCIENCE

BY

GARISEB SIKHOEB NICLAAS

2013

A COMPUTATIONAL STUDY OF THE STRUCTURE, BONDING, AND THERMOCHEMICAL PROPERTIES OF PRIMARY OZONIDES DERIVED FROM SUBSTITUTED PHENOL AND THIOPHENOL

A THESIS SUBMITTED IN PARTIAL FULFILLMENT OF THE REQUIREMENTS FOR THE DEGREE OF

MASTER OF SCIENCE

OF

THE UNIVERSITY OF NAMIBIA

BY

GARISEB SIKHOEB NICLAAS

JANUARY 2013

Supervisor: **Prof. Edet F. Archibong** (**Department of Chemistry and Biochemistry, University of Namibia)**

This work was carried out from December 2009 to November 2011 in the Computational Laboratory, in the Department of Chemistry and Biochemistry at the University of Namibia under the supervision of Prof. Edet F. Archibong.

ABSTRACT

Ozone (O_3) is an allotrope of oxygen occurring naturally in the earth's atmosphere. Its importance in environmental issues is well documented and cannot be overemphasized. Ozone reacts with carbon-carbon multiple bonds such as in alkenes via the ozonolysis process. The first step of ozonolysis involves the formation of an important but very unstable primary ozonide (POZ) which after formation, immediately rearranges to the more stable secondary ozonide (SOZ). Due to its instability, it is difficult to determine experimentally the structure, bonding and thermochemical properties of a POZ. Hence, theoretical methods are often used to compute the properties of this class of transient chemical species.

The results of density functional theory for the 1,3-cycloadditions of ozone to chlorophenol, dihydroxybenzene and hydroxythiophenol are presented here. Theoretical calculations for the chlorophenol, dihydroxybenzene and hydroxythiophenol ozonolysis yields reaction barriers of 56.8, 11.2 and 10.4 kcal/mol for the formation of the most stable POZs, respectively. The lowest energy POZs for chlorophenol, dihydroxybenzene and hydroxythiophenol are located at 19.1, 22.1 and 19.4 kcal/mol below the reactants, respectively. For the chlorophenol POZ, the calculated reaction enthalpies ($\Delta_r H°$) and Gibbs free energies ($\Delta_r G°$) are 20.0 and 6.8 kcal/mol below those of the reactants, respectively. For the dihydroxybenzene POZ, the calculated reaction enthalpies ($\Delta_r H°$) and Gibbs free energies ($\Delta_r G°$) are 23.1 and 9.9 kcal/mol below those of the reactants, respectively. For the hydroxythiophenol POZ, the calculated reaction enthalpies ($\Delta_r H°$)

and Gibbs free energies ($\Delta_r G°$) are 20.3 and 6.9 kcal/mol below those of the reactants, respectively.

Structurally, the carbon rings in the primary ozonides of chlorophenol, dihydroxybenzene and hydroxythiophenol are found to retain their planarity. This research determines that the most feasible pathway for the formation of the POZ of chlorophenol, dihydroxybenzene and hydroxythiophenol involve the addition of ozone to the 3,4-, 1,2- and 2,3-positions, respectively.

Table of Contents **Page**

ABSTRACT iii

LIST OF ABBREVIATIONS AND SYMBOLS viii

LIST OF SCHEMES ix

LIST OF TABLES x

LIST OF FIGURES xii

ACKNOWLEDGEMENTS xv

DECLARATIONS xvi

DEDICATIONS xvii

CHAPTER 1: INTRODUCTION **1**

1.1 Chemistry of ozone 1

1.1.1 What is ozone? 1

1.1.2 Ozone in the atmosphere 2

1.1.3 Ozone in aqueous solution 6

1.1.4 The significance of ozone 9

1.1.5 Industrial applications of ozone 11

1.2 Phenols and Thiophenols 14

1.3 Problem Statement 18

1.4 Objective 19

1.5 Relevance and Significance of the Study 20

1.6 Limitation of the Study 21

CHAPTER 2: LITERATURE REVIEW **22**

2.1 Reactions of ozone with compounds containing C=C 22

(a) With Olefins 22

(b) With aromatic compounds 27

2.2 Density Functional Theory (DFT) 30

2.3 Basis Sets 31

2.4 Computational Methods 38

2.5 Data Analysis 43

CHAPTER 3: MATERIALS AND METHODS 46

3.1 Substances studied 46

3.2 Computational methods utilized 47

CHAPTER 4: RESULTS AND DISCUSSION 48

4.1 Minima of conformers studied: Best 5 isomers per group and globally 49

4.1.1 Chlorophenol POZs 49

4.1.1.1 The 1,2-POZs of chlorophenol 50

4.1.1.2 The 2,3-POZs of chlorophenol 53

4.1.1.3 The 3,4-POZs of chlorophenol 56

4.1.2 Dihydroxybenzene POZs 62

4.1.2.1 The 1,2-POZs of dihydroxybenzene 63

4.1.2.2 The 2,3-POZs of dihydroxybenzene 67

4.1.2.3 The 3,4-POZs of dihydroxybenzene 71

4.1.3 Hydroxythiophenol POZs 77

4.1.3.1 The 1,2-POZs of hydroxythiophenol 78

4.1.3.2 The 2,3-POZs of hydroxythiophenol 82

4.1.3.3 The 3,4-POZs of hydroxythiophenol 86

4.3 General Discussion 92

4.3.1 Reaction of Ozone with Chlorophenol 92

4.3.2 Reaction of Ozone with Dihydroxybenzene 95

4.3.3 Reaction of Ozone with Hydroxythiophenol 99

CHAPTER 5: CONCLUSIONS 105

CHAPTER 6: REFERENCES 108

APPENDICES 115

LIST OF ABBREVIATIONS AND SYMBOLS

Abbreviation/symbol	Meaning
ACM	- Adiabatic connection method
AO	- Atomic orbital
AOP	- Advanced oxidation process
CCSD(T)	- Coupled-cluster singles and doubles model with a perturbation correction for triples
DFT	- Density functional theory
GAC	- Granular active carbon
GGA	- Generalized gradient approximation
GTO	- Gaussian-type orbital
HF	- Hartree-Fock
LDA	- Local density approximation
LSD	- Local spin-density approximation
MO	- Molecular orbital
MP2	- 2^{nd} order Möller-Plesset perturbation theory
NOM	- Natural organic matter
POZ	- Primary ozonide
SOZ	- Secondary ozonide
STO	- Slater-type orbital
VOC	- Volatile organic compound
ZPE	- Zero-point vibrational energy

LIST OF SCHEMES

Scheme 1 The Criegee component in the reaction of ozone with 1,2-dimethoxy-benzene..... … 7

Scheme 2 Synthesis of phenol ..... …15

Scheme 3 Formation of a SOZ ..... … 22

Scheme 4 Rearrangement of a POZ to a SOZ ..... … 23

Scheme 5 Decomposition of a POZ in a protonic solvent..... … 23

Scheme 6 A reductive workup (top) and an oxidative workup (bottom) of a SOZ.. … 24

Scheme 7 The mechanism of ozone reaction with an olefin ..... … 25

Scheme 8 Criegee Mechanism of Ethylene Ozonolysis ..... … 26

Scheme 9 Mechanism of the ozonolysis of benzene ..... … 28

Scheme 10 The mechanism of ozone reaction with benzene ..... …28

Scheme 11 Bailey's mechanism for the reaction of ozone with phenol..... … 29

LIST OF TABLES

Table 1 Names and representative structures of the compounds from which the POZs investigated in this work were derived..... 46

Table 2 Relative energies and thermochemical properties of the minima of the five (5) most stable chlorophenol 1,2-POZs at the B3LYP/6-31G(d) level 50

Table 3 Relative energies and thermochemical properties of the minima of the five (5) most stable chlorophenol 2,3-POZs at the B3LYP/6-31G(d) level 53

Table 4 Relative energies and thermochemical properties of the minima of the five (5) most stable chlorophenol 3,4-POZs at the B3LYP/6-31G(d) level 56

Table 5 Relative energies and thermochemical properties of the minima of the five (5) most stable chlorophenol POZs at the B3LYP/6-31G(d), B3LYP/6-31G(d,p) and B3LYP/6-311+G(2df) levels..... 60

Table 6 Relative energies and thermochemical properties of the minima of the five (5) most stable dihydroxybenzene 1,2-POZs at the B3LYP/6-31G(d) level..... 63

Table 7 Relative energies and thermochemical properties of the minima of the five (5) most stable dihydroxybenzene 2,3-POZs at the B3LYP/6-31G(d) level..... 67

Table 8 Relative energies and thermochemical properties of the minima of the five (5) most stable dihydroxybenzene 3,4-POZs at the B3LYP/6-31G(d) level..... 71

Table 9 Relative energies and thermochemical properties of the minima of the five (5) most stable dihydroxybenzene POZs at the B3LYP/6-31G(d), B3LYP/6-31G(d,p) and B3LYP/6-311+G(2df) levels..... 75

Table 10 Relative energies and thermochemical properties of the minima of the five (5) most stable hydroxythiophenol 1,2-POZs at the B3LYP/6-31G(d) level 78

Table 11 Relative energies and thermochemical properties of the minima of the five (5) most stable hydroxythiophenol 2,3-POZs at the B3LYP/6-31G(d) level 82

Table 12 Relative energies and thermochemical properties of the minima of the five (5) most stable hydroxythiophenol 3,4-POZs at the B3LYP/6-31G(d) level 86

Table 13 Relative energies and thermochemical properties of the minima of the five (5) most stable hydroxythiophenol POZs at the B3LYP/6-31G(d), B3LYP/6-31G(d,p) and B3LYP/6-311+G(2df) levels 90

Table 14 Relative energies and thermochemical properties of the minima of the three (3) most stable chlorophenol POZs at the B3LYP/6-311+G(2df) level 92

Table 15 Relative energies and thermochemical properties of the minima of the three (3) most stable dihydroxybenzene POZs at the B3LYP/6-311+G(2df) level 96

Table 16 Relative energies and thermochemical properties of the minima of the three (3) most stable hydroxythiophenol POZs at the B3LYP/6-311+G(2df) level 99

LIST OF FIGURES

Figure 1 Resonance structures of the ozone molecule 1

Figure 2 Structure of phenol..... 14

Figure 3 Resonance structures of the conjugate base of phenol..... 14

Figure 4 Structure of thiophenol 16

Figure 5 1,3-Cycloaddition of ozone on phenol/thiophenol: schematic representation of the three modes of addition 48

Figure 6 Absolute relative electronic energies (+ZPE) of the five (5) most stable chlorophenol 1,2-POZs at the B3LYP/6-31G(d) level..... 51

Figure 7 Absolute relative electronic energies (+ZPE) of the five (5) most stable chlorophenol 1,2-POZs at the B3LYP/6-31G(d,p) level..... 52

Figure 8 Structure of 2-Cℓ-*endo*-H-*exo*-O-1,2-poz..... 53

Figure 9 Absolute relative electronic energies (+ZPE) of the five (5) most stable chlorophenol 2,3-POZs at the B3LYP/6-31G(d) level..... 54

Figure 10 Absolute relative electronic energies (+ZPE) of the five (5) most stable chlorophenol 2,3-POZs at the B3LYP/6-31G(d,p) level..... 55

Figure 11 Structure of 2-Cℓ-*endo*-H-*exo*-O-2,3-poz..... 56

Figure 12 Absolute relative electronic energies (+ZPE) of the five (5) most stable chlorophenol 3,4-POZs at the B3LYP/6-31G(d) level..... 57

Figure 13 Absolute relative electronic energies (+ZPE) of the five (5) most stable chlorophenol 3,4-POZs at the B3LYP/6-31G(d,p) level..... 58

Figure 14 Structure of 4-Cℓ-*endo*-H-*exo*-O-3,4-poz..... 59

Figure 15 Absolute relative electronic energies (+ZPE) of the five (5) most stable dihydroxybenzene 1,2-POZs at the B3LYP/6-31G(d) level 64

Figure 16 Absolute relative electronic energies (+ZPE) of the five (5) most stable dihydroxybenzene 1,2-POZs at the B3LYP/6-31G(d,p) level 65

Figure 17 Structure of 2-OH-*endo*-H-*exo*-O-*endo*-H-1,2-poz 66

Figure 18 Absolute relative electronic energies (+ZPE) of the five (5) most stable dihydroxybenzene 2,3-POZs at the B3LYP/6-31G(d) level 68

Figure 19 Absolute relative electronic energies (+ZPE) of the five (5) most stable dihydroxybenzene 2,3-POZs at the B3LYP/6-31G(d,p) level 69

Figure 20 Structure of 2-OH-*endo*-H-*exo*-O-*endo*-H-2,3-poz 70

Figure 21 Absolute relative electronic energies (+ZPE) of the five (5) most stable dihydroxybenzene 3,4-POZs at the B3LYP/6-31G(d) level 72

Figure 22 Absolute relative electronic energies (+ZPE) of the five (5) most stable dihydroxybenzene 3,4-POZs at the B3LYP/6-31G(d,p) level 73

Figure 23 Structure of 3-OH-*endo*-H-*exo*-O-*endo*-H-3,4-poz 74

Figure 24 Absolute relative electronic energies (+ZPE) of the five (5) most stable hydroxythiophenol 1,2-POZs at the B3LYP/6-31G(d) level 79

Figure 25 Absolute relative electronic energies (+ZPE) of the five (5) most stable hydroxythiophenol 1,2-POZs at the B3LYP/6-31G(d,p) level 80

Figure 26 Structure of 2-OH-*endo*-H-*exo*-O-*exo*-H-1,2-poz 81

Figure 27 Absolute relative electronic energies (+ZPE) of the five (5) most stable hydroxythiophenol 2,3-POZs at the B3LYP/6-31G(d) level 83

Figure 28 Absolute relative electronic energies (+ZPE) of the five (5) most stable hydroxythiophenol 2,3-POZs at the B3LYP/6-31G(d,p) level 84

Figure 29 Structure of 2-OH-*exo*-H-*exo*-O-*endo*-H-2,3-poz 85

Figure 30 Absolute relative electronic energies (+ZPE) of the five (5) most stable hydroxythiophenol 3,4-POZs at the B3LYP/6-31G(d) level 87

Figure 31 Absolute relative electronic energies (+ZPE) of the five (5) most stable hydroxythiophenol 3,4-POZs at the B3LYP/6-31G(d,p) level 88

Figure 32 Structure of 3-OH-*endo*-H-*exo*-O-*exo*-H-3,4-poz 89

Figure 33 Activation barrier (kcal/mol) and exothermicity (kcal/mol) of 4-Cℓ-*endo*-H-*exo*-O-3,4-poz 93

Figure 34 Geometry of most stable chlorophenol POZ intermediate (4-Cℓ-*endo*-H-*exo*-O-3,4-poz) 94

Figure 35 Activation barrier (kcal/mol) and exothermicity (kcal/mol) of 2-OH-*endo*-H-*exo*-O-*endo*-H-1,2-poz 97

Figure 36 Geometry of most stable dihydroxybenzene POZ intermediate (2-OH-*endo*-H-*exo*-O-*endo*-H-1,2-poz) 98

Figure 37 Activation barrier (kcal/mol) and exothermicity (kcal/mol) of 2-OH-*exo*-H-*exo*-O-*endo*-H-2,3-poz 100

Figure 38 Geometry of most stable hydroxythiophenol POZ intermediate (2-OH-*exo*-H-*exo*-O-*endo*-H-2,3-poz) 101

ACKNOWLEDGEMENTS

First of all, I would like to take this opportunity to thank my creator, the Almighty God, for giving me the strength, courage and willpower to carry out this research. I would also like to acknowledge Prof. E. F. Archibong, my supervisor, for his expertise and advice provided as well as for being patient. The computational equipment provided by the Department of Chemistry and Biochemistry of the University of Namibia is also acknowledged.

DECLARATIONS

I, Niclaas Sikhoeb Gariseb, declare hereby that this study is a true reflection of my own research, and that this work, or part thereof has not been submitted for a degree in any other institution of higher education.

…… Date: 25 March 2013

Niclaas Sikhoeb Gariseb

To my beloved family: my mother, Magdalena Johnson; my aunt, Rudolfine Noabes; and my brothers, Phillips Robert Gariseb and Etienne Ernst Gariseb.

CHAPTER 1

INTRODUCTION

1.1 Chemistry of ozone

1.1.1 What is ozone?

Ozone is an allotrope of oxygen occurring naturally in the Earth's atmosphere. Ozone molecule contains three oxygen atoms and its molecular formula is O_3. According to spectroscopic measurements the O_3 molecule is bent, characterized by a bond angle of 116.5º and a O-O bond length of 1.278 Å. In its ground state, ozone exists as a singlet diradical **1** (Hay & Goddard III, 1972).

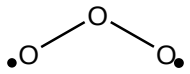

1

Its chemical structure can be described as a resonance hybrid of four canonical forms exhibiting a dipolar character as shown in Figure 1.

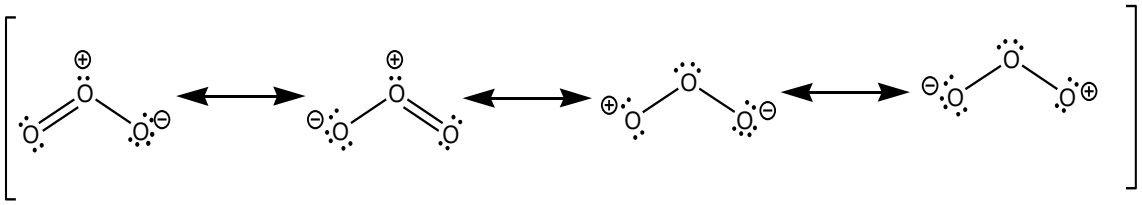

Figure 1 Resonance structures of the ozone molecule.

Ozone is an irritating pale blue gas, heavier than the air with a density of 2.14 kg/m^3. It is very reactive and unstable and cannot be stored and transported, therefore it has to be generated "in situ". It is explosive and toxic, even at low concentrations (*The*

Ozone, n.d.). Ozone has low melting and boiling points which are -192.5 °C and -111.9 °C, respectively (Chang, 1998). Ozone is soluble in many substances, forming either stable or metastable solutions. In water, ozone is about 14 times more soluble than oxygen, but forms a metastable solution. The stability is influenced by the presence of sensitizing impurities, such as heavy-metal cations and metal oxides, and by temperature and pressure: generally, an increase of the pressure or decrease of the temperature enhances the solubility of ozone in the aqueous phase (*The Ozone*, n.d.).

1.1.2 Ozone in the atmosphere

Most of the ozone in the earth's atmosphere is found in the stratosphere (15-50 km above the earth's surface). This layer of ozone plays a crucial role, protecting animals and plants from the sun's harmful ultraviolet (UV) rays and stabilising the earth's climate. The ozone layer is incredibly unstable, since it is constantly being formed and destroyed through interactions with UV radiation. Ozone absorbs UV radiation in its formation and breakdown: O_2 absorbs UV light to form 2 atomic oxygens as shown below [Reaction (1)]:

$$O_2 + h\nu \rightarrow 2O \quad (1)$$

The atomic oxygens can then react in one of three ways [Reactions (2) – (4)]:

$$O + O_2 \rightarrow O_3 \quad (2)$$

$$2O \rightarrow O_2 \quad (3)$$

$$O + O_3 \rightarrow 2O_2 \quad (4)$$

The ozone produced in reaction (2) can absorb UV radiation of wavelength 10.1-14.0 x 10^{14} Hz and undergo photodissociation as follows:

$$O_3 + h\nu \rightarrow O_2 + O \qquad (5)$$

Reaction (5) above is the most vital in shielding the earth from the sun's UV radiation (Stattersfield, 2001b).

Ozone is also present in the lower atmosphere, i.e. in the troposphere. Tropospheric ozone is man-made and it is produced in a cycle of reactions involving two basic classes of compounds, namely nitrogen oxides (NO_x) and hydrocarbons or volatile organic compounds (VOCs). Tropospheric ozone is found in photochemical smog, a complex pollutant generated when hydrocarbons and nitrogen oxides react in strong sunlight (Freudenrich, 2001; Stattersfield, 2001c). The formation of photochemical smog is typically initiated by photolysis of nitrogen dioxide, which leads to the production of ozone and in turn the reformation of NO_2. Reaction (6) below is one of the most important photochemical reactions in the lower atmosphere:

$$NO_2 + h\nu \rightarrow {}^{\cdot}NO + O^{\cdot} \qquad (6)$$

When nitrogen dioxide is excited by light, nitric oxide and atomic oxygen are formed. This reaction follows a first order kinetics: $k_1[NO_2]$ where k_1 is the rate coefficient and $[NO_2]$ represents molar concentration of NO_2. At night k_1 approaches 0 and reaches its maximum during hours of high sunlight intensity.

The first reaction of the atomic oxygen tends to be with the more abundant diatomic oxygen (O_2) to produce the ozone (O_3) molecule:

$$O_2 + O + M \rightarrow O_3 + M \qquad (7)$$

In reaction (7), M is an unreactive 3rd molecule which is needed to absorb excess energy from the reaction. The rate coefficient of this reaction is k_2. There is a third and final reaction which competes with this reaction [Reaction (8)]:

$$O_3 + {}^{\cdot}NO \rightarrow NO_2 + O_2 \qquad (8)$$

This reaction has the rate coefficient k_3.

Each of the 3 reactions [Reactions (6), (7) and (8)] is very fast, and a photostationary state of equilibrium is established. This governs the ratio of NO_2/NO in air, which in turn can be shown to be proportional to the concentration of ozone [Equation (1)].

$$[NO_2]/[{}^{\cdot}NO] = k_3[O_3]/k_1 \qquad \text{Eqn (1)}$$

So as k_1 approaches 0 (night time conditions), the presence of excess ozone increases and the lowest $[NO_2]/[NO]$ ratios are during hours of extreme day light, i.e. around midday.

Reactions (6) and (7) produce mono-atomic oxygen and ozone, respectively, which go on to react with hydrocarbons released from fossil fuels. Alkenes are particularly susceptible to attack from these oxygen allotropes. A typical reaction [Reaction (9)] is shown below:

$$CH_3CH{=}CHCH_3 + O_3 \rightarrow CH_3CHO_2 + CH_3CHO \qquad (9)$$

The reaction chain is then propagated:

$$C_2H_5 + O_2 \rightarrow C_2H_5O_2 \qquad (10)$$

$$C_2H_5O_2 + {}^{\cdot}NO \rightarrow C_2H_5O + NO_2 \qquad (11)$$

$$C_2H_5O + O_2 \rightarrow CH_3CHO + HO_2 \qquad (12)$$

$$HO_2 + {}^{\cdot}NO \rightarrow NO_2 + {}^{\cdot}OH \qquad (13)$$

Reactions (11) and (13) convert ˙NO to NO_2 without the use of ozone, keeping ˙NO concentrations reasonably low. Reaction (8) is relatively unimportant and high levels of ozone are able to build up (Stattersfield, 2001c).

Ozone is also a very strong oxidising agent as shown in reaction (14) below (Stattersfield, 2001a):

$$2Fe^{2+} + 2H^{+} + O_3 \rightarrow 2Fe^{3+} + H_2O + O_2 \qquad (14)$$

This reaction indicates one of the ways through which ozone is being depleted or destroyed in the atmosphere.

The same photons that break oxygen molecules apart to produce oxygen atoms can also break chlorofluorocarbons (CFCs), such as coolants, aerosols, and fire extinguishers, apart to release chlorine radicals, among other things.

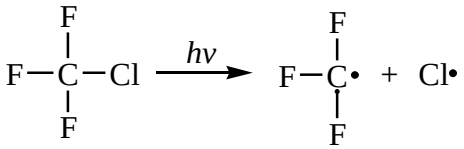

(15)

Radicals are very reactive because of the unpaired electron, so chlorine radical reacts easily with ozone molecules. When a chlorine radical encounters an ozone molecule, it takes one of the oxygen atoms away, leaving O_2 and chlorine oxide radical (ClO•).

$$O_3 + Cl\bullet \longrightarrow ClO\bullet + O_2 \qquad (16)$$

Chlorine oxide radical is also a reactive radical and it reacts quickly with another ozone molecule, converting it to two O_2 molecules, and freeing the Cl• to do still more damage. Since the Cl• starts this whole reaction, but is not consumed in the process, it is

a catalyst for the ozone destruction reaction (Chemical Heritage Foundation [CHF], 2001).

$$ClO\bullet + O_3 \longrightarrow Cl\bullet + 2O_2 \qquad (17)$$

Nitrogen oxide gases (NO_x) and volatile organic compounds (VOCs) are emitted by automobiles, gasoline vapors, fossil fuel power plants, refineries, and certain other industries. NO_x, VOCs and CFCs are carried into the ozone layer by strong winds (*Tropospheric Ozone*, n.d.).

The processes described above in one form or another results in the depletion of ozone in the atmosphere. It is thought that a reduction of 1% of the ozone in the stratosphere could lead to an increase in skin cancers in animals and humans; a suppression of the human immune systems; some inhibition to plant life, and an increased susceptibility to pests; reduction in growth of phytoplankton, endangering the food chain and a decrease in aquatic life forms (Stattersfield, 2001b).

1.1.3 Ozone in aqueous solution

Ozonation is widely used in drinking-water processing for disinfection as well as for the removal of unwanted contaminants, in particular organic pollutants (Mvula & Von Sonntag, 2003). The organic pollutants are removed from wastewater and process water by advanced oxidation processes (AOPs). This is due to the fact that traditional methods like the use of zeolites, activated carbon, reverse osmosis and electrodialysis are not fully able to remove the organic contaminants. The AOP technique seems very

suitable to break down organic pollutants such as recalcitrant aromatic compounds to smaller oxygenated and more water soluble fragments. In this way, biologically degradable molecules are formed which can be eliminated in conventional biological water purification systems. These AOPs are more environmentally friendly than the strong oxidizers such as permanganate, chromate, or chlorine. Chlorination which is the most widely used disinfecting method does not destroy most of the dissolved organic compounds and may result in the formation of trihalomethanes (THMs) which are suspected carcinogens. Organic pollutants of high relevance in this context are those containing aromatic ring structures such as phenolic compounds (Hendrickx & Vinckier, 2003; Mvula, 2002).

An example of a reaction of ozone with a phenolic compound is the reaction between ozone and 1,2-dimethoxybenzene. In this reaction, hydrogen peroxide is likely to be formed via a Criegee-type reaction pathway (Scheme 1) (Mvula, 2002).

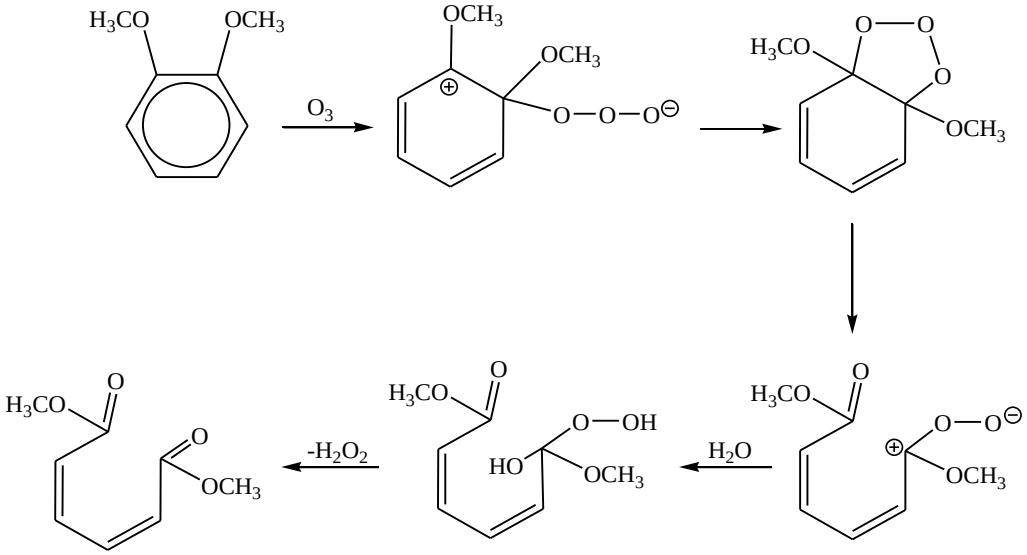

Scheme 1 The Criegee component in the reaction of ozone with 1,2-dimethoxybenzene.

Ozone is widely used for drinking water treatment, because of its excellent disinfection and oxidation qualities. Ozone can be added at several points throughout the treatment system, such as during pre-oxidation, intermediate oxidation or final disinfection. Usually, it is recommended to use ozone for pre-oxidation, before a sand filter or a granular active carbon (GAC) filter. After ozonization, these filters can remove the remaining organic matter which is important for the final disinfection.

Ozone improves the removal process of natural organic matter (NOM) by a subsequent filter when it is used as a pre-oxidant as it seldom achieves a complete mineralisation of NOM. Ozone can be very effective for the oxidation of several pesticides. At a water treatment plant in Zevenbergen (Holland) it was proved that three barriers (storage–ozonation–granular active carbon filter (GAC filter) are effective and safe enough for the removal of pesticides. From 23 tested pesticides, 50 % was degraded sufficiently (80 % degradation). Ozone is a more effective disinfectant than chlorine, chloramines, and even chlorine dioxide. An ozone dose of 0,4 mg L^{-1} for 4 minutes is usually effective for pre-treated water (low NOM concentration). Several studies proved that ozone, unlike chlorine products, can deactivate resistant micro-organisms. However, as ozone rapidly decomposes in water, its life-span in aqueous solutions is very short.

Ozone can oxidize compounds in a range of 20–90 % (depending on the type of compound). Ozone is more effective for the oxidation of unsaturated compounds. Geosmin and 2-methylisoborneol (MIB) are examples of resistant odorous compounds, which are often present in the water. These are produced by algae and have a low odor and taste threshold. Nevertheless, ozone still very effectively removes these compounds

(Lenntech Water treatment, 2009).

1.1.4 The significance of ozone

The ozone layer in the atmosphere is significant because in the stratosphere it is responsible for the protection of life, whereas in the troposphere it is harmful to both humans and ecosystems. The stratospheric ozone layer is a diluted veil of ozone gas that stretches from about 10-40 km above the ground (Velders, Slaper, Pearce, & Howarth, n.d.). The stratospheric ozone layer protects the Earth by absorbing the sun's harmful ultraviolet (UV) radiation (Scannell et al., 2011).

However, since the mid 1980's a noticeable severe depletion of stratospheric ozone mainly by chlorine- and bromine-containing substances has been observed annually over the Antarctic region during the polar springtime (i.e. August to November) (Velders et al., n.d.). The area of severe depletion of stratospheric ozone in the Antarctic region is what is referred to as the 'ozone hole'. During the polar springtime it has been established that there is an increase in the level of UV radiation reaching the Earth's surface in the ozone hole region. This in turn leads to adverse impacts on human health in parts of Australia and South America due to their close proximity to the Antarctic ozone hole (Scannell et al., 2011).

Stratospheric ozone has decreased over the past decades, whereas tropospheric ozone has increased over the last century. These ozone changes have a subsequent impact on the climate. A statistically significant cooling has occurred in the lower stratosphere and in the upper stratosphere. The lower stratospheric cooling is attributable

largely to the observed ozone reduction there. The upper stratospheric cooling will slow down the natural ozone destruction cycles, first offsetting any chlorine-catalyzed ozone destruction there and eventually leading to ozone increases compared to pre-ozone hole conditions (European Commission, 2003).

Ozone is also a ‘greenhouse gas’ like carbon dioxide and water vapour. A greenhouse gas is one that is transparent to incoming solar radiation, but traps long-wave infrared (IR) radiation. They trap heat in the atmosphere by absorbing IR radiation from the Earth and by so doing become heated and then the IR radiation is reflected back to the Earth. Because of the presence of greenhouse gases such as ozone in the troposphere, the Earth's average temperature is higher than it would be if these gases were absent. This phenomenon is known as the greenhouse effect. The increase in tropospheric ozone has led to a gradual increase in the Earth’s average temperature. This gradual increase in the Earh’s average temperature due to the greenhouse effect is referred to as global warming (Marinelli & Worth, 1994).

To sum up, the ozone layer in the upper stratosphere blocks the penetration of radiation from the sun. With a thinning protective ozone layer, the Earth is hit by more of the sun’s radiation. The greenhouse gases including ozone absorb the Earth’s outgoing long-wave radiation in the troposphere. These gases essentially block the release of infrared radiation and thereby disrupt the heat balance of the Earth. Warming by greenhouse gases may be offset by cooling from stratospheric ozone depletion; diminished amounts of ozone decrease the amount of solar and long-wave radiation

absorbed. Thus the net effects of ozone depletion on global warming depend on where in the atmosphere the ozone is destroyed (Marinelli & Worth, 1994).

1.1.5 Industrial applications of ozone

Ozone has many applications in the industries. The following are some of the industrial applications of ozone:

Waste water processing

Ozone is an effective disinfectant for treating municipal and industrial waste water. Ozone has the ability to disinfect the final stage of effluent and reduce odour emissions by breaking down organic materials and chemicals in waste water. Ozone will reduce the biochemical oxygen demand (BOD) of the waste and so reduce its disposal costs because municipal processing fees and charges are often based on the BOD. Recycled water is now very common for irrigation purposes, but must be treated so that it is free of organisms that can cause harm. Ozone will sanitize the waste water prior to agricultural use allowing it to comply with health regulations (Franken, 2005).

Fruit and vegetable cleaning and storage

During post-harvest storage, surface infections on produce can spread and cause significant losses of the crop. The use of ozonated water for washing and disinfecting can reduce these losses and maximize returns. Ozonated water is a convenient way to wash fruit and vegetables. The shelf life of produce in cold storage can also be extended by the use of gaseous ozone. Ozone in the air within a cold storage room can retard the

growth of microorganisms in the air and on the surface of the produce. Ozone is also effective in breaking down ethylene gas which is given off by some fruits and accelerates the ripening process. The reduction of ethylene gas will effectively reduce the ripening effect of mixed produce held in the same area (*Industries*, n.d.).

Aquaculture

With the increase in demand for seafood and the reduction of ocean fish stock aquaculture is now a growing industry. Growing healthy fish stock requires waste matter removal and water treatment to provide a healthy environment for the stock. Ozone can be used to reduce toxicity allowing water to be recycled through the system in a closed loop thereby reducing the need for large amounts of fresh water being continuously added. Ozone can sanitize small or large quantities of water by altering the dose being added accordingly. Using ozone instead of chlorine has some significant advantages. Firstly, the ozone gas will increase the dissolved oxygen level in the fish tanks. Secondly, the fish will not be exposed to the by-products of chlorination with all the ramifications that are entailed (*Industries*, n.d.).

Wineries

Ozone has many uses in wineries as is outlined below:

- Storage tanks rinsed using ozonated water will have a significant reduction of organisms on the internal tank surfaces and fittings. Often this replaces the need to use caustic products.

- Pipework free from organic material can be sanitized by the use of ozonated water instead of sodium hydroxide or as a supplement to the use of sodium hydroxide.
- Ozone will sanitize bottling equipment simply and without the use of chemicals.
- In barrels, the use of ozonated water as a rinse after hot water, or on its own for those who use cold rinse only, will reduce or eliminate bacteria and yeasts including *Brettanomyces* (Franken, 2005).

Bottled water

Bottled water is a part of everyday life and ozone is commonly used to process that water. Not all sparkling springs are clear of bacteria which can be carried by the water as it travels through to the water table. This water is often treated with ozone which acts on the bacteria and in the process it breaks down to oxygen and then dissipates leaving no residues behind except sanitized water. Ozone can also be used to sanitize bottles and caps prior to bottling, making it perfect for bottling plants (*Industries*, n.d.).

Pulp and paper manufacturing

The main steps in pulp and paper manufacturing are raw material preparation, such as wood debarking and chip making; pulp manufacturing; pulp bleaching; paper manufacturing; and fiber recycling. Manufactured pulp is used as a source of cellulose for fiber manufacture and for conversion into paper or cardboard. In the manufacturing

of pulp, ozone is used during the bleaching process to transform lignin into an alkali-soluble form and to give paper its white color. Ozone can also be applied as a final polishing treatment to the waste effluent from the plant to reduce odour emissions which emanates from the process (World Bank Group, 1998).

1.2 Phenols and Thiophenols

Phenols

Phenol is the simplest aromatic alcohol. It consists of a hydroxyl group (-OH) bonded to the aromatic ring. The structure of phenol is shown in Figure 2 below:

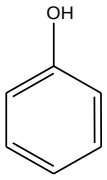

Figure 2 Structure of phenol.

The conjugate base of phenol has four contributors (resonance structures) which are shown in Figure 3 below:

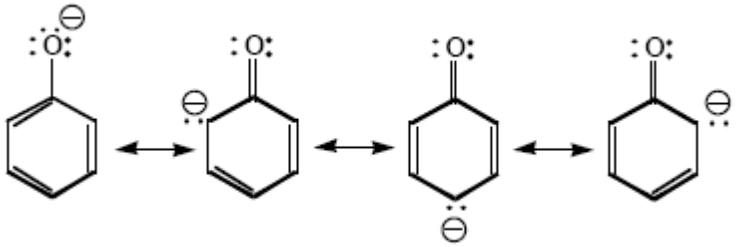

Figure 3 Resonance structures of the conjugate base of phenol.

Phenol is found naturally in decaying dead organic matter like rotting vegetables and in coal. Phenol is stable under ordinary (normal) conditions. It was first isolated in 1834 from coal tar and this remained the main source of phenol until the First World War. The first synthetic method was then devised and all of the phenol today is man-made (Harrison, 2007). Phenol is synthesized via the reactions shown in Scheme 2 below (Carey, 2000):

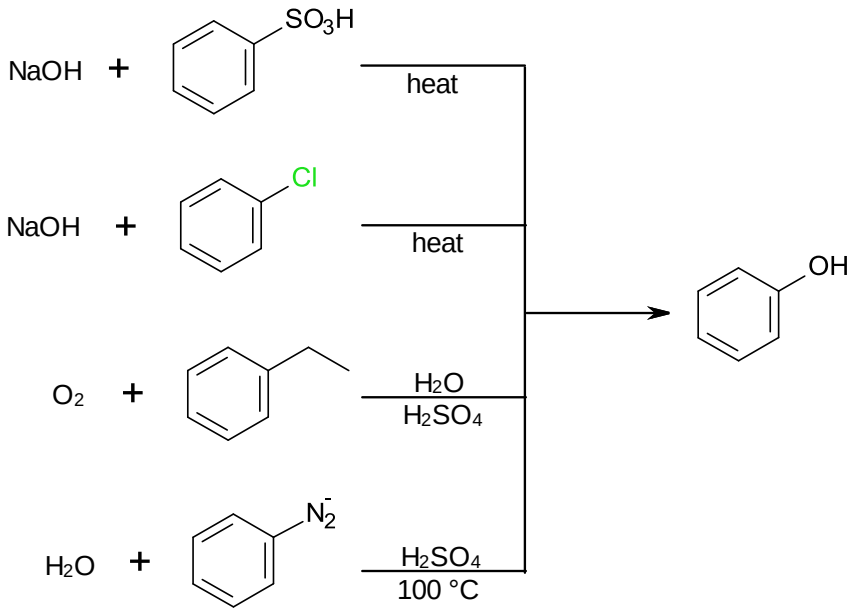

Scheme 2 Synthesis of phenol.

Phenol has a sweet odour which enables it to be used in air fresheners. The largest use for phenol is in low cost, versatile resins. They are mainly thermoset resins used in plywood adhesion, construction and the motorcar industry. Another use for phenol includes an intermediate stage in the process of producing caprolactam, which is used in nylon and many other man-made fibres. Phenol is also a powerful disinfectant and bacteria killer. This is ideal for not only air fresheners, but also for other products

like medicinal ointments and lotions. However, the chemical is highly corrosive and moderately toxic. It affects humans by burning the skin and other tissues that it comes into contact with. This gives severe skin burning and if inhaled, it can cause serious internal corrosion. The skin burning is not initially felt, because the phenol has a local anaesthetic effect. It can affect the central nervous system, which will at first lead to sweating, weakness, dizziness and twitching, but with prolonged exposure leads to nausea, vomiting and coma. If ingested, even a small dose can lead to be fatal in humans and therefore care must be taken at all times when phenol-containing products are used (Harrison, 2007).

Thiophenols

Thiophenol is an aromatic thiol which is structurally analogous to phenol; the hydroxyl group (-OH) bonded to the aromatic ring in phenol is replaced by a sulfhydryl group (-SH) in thiophenol. This structure (Figure 4) means that the oxygen atom of the hydroxyl group in phenol is replaced by a sulfur atom in thiophenol (*Thiophenol*, 2008).

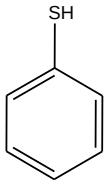

Figure 4 Structure of thiophenol.

Thiophenol is found naturally in natural gas. Thiophenol can be synthesized by the Leuckart Thiophenol Reaction or by the reduction of sulfonyl chlorides by zinc dust and sulfuric acid as shown below:

Leuckart Thiophenol Reaction

The first step is the reaction of an aryl diazonium salt with a potassium alkyl xanthate to give an aryl xanthate, which affords a phenyl mercaptan (thiophenol) upon basic hydrolysis [Reactions (18) and (19)] (*Leuckart Thiophenol Reaction*, n.d.).

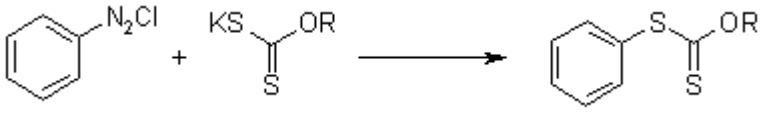

(18)

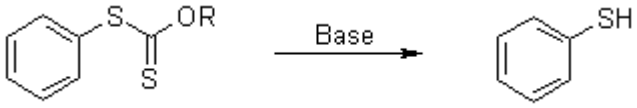

(19)

Reduction of sulfonyl chlorides by zinc dust and sulfuric acid

In this method, sulfonyl chlorides are reduced by zinc dust and sulfuric acid [Reaction (20)] (*Thiophenol*, 2007).

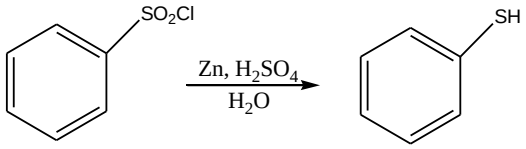

(20)

Thiophenols have many important uses. They can form thiophenolate anions by losing sulfhydryl H^+ ions. The ring closure reaction of *o*-amino thiophenol produces benzothiazole, an important industrial product. Thiophenol itself is used as an antinematodal agent. Thiophenols are also used as anthelminthics, polymerization stabilizers, complexing agents for metal extraction or flotation benefaction, flame resistant polymers; rubber chemicals, such as accelerators, inhibitors, anti-oxidants and anti-ozonants; fragrances and flavors, arctic oils and as intermediates for making other

compounds such as the insecticides. However, thiophenol is also toxic. They pose a problem to humans. Thiophenols may be toxic to kidneys, lungs and liver. Repeated or prolonged exposure to thiophenols can produce target organs damage. Repeated exposure to highly toxic thiophenols may produce general deterioration of health by an accumulation in one or many human organs (*Production of Thiophenols*, 2009; Sciencelab, 2008; *Thiophenol*, 2008).

1.3 Problem Statement

Experimentally it is difficult to determine the stability, bonding and thermochemical properties of compounds that enjoy only a transient existence. POZs derived from phenol and substituted phenol and thiophenol fall into this class. Most of the intermediates and products that are formed during ozonolysis are short-lived and cannot be studied experimentally. For these reasons, a computational approach provides an alternative and reliable path of investigating the stability of the transient intermediates and products that will be formed from the reaction of ozone with substituted phenol and thiophenol compounds.

The different substituents on phenol and thiophenol compounds have an effect on the stability of the POZ that will be formed from the reaction with ozone. If it is established from computational studies that a POZ having a specific substituent is stable, then this will motivate the experimental chemist and give the assurance that the specific POZ can be isolated or synthesized in the laboratory.

Despite compilations of experimental thermochemical data of many molecules, there are numerous species, including POZs derived from phenols and substituted phenol and thiophenol, for which no data are available. And for those cases where thermochemical data are available, sometimes they are incorrect and unreliable for species that are unstable. Further, experimental measurements of thermochemical data are often expensive and difficult, so it is highly desirable to employ computational methods that can make reliable predictions.

Thermochemical data are very imperative as they provide information on stabilities and reactivities of molecules that are used, for example, in modeling reactions occurring in combustion, the atmosphere, and chemical vapor deposition. Themochemical data is a key factor in the safe and successful scale-up of chemical processes in the chemical industry (Curtiss & Pople, 1999).

This work investigates, for the first time, the potential energy surfaces of substituted phenol and thiophenol primary ozonides (POZs), specifically chlorophenol, dihydroxybenzene and hydroxythiophenol, using density functional theory (DFT). The focus was on processes involving the formation of POZs as intermediates in the ozonolysis of substituted phenol and thiophenol. Consequently, the structures, stability and thermochemical properties of the POZ are computed in the gas phase.

1.4 Objective

- The cardinal objective is to investigate the structures, stability and thermochemical properties of primary ozonides (POZs) derived from substituted

phenol and thiophenol in order to predict and complement future experimental results involving the ozonolysis of substituted phenol and thiophenol.

1.5 Relevance and Significance of the Study

Thermochemical properties such as enthalpy, entropy and Gibb's free energy are not available for the POZs of phenol and substituted phenol and thiophenol which are the ubiquitous intermediates in the ozonolysis process. The reason for the unavailability of these data is that experimentally it is not easy to isolate the primary ozonides (POZs). Computational studies can be used to study these POZs and predict these thermal quantities. Based on these theoretical data, experiments can be designed to measure the properties. While studies on the kinetics of 1,2-benzenediol (catechol) POZs have been done (Tomas et al., 2001), kinetics alone does not tell the researcher anything about the structure, bonding and thermochemical properties. Kinetics provide only the rates of the reaction. This research investigates the structure, bonding and thermochemical properties of POZs derived from substituted phenol and thiophenol, specifically chlorophenol, dihydroxybenzene and hydroxythiophenol. And thus provides essential data.

Hendrickx and Vinckier (2003) have reported the only computational study of the reaction of ozone with phenol. However, the latter report was only concerned with the electronic energy differences, ΔE_e, and the zero-point vibrational energies, *ZPE*. This research goes further by computing the thermochemical properties (including enthalpies (ΔH), Gibbs free energies (ΔG) and entropies (ΔS)) of the POZs derived from substituted

phenol. And for the first time thermochemical data are made available for the POZs derived from substituted thiophenol for which no study has been done up to date.

The results of this research will serve as a guide to experimentalists and some of the computed parameters can be used to identify and characterize the compounds detected in future experiments. Additionally, the investigation of the potential energy surface of ozone reactions with compounds likely to be found in both natural and waste-waters would help with the understanding of the mechanism of such reactions.

1.6 Limitation of the Study

It would have been much desirable to conduct this research at the highest level of theory using coupled cluster approach and very large one-particle basis set. However, the computational resources at UNAM are very much limited. The laboratory has only single-processor machines with not more than 1GB of RAM. This places a limitation on the sophistication of the calculations and confines us to a decent theoretical level of density functional theory (DFT).

CHAPTER 2

LITERATURE REVIEW

2.1 Reactions of ozone with compounds containing C=C

(a) With olefins

Ozonolysis is an important oxidation pathway for gaseous and condensed-phase alkenes in the troposphere. Ozonolysis is a process in which ozone reacts with a carbon-carbon multiple bond as in alkene. The first step of ozonolysis involves the formation of a very unstable five-membered ring consisting of 3 oxygen atoms in a row and 2 carbon atoms. This species is known as a primary ozonide (POZ) or 1,2,3-trioxolane. The ozone molecule reacts very fast with alkenes through a 1,3-dipolar cycloaddition reaction to form the POZ. The unstable POZ rearranges almost immediately to the more stable secondary ozonide (SOZ or 1,2,4-trioxolane) via a reverse 1,3-dipolar addition (Scheme 3). The reason why the POZ is less stable than the SOZ is because the POZ has two weak oxygen-oxygen bonds, whereas the SOZ has only one weak oxygen-oxygen bond in its structure (*Reactions of alkenes*, n.d.).

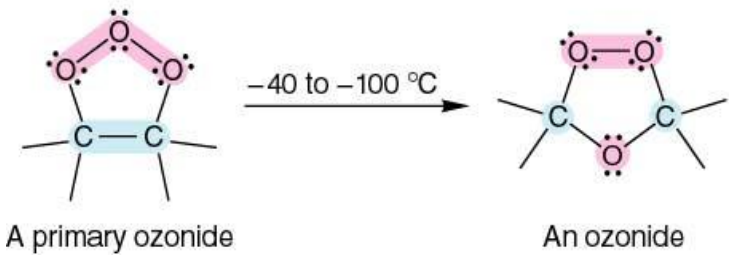

Scheme 3 Formation of a SOZ.

During the rearrangement to the SOZ, the POZ decomposes into a carbonyl compound and a carbonyl oxide as shown in Scheme 4:

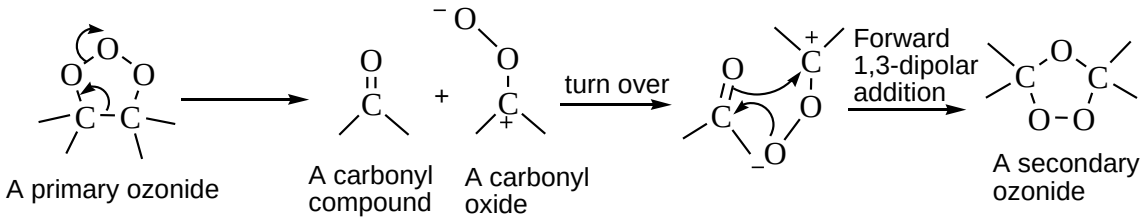

Scheme 4 Rearrangement of a POZ to a SOZ.

In a protonic solvent such as water, the primary ozonide decomposes into a carbonyl compound (aldehyde or ketone) and a zwitterion (**I**) that quickly leads to a hydroxy-hydroperoxide (**II**) stage that, in turn, decomposes into a carbonyl compound and hydrogen peroxide (see Scheme 5) (*The Ozone*, n.d.).

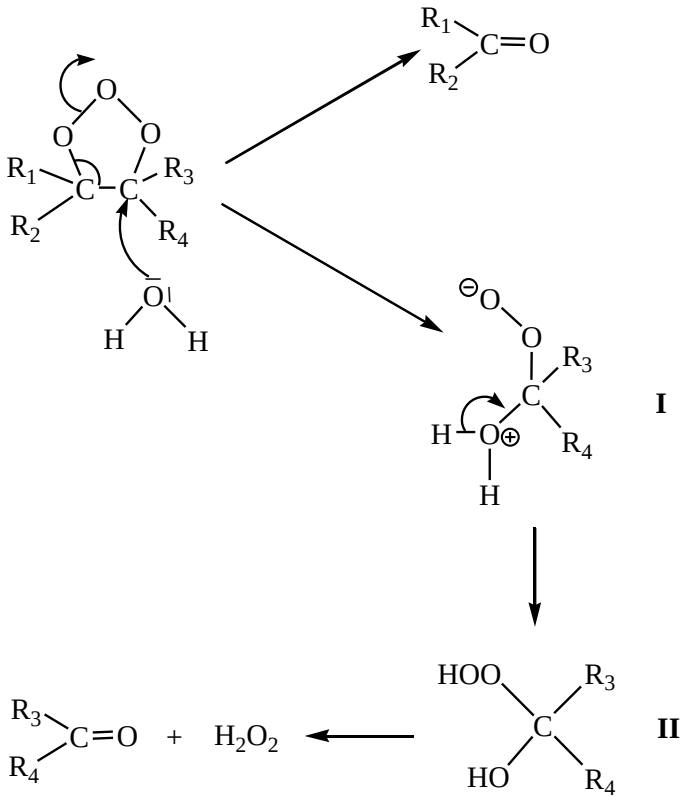

Scheme 5 Decomposition of a POZ in a protonic solvent.

A reductive workup of a SOZ, i.e. reaction with either Me_2S, PPh_3 or Zn, leads to aldehydes and ketones and an oxidative workup of a SOZ, i.e. reaction with H_2O_2, leads to ketones and carboxylic acids (Scheme 6) (*Reactions of alkenes*, n.d.).

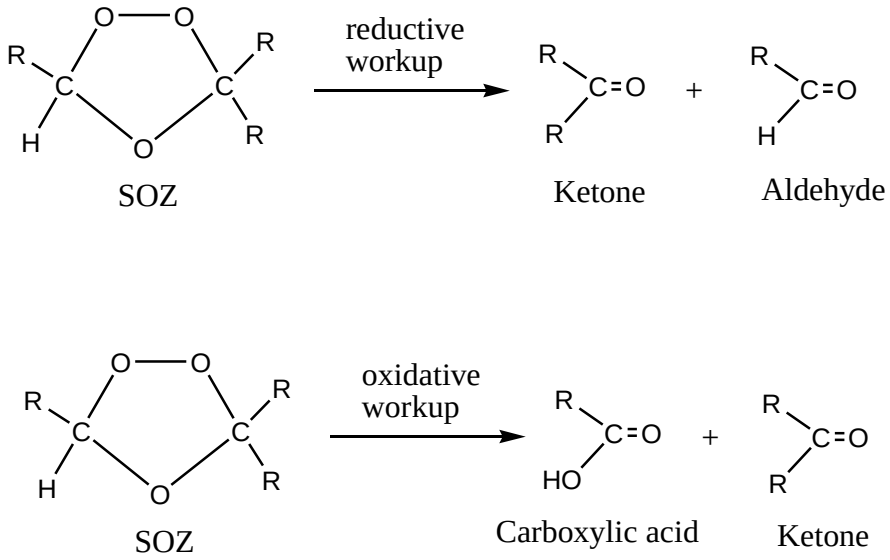

Scheme 6 A reductive workup (top) and an oxidative workup (bottom) of a SOZ.

The reaction between ozone and an olefin has been categorized as an ozone 1,3-dipolar cycloaddition reaction and is well described in terms of the Criegee mechanism (Scheme 7). The initial encounter results in the formation of a π-complex, which gives rise to a zwitterion σ-complex **1** [reaction (21)] followed by ring closure to form the primary ozonide (POZ) **2** also known as 1,2,3-trioxolane [reaction (22)]. The POZ **2** decomposes into the zwitterion **3** which decomposes further into another zwitterion **4** and a carbonyl compound **5** [reaction (23) and (24)]. The zwitterion **4** reacts with water [reaction (25)] to give an α-hydroxyalkylhydroperoxide **6** which is in equilibrium with hydrogen peroxide **10** and a carbonyl compound **9** [equilibrium (27)]. In water, reaction

(25) does not compete with reaction (26). However, in organic solvents, the zwitterion **4** and carbonyl compound **5** can react to form the Criegee ozonide **7**. In aqueous solution, compound **8** would hydrolyze yielding two moles of carbonyl compound **9** and one mole of hydrogen peroxide **10** [reaction (29)] (Mvula, 2002).

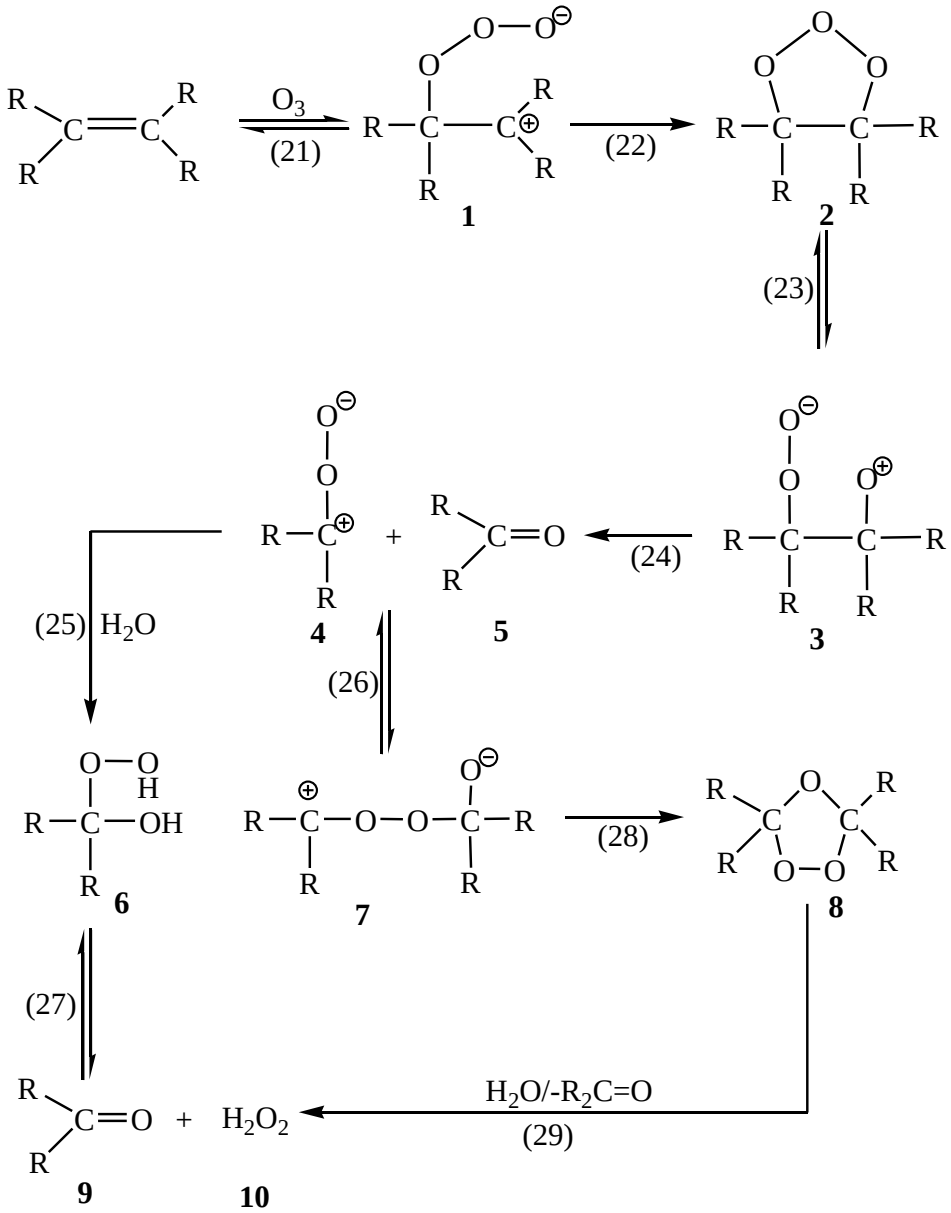

Scheme 7 The mechanism of ozone reaction with an olefin.

An example of a reaction of ozone with an olefin is the reaction of ozone with ethylene which mechanism involves three-steps having three intermediates, namely the primary ozonide, **III** (POZ), the secondary ozonide , **V** (SOZ); and a carbonyl oxide, **IV**, sometimes referred to as the Criegee intermediate (CI) (Scheme 8). The POZ's are more reactive than the SOZ's. The POZ's were first directly observed by NMR and by infrared spectroscopies in low-temperature matrices, and more recently the microwave spectrum of the ethylene POZ was obtained in a seminal paper by Gillies J., Gillies C., Suenram, and Lovas (Hendrickx & Vinckier, 2003; *The Ozone*, n.d.; Samuni, Fraenkel, Haas, Fajgar, & Pola, 1996).

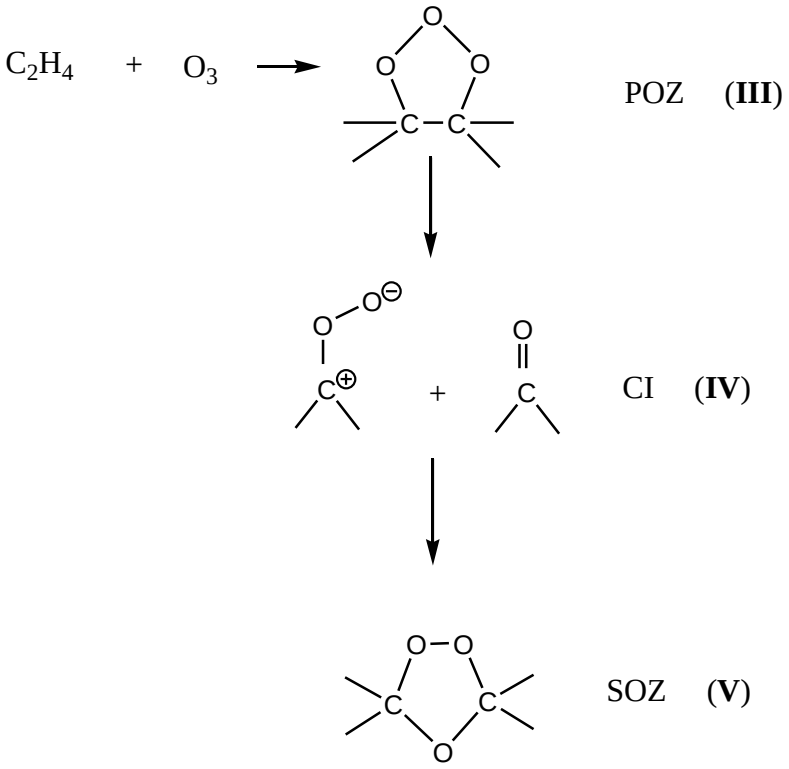

Scheme 8 Criegee Mechanism of Ethylene Ozonolysis.

(b) With aromatic compounds

An example is the reaction of ozone with benzene. From preliminary calculations that were done by Hendrickx and Vinckier (2003), it was deduced that the reaction between ozone and benzene proceeds in a concerted fashion. In this case the addition can occur on two carbons in the α, β or γ position to each other. The α addition was found to produce POZ structures that were the most stable (Scheme 9). The reason for this could most probably be attributed to a 1,3-butadiene-like moiety, which is only present in the product of the α addition. Optimization of the γ structure (Scheme 9) yielded a local minimum on the potential energy surface, which at the CCSD(T) level is 15 kcal/mol higher than the α-POZ. A detailed search did not yield a stable structure in which the ozone molecule is bound to two carbon atoms that are in β position with respect to each other. All attempts collapsed to either α- or γ-POZ. Even if the study was confined to the α type addition, still two mechanistically different approaches should be considered: the middle oxygen atom of ozone is either directed toward the benzene ring (*endo*-type) or directed away from this ring structure (*exo*-type). Hendrickx and Vinckier (2003) arrived at the conclusion that at the B3LYP and CCSD(T) levels, the energetic positions of the two conformers (i.e. *endo*- and *exo*-type) of the POZ are nearly identical, the difference being less than 0.5 kcal/mol.

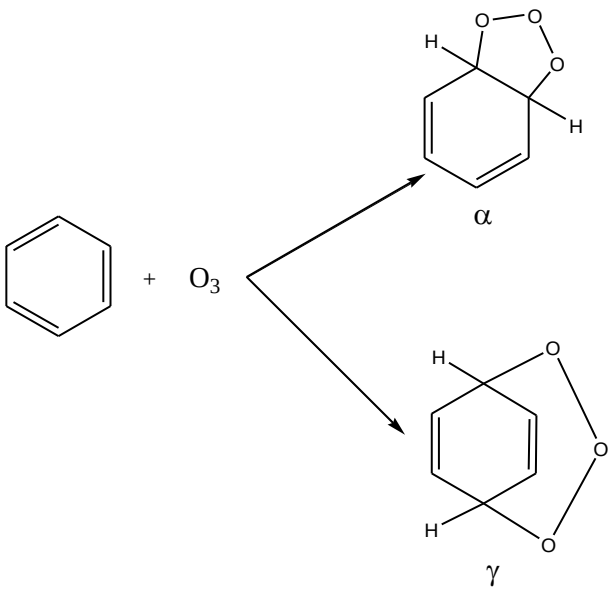

Scheme 9 Mechanism of the ozonolysis of benzene.

Another mechanism that was proposed for the ozonolysis of benzene in experimental kinetic studies by Razumovskii and Zaikov (n.d.) involves the formation of polymeric ozonides (Scheme 10).

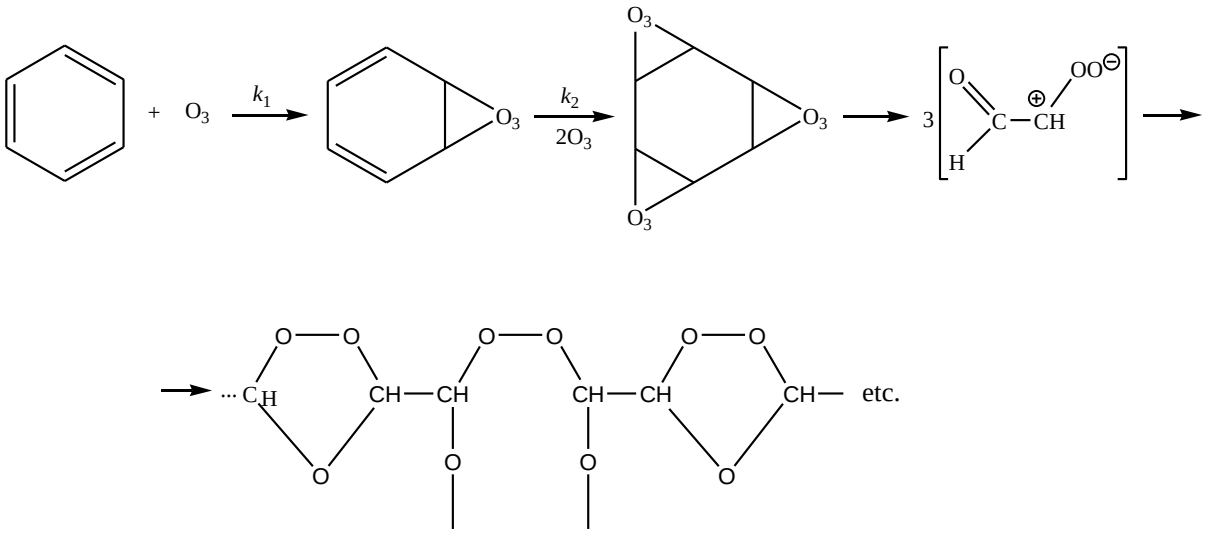

Scheme 10 The mechanism of ozone reaction with benzene.

Another example of the reaction between ozone and an aromatic compound is the reaction of ozone with phenol. The mechanism which was proposed by Bailey (1978) is given in Scheme 11. It was suggested that catechol **11** and hydroquinone **12** are formed as a result of ozone attack at the *ortho*- and *para*-position, respectively, followed by the O_2 elimination reaction of intermediate **14** and **15** [reactions (30) - (33)]. In this mechanism, a 1,3 dipolar cycloaddition similar to that of simple olefins also occurs from reaction (34), in which the 1,2-POZ **16** is formed, to reaction (36) which ultimately results in the formation of *cis*,*cis*-muconic acid **13** (Mvula, 2002). For all these reactions, no thermodynamic studies were carried out.

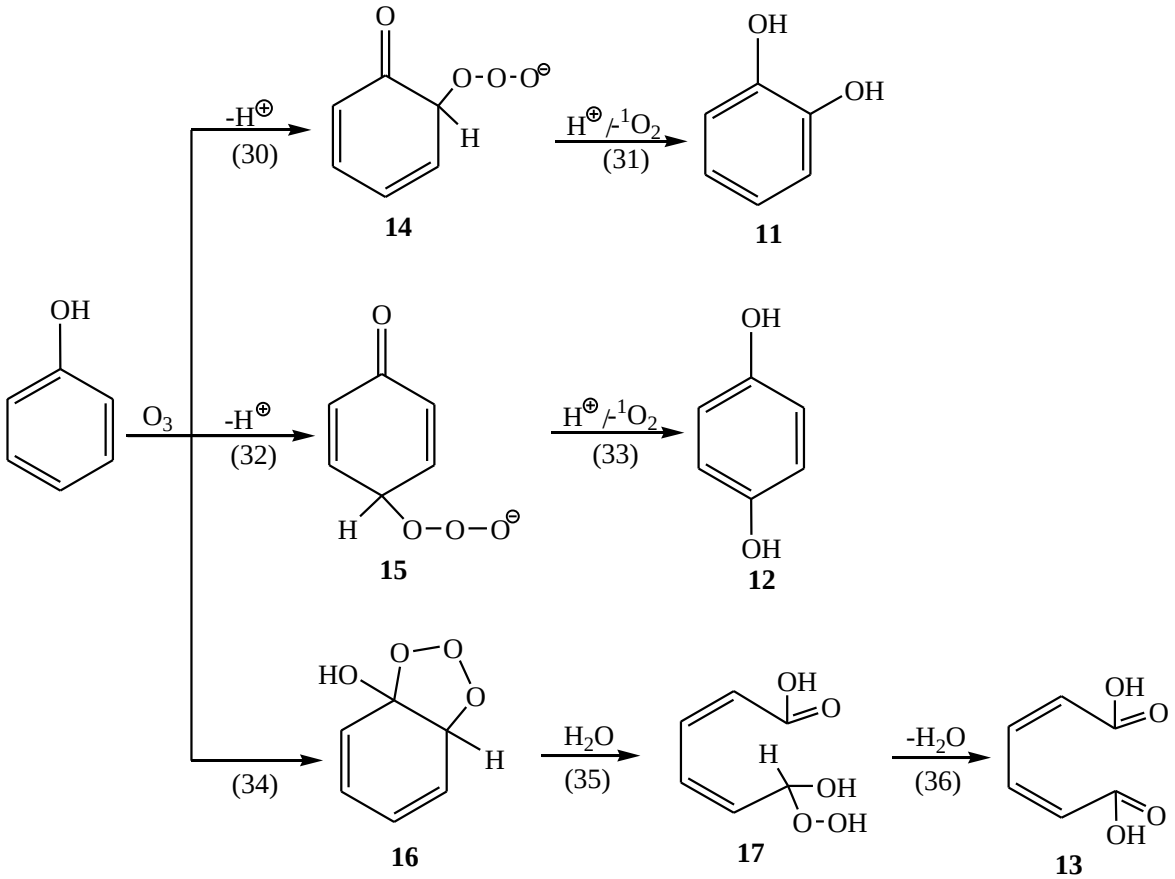

Scheme 11 Bailey's mechanism for the reaction of ozone with phenol.

2.2 Density Functional Theory (DFT)

Density functional theory (DFT) is a method that can be used in the computational studies of the structures, bondings and thermochemical properties of molecules.

The aim of DFT as formulated by Hohenberg and Kohn is to describe the properties of the ground state of a many-electron system solely by the electron density without making any explicit reference to the many-body wave function. In other words every ground-state property, and in particular the ground-state energy, is a functional of the electron density (*Density-Functional Theory*, n.d.; Simons, 1991). The Hohenberg and Kohn formulation can be expressed mathematically by equation (2):

$$E(\rho) = F(\rho) + \int \rho(r) V_{ext}(r) dr \qquad \text{Eqn (2)}$$

In equation (2), $E(\rho)$ is the ground state energy or the total energy functional; $V_{ext}(r)$ is the external potential and it includes the potential from the nuclei; $F(\rho)$ is the universal functional which is unknown, it contains the kinetic energy and the electron-electron interaction energy and it does not depend on V_{ext}; and $\rho(r)$ is the electron density.

The advantages of such a theory are clear. Whereas the complicated many-body wave function depends on three spatial variables for each of the N electrons, the electron density is a collective variable which only depends on three spatial variables, i.e. the spatial coordinates x, y, and z, making the electron density a quantity that is easier to deal with in practice (*Density-Functional Theory*, n.d.).

DFT has got several advantages over *ab initio* methods of which the most commonly used type of *ab initio* calculation is called a Hartree-Fock calculation (abbreviated HF). HF misses the Coulomb correlation, whereas DFT to some extent includes both the Coulomb and Exchange correlation. The performance of DFT is as good as that of HF and MP2 or better, with less effort. And DFT can be used for transition metals, whereas HF will give a lousy result.

Although DFT is formally exact as aforementioned, the exact functional is unknown. The exact functional probably does not have a closed form, and would be extremely non-local. Nevertheless, very good approximations are known which work well for many systems. In practice, DFT is good for structural stability, vibrational properties, elasticity, and equations of state. DFT is also used in thermochemistry which is the study of the effects of work, heat and energy on a system. The thermochemical properties of molecules, e.g. enthalpy, entropy and Gibb's free energy, that are obtained with the help of DFT are of major importance in the chemical sciences and are essential to many technologies.

2.3 Basis Sets

Basis sets are mathematical functions that are used to represent atomic and molecular orbitals in electronic structure calculations (Archibong, 2007). Early, the Slater Type Orbitals (STOs) were used as basis functions due to their similarity to atomic orbitals of the hydrogen atom. In spherical coordinates, they are described as follows [Equation (3)]:

$$\phi_i(\varsigma, n, l, m; r, \theta, \phi) = \boldsymbol{N} r^{n-1} e^{-\varsigma r} \boldsymbol{Y}_{lm}(\theta, \phi) \qquad \text{Eqn (3)}$$

$\boldsymbol{N}$ is a normalization constant and ζ is called "exponent". The r, θ, and ϕ are spherical coordinates, and $\boldsymbol{Y}_{lm}$ is the angular momentum part (function describing "shape"). The n, l, and m are principal, angular momentum, and magnetic quantum number, respectively. Unfortunately, functions of this kind are not suitable for fast calculations of necessary two-electron integrals. Consequently, the Gaussian Type Orbitals (GTOs) were introduced whereby the shape of the STO function was approximated by summing up a number of GTOs with different exponents and coefficients.

The GTO in cartesian form is expressed as [Equation (4)]:

$$g(\alpha, l, n, m; x, y, z) = \boldsymbol{N} e^{-\alpha r^2} x^l y^m z^{\boldsymbol{n}} \qquad \text{Eqn (4)}$$

$\boldsymbol{N}$ is a normalization constant and α is called the "exponent" of the Gaussian. The x, y, and z are cartesian coordinates. The l, m, and n are not quantum numbers, but simply integral exponents at cartesian coordinates $r^2 = x^2 + y^2 + z^2$. GTOs are simpler functions which are also referred to as gaussian primitives (Labanowski, 1996).

Gaussian primitives are usually obtained from quantum calculations on atoms. Typically, the exponents are varied until the lowest total energy of the atom is achieved. In some cases, the exponents are optimized independently. In others, the exponents are related to each other by some equation, and parameters in this equation are optimized. The primitives so derived describe isolated atoms and cannot accurately describe deformations of atomic orbitals brought by the presence of other atoms in the molecule. Basis sets for molecular calculations are therefore frequently augmented with other functions of which the most popular are the polarization and diffuse functions.

For molecular calculations, the gaussian primitives have to be contracted, i.e., certain linear combinations of them will be used as basis functions. The term contraction means "a linear combination of gaussian primitives to be used as a basis function". Such a basis function will have its coefficients and exponents fixed. The contractions are sometimes called Contracted Gaussian Type Orbitals (CGTO). The notations that are used to specify the number of primitives and contractions explicitly are the parentheses, i.e. ( ), and the square brackets, i.e. [ ]. The parentheses embrace the number of primitives that are given in the order of angular momentum quantum number, whereas the square brackets are used to specify the number of resulting contractions. When specifying structure of the basis sets for the entire molecule, slashes, i.e /, are used to separate information for different atoms. The information is given starting from the heaviest atoms (Labanowski, 1996).

There are different types of basis sets ranging from the minimal basis sets to the more extended basis sets. Some of the basis sets commonly used in electronic structure calculations are discussed below.

Minimal basis sets

The minimal basis set is the smallest possible set, i.e., it contains only one function per occupied atomic orbital. The most popular minimal basis sets are the STO-nG, where n denotes the number of primitives in the contraction. These sets were obtained by least square fit of the combination of n gaussian functions to a Slater type orbital of the same type with zeta = 1.0 (Labanowski, 1996).

Perhaps the most widely used minimal basis set of all time is the STO-3G minimal basis developed by Pople and co-workers. The main attraction of this basis, other than its small size, is its effectiveness in predicting geometries (Davidson & Feller, 1986). Minimal basis sets do not adequately describe non-spherical (anisotropic) electron distribution in molecules (as in polar covalent bonds) (*Session 2*, 2008).

Split-valence (SV) or Pople basis sets

Valence orbitals of atoms are more affected by bond formation than the inner (core) orbitals. Consequently, more basis functions are assigned to describe the valence orbitals. This prompted the development of split-valence (SV) or Pople's basis sets, i.e., basis sets in which more contractions are used to describe valence orbitals than core orbitals. The notation that is used for SV basis sets is n-ijG (or n-ijkG), where n is the number of sp-type inner shell primitive GTOs, i is the number of inner valence s- and p-type primitive GTOs and j is the number of outer valence s- and p-type primitive GTOs (Labanowski, 1996; *Session 2*, 2008).

Examples: **4-21G and 3-21G.** These "split valence" basis sets were a compromise between the speed obtainable using the STO-3G basis set and the accuracy of larger, slower basis sets. The 4-21G basis set represents the (421,21)/(21) split, or (7s,3p/3s) → [3s,2p/2s] contraction and it was designed for efficient use in geometry optimizations which utilize analytical gradients. The 3-21G basis sets represent the (321,21)/(21) split, or (6s,3p/3s) → [3s,2p/2s] contraction and they have been constructed for first and second-row elements of the periodic table (Davidson & Feller, 1986).

4-31G, 5-31G, and 6-31G. By increasing the number of primitives devoted to the core and first valence function, the 4-31G, 5-31G, and 6-31G bases improve upon 3-21G energetics at the expense of increased computer times. The 6-31G basis set represents the (631,31)/(31) split, or (10s,4p/4s) → [3s,2p/2s] contraction. SV basis sets were developed to overcome problems of inadequate description of anisotropic electron distributions using minimal basis sets (size is adjusted) (Davidson & Feller, 1986; *Session 2*, 2008).

Polarization functions

The polarization functions are simply functions having higher values of angular momentum than those present in occupied atomic orbitals for the corresponding atom. The polarization functions are important for reproducing chemical bonding (Labanowski, 1996). Polarization functions are functions that are used to describe the polarization (distortion) of atomic orbitals (AOs) in molecular orbitals (MOs) as the AOs become distorted in shape when a molecule is formed (Archibong, 2007). They were frequently derived from optimizing exponents for a set of molecules (Labanowski, 1996). Polarization functions are required at least for the heavier elements, because of the electric field that is polarizing the calculated AOs in the non-spherical MO environment (Drees, 2008).

Augmenting Pople's basis sets with d type and f type polarization functions adds 5 (or 6) and 7 (or 10) basis functions on heavy atoms, respectively. This is denoted as n-ijG* (or n-ijkG*) which is synonymous to n-ijG(d) (or n-ijkG(d)). Polarization

functions can also be added on all atoms. In this case, d type and f type polarization functions will be added on heavy atoms, whereas p type polarization functions will be added on hydrogen atoms. This is denoted as n-ijG** or n-ijkG** which is synonymous to n-ijG(d,p) (or n-ijkG(d,p)) (Labanowski, 1996).

Examples: **6-31G*** (or 6-31G(d)) **and 6-31G**** (or 6-31G(d,p))**.** Adding all six components of a Cartesian d function to the 6-31G basis set for first-row atoms gives the 6-31G* basis. Further addition of p functions to hydrogen results in the 6-31G** basis. The 6-31G* (or 6-31G(d)) basis set represents the (631,31,1)/(31) split, or (10s,4p,1d/4s) → [3s,2p,1d/2s] contraction and it is available for the first- and second-row atoms (Davidson & Feller, 1986).

6-31lG.** All previously described Pople basis sets have been optimized at the Hartree-Fock level. These sets are somewhat deficient for use in post-HF calculations, so a 6-311G** basis (single zeta core, triple zeta valence, and polarization functions on all atoms) was developed which performs better at the MP2 level. The 6-311G** (or 6-311G(d,p)) basis set would involve the following contractions: (6311,311,1)/(311,1) or (11s,5p,1d/5s,1p) → [4s,3p,1d/3s,1p] (Davidson & Feller, 1986).

Diffuse functions

Diffuse functions have very small exponents and decay slowly with distance from the nucleus (Labanowski, 1996). Diffuse functions are functions that are used to describe the outer part (peripheral) of a system (Archibong, 2007). Diffuse gaussians are usually of s and p type, however sometimes diffuse polarization functions are also used.

Diffuse functions are necessary for correct description of anions and weak bonds (e.g. hydrogen bonds) and are frequently used for calculations of properties (e.g. dipole moments, polarizabilities, etc.). For the Pople's basis sets the following notation is used: n-ij+G (or n-ijk+G) when 1 diffuse s-type and p-type gaussian with the same exponents are added to a standard basis set on heavy atoms. The n-ij++G (or n-ijk++G) are obtained by adding 1 diffuse s-type and p-type gaussian on heavy atoms and 1 diffuse s-type gaussian on hydrogens.

Example: **6-31+G**. The 6-31+G basis set represents the (6311,311)/(31) split or (11s,5p/4s) → [4s,3p/2s] contraction (Labanowski, 1996).

More Extended Pople Basis Sets

If accuracy beyond that obtainable with the 6-311G** basis is desired, more flexibility must be introduced into the polarization space. The set must also be supplemented with diffuse functions for description of anions. With these goals in mind Pople and co-workers have developed several basis sets, the largest of which goes by the unwieldy name of 6-311++G(3df,3pd). The "++" indicates that there are additional diffuse functions on all atoms. The "3df" means that three 5-component d functions and one 7-component f function are included on all first-row atoms. The "3pd" means three p functions and one d function are included on hydrogen (Davidson & Feller, 1986).

Example: **6-311++G(3df,3pd).** The 6-311++G(3df,3pd) basis set represents the (63111,3111,111,1)/(3111,111,1) split, or (12s,6p,3d,1f/6s,3p,1d) → [5s,4p,3d,1f/4s,3p,1d] contraction (Labanowski, 1996).

2.4 Computational Methods

A functional by definition is a function of a function. Exchange-correlation functionals, denoted as E_{xc}, account for the difference between the so-called classical and quantum mechanical electron-electron repulsion and they also include the difference in kinetic energy between the fictitious non-interacting system and the real system (Cramer, 2004).

The exchange (or Fermi) correlation is as a result of the probability of finding two electrons with the same spin at the same point in space being exactly zero. Electrons of like spin thus do not move independently from each other. Exchange correlation is in no way connected to the charge of the electrons, but it is a direct consequence of the Pauli Exclusion principle. The Coulomb correlation is as a result of the charge of the electrons. The electrostatic repulsion prevents the electrons from coming too close to each other. This effect is, of course, independent of the spin of the electrons and it is simply referred to as the electron correlation (Koch & Holthausen, 2000).

Different types of E_{xc} have been developed over the years. These include local density approximation (LDA), local spin-density approximation (LSD), generalized gradient approximation (GGA) and Hybrid or adiabatic connection method (ACM) functional.

In the LDA, the functional depends only on the density of the coordinate where the functional is evaluated. When the E_{xc} is written in the following form, i.e. E_{xc}^{LDA}, it defines the LDA:

$$E_{xc}^{LDA}[\rho] = \int \rho(\mathbf{r})\varepsilon_{xc}\big(\rho(\mathbf{r})\big)\,d\mathbf{r} \qquad \text{Eqn (8)}$$

In equation (8), $\varepsilon_{xc}(\rho(\mathbf{r}))$ is the exchange-correlation energy per particle, i.e. the so-called 'energy density' and $\rho(\mathbf{r})$ is the electron density. The quantity $\varepsilon_{xc}(\rho(\mathbf{r}))$ can be further split into exchange, $\varepsilon_x(\rho(\mathbf{r}))$, and the correlation, $\varepsilon_c(\rho(\mathbf{r}))$, contributions:

$$\varepsilon_{xc}(\rho(\mathbf{r})) = \varepsilon_x(\rho(\mathbf{r})) + \varepsilon_c(\rho(\mathbf{r})) \qquad \text{Eqn (9)}$$

The ε_x part was originally derived by Bloch and Dirac in the late 1920's:

$$\varepsilon_x = -\frac{3}{4}\sqrt[3]{\frac{3\rho(\mathbf{r})}{\pi}} \qquad \text{Eqn (10)}$$

This exchange functional is frequently called Slater exchange and is abbreviated by S. No such explicit expression is known for the correlation part, ε_c**.** The most widely used representations of ε_c are the ones developed by Vosko, Wilk, and Nusair (in 1980) abbreviated as VWN and the most recent one has been given by Perdew and Wang (in 1992). There are two variants or forms of the VWN, i.e. VWN3 and VWN5. The LDA functional have been derived from the analysis of the uniform electron gas (where the density has the same value at every position).

The LSD is a straightforward generalization of the LDA to include electron spin (e.g. open-shell systems). When the E_{xc} is written in the following form, i.e. E_{xc}^{LSD}, it defines the LSD:

$$E_{xc}^{LSD}[\rho_\alpha, \rho_\beta] = \int \rho(\mathbf{r})\varepsilon_{xc}\left(\rho_\alpha(\mathbf{r}), \rho_\beta(\mathbf{r})\right)\,d\mathbf{r} \qquad \text{Eqn (11)}$$

In equation (11), the subscripts α and β represent electrons, $\rho_\alpha(\mathbf{r})$ and $\rho_\beta(\mathbf{r})$ are the spin densities of the α and β electrons, respectively, with $\rho_\alpha(\mathbf{r}) + \rho_\beta(\mathbf{r}) = \rho(\mathbf{r})$. LSD

calculations that employ a combination of Slater exchange and the VWN correlation energy expression are sometimes referred to as using the SVWN method.

The only moderate accuracy that the local (spin) density approximation delivers is certainly insufficient for most applications in chemistry. Moreover, in a molecular system, the electron density is typically rather far from spatially uniform, so there is good reason to believe that the LDA or LSD approach will have limitations. One obvious way to improve the correlation functional is to make it depend not only on the local value of the density, but on the extent to which the density is locally changing, i.e. the gradient of the density. The more common term in modern nomenclature for a functional that depends on both the density and the gradient of the density is 'gradient-corrected'. Including a gradient correction defines the 'generalized gradient approximation' or GGA. The GGA is defined with the E_{xc} written as shown in equation 12:

$$E_{xc}^{GGA}[\rho_\alpha, \rho_\beta] = \int f(\rho_\alpha, \rho_\beta, \nabla\rho_\alpha, \nabla\rho_\beta)\, d\mathbf{r} \qquad \text{Eqn (12)}$$

In equation (12), f is the integrand which depends on the densities and their gradients, $\nabla\rho_\alpha$ and $\nabla\rho_\beta$ are the gradients of the charge densities of the α and β electrons, respectively. In practice, the E_{xc}^{GGA} is usually split into its exchange, E_x^{GGA}, and the correlation, E_c^{GGA}, contributions:

$$E_{xc}^{GGA} = E_x^{GGA} + E_c^{GGA} \qquad \text{Eqn (13)}$$

The first widely popular class of GGA exchange functional was developed by Becke (in 1986). Usually abbreviated simply as 'B', this functional adopts a mathematical form

that has correct asymptotic behavior at long range for the energy density, and it further incorporates a single empirical parameter the value of which was optimized by fitting to the exactly known exchange energies of the six noble gas atoms He through Rn. Other exchange functionals similar to the Becke example in one way or another have appeared, including CAM(A) and CAM(B) functional developed by Handy and co-workers (in 1993), FT97 functional developed by Filatov and Thiel (in 1997), and the PW91 exchange functional (Perdew (in 1991), and Burke, Perdew, and Wang (in 1998)) (Cramer, 2004; Koch & Holthausen, 2000).

The second class of GGA exchange functionals have been developed based on rational function expansions of the reduced gradient. These functionals which contain no empirically optimized parameters, include early functionals by Becke in 1986 (B86) and Perdew in 1986 (P), the functional by Lacks and Gordon in 1993 (LG) or the recent implementation of Perdew, Burke, and Ernzerhof in 1996 (PBE).

Among the most widely used gradient-corrected correlation functional is the correlation counterpart of the 1986 Perdew exchange functional, usually termed P (or P86). This functional employs an empirical parameter, which was fitted to the correlation energy of the Ne atom. A few years later Perdew and Wang (in 1991), refined their correlation functional, leading to the parameter free PW91. Another, nowadays even more popular correlation functional is due to Lee, Yang, and Parr, 1988 (LYP). Unlike all the functionals mentioned so far, LYP is not based on the uniform electron gas, but is derived from an expression for the correlation energy of the He atom

based on an accurate, correlated wave function presented in the context of wave function based theory by Colle and Salvetti in 1975 (Cramer, 2004).

In principle, each exchange functional could be combined with any of the correlation functionals, but only a few combinations are currently in use. The exchange part is almost exclusively chosen to be Becke's functional which is either combined with Perdew's 1986 correlation functional or the Lee, Yang, Parr one - levels usually abbreviated as BP86 and BLYP, respectively.

Functionals where a certain amount of exact exchange from Hartree-Fock (HF) theory is incorporated to the exchange-correlation energy functional in DFT are frequently called DFT/HF hybrid functionals. They are also referred to as adiabatic connection method (ACM) functionals. This highly relieves the difficulties in expressing the exchange part of the energy. The expression for a hybrid functional is written as follows:

$$\mathrm{E_{xc}} = (1-a)\mathrm{E_{xc}^{DFT}} + a\mathrm{E_{x}^{HF}} \qquad \text{Eqn (14)}$$

In equation (14), *a* is an unknown variable. If one is forced to estimate a constant like *a*, one might just as well choose a value that maximizes the utility of the method. And one may legitimately ask whether inclusion of additional empirical parameters results in sufficient improvement to make such inclusion worthwhile. Becke was the first to do this, developing the 3-parameter functional expression:

$$\mathrm{E_{xc}^{B3PW91}} = (1-a)\mathrm{E_{x}^{LSD}} + a\mathrm{E_{x}^{HF}} + b\mathrm{E_{x}^{B}} + \mathrm{E_{c}^{LSD}} + c\mathrm{E_{c}^{PW91}} \qquad \text{Eqn (15)}$$

In equation (15), *a*, *b* and *c* were optimized to 0.20, 0.72 and 0.81, respectively. The name of the functional, B3PW91, implies its use of a three-parameter scheme, as well as the GGA exchange and correlation functional B and PW91, respectively.

Subsequently, Stevens et al. modified this functional to use LYP instead of PW91. Because LYP is designed to compute the full correlation energy and not a correlation to LSD, the B3LYP model is defined by equation (16):

$$E_{xc}^{B3LYP} = (1-a)E_x^{LSD} + aE_x^{HF} + bE_x^{B} + (1-c)E_c^{LSD} + cE_c^{LYP} \quad \text{Eqn (16)}$$

where *a*, *b* and *c* have the same values as in B3PW91 (Cramer, 2004; Koch & Holthausen, 2000).

2.5 Data Analysis

Calculating Thermochemical Parameters

The basic equations used to calculate thermochemical quantities are based on those given in standard texts on thermodynamics. The thermochemical parameters result from the interactions of large collections of like molecules. In other words, the results of a calculation performed on a single molecule need to be related to the macroscopic properties, such as enthalpy (H), entropy (S), and Gibbs free energy (G). Statistical mechanics relates the microscopic calculations to the macroscopic properties of interest through the molecular partition function, *q*. For a single molecule, *q* is the sum of exponential terms involving all possible quantum energy states ε_i (Gotwals & Sendlinger, 2007; Ochterski, 2000).

$$q = \sum_i^{all\ states} e^{-\varepsilon_i/k_B T} \qquad \text{Eqn (17)}$$

In equation (17), k_B is the Boltzmann constant and T is the temperature in Kelvin. Once the molecular partition function (q) is known, the partition function (Q) for N identical molecules can easily be found via equation (18) (Gotwals & Sendlinger, 2007):

$$Q = {q^N}/{N!} \qquad \text{Eqn (18)}$$

Once the partition function Q is found, a number of thermochemical parameters and macroscopic observables can be calculated. Using Q, the thermochemical parameters H, S, and G are obtained as follows (Gotwals & Sendlinger, 2007):

$$H = U + PV = k_B T^2 \left(\frac{\partial \ln Q}{\partial T}\right)_V + k_B TV \left(\frac{\partial \ln Q}{\partial V}\right)_T \qquad \text{Eqn (19)}$$

$$S = \frac{H - G}{T} = k_B T \left(\frac{\partial \ln Q}{\partial T}\right)_V + k_B \ln Q \qquad \text{Eqn (20)}$$

$$G = H - TS = k_B TV \left(\frac{\partial \ln Q}{\partial V}\right)_T - k_B T \ln Q \qquad \text{Eqn (21)}$$

where U is the internal energy,

P is the pressure,

V is the volume and

T is the temperature (default is 298.15 K).

The vibrational partition function depends on the frequencies, necessitating calculation of the harmonic vibrational frequencies of optimized structures. For

electronic contributions to the partition function, it is assumed that the first and all higher states are inaccessible at the temperature the calculation is done. The data generated by the Gaussian program were used to calculate heats and free energies of reactions as well as absolute rate information (Ochterski, 2000). For example, the standard enthalpy, ΔH_r^o, and the Gibbs free energy, ΔG_r^o, of a reaction will be calculated using equations (22) and (23), respectively (Ochterski, 2000):

$$\Delta H_r^o = \sum(E_o + H_{corr})_{products} - \sum(E_o + H_{corr})_{reactants} \quad \text{Eqn (22)}$$

$$\Delta G_r^o = \sum(E_o + G_{corr})_{products} - \sum(E_o + G_{corr})_{reactants} \quad \text{Eqn (23)}$$

where E_o is the total electronic energy,

H_{corr} is the correction to the enthalpy due to internal energy and

G_{corr} is the correction to the Gibbs free energy due to internal energy.

The quantities E_o, H_{corr} and G_{corr} will be obtained from the Thermochemistry section of the Gaussian output file after the frequency calculations are done. The entropy of a reaction, $\Delta S_r°$, will be calculated using $\Delta S_r° = (\Delta H°_r - \Delta G°_r)/T$ (Ochterski, 2000). The calculations that will be carried out to obtain ΔH_r^o, ΔG_r^o and $\Delta S_r°$ will be done using MS Excel.

CHAPTER 3

MATERIALS AND METHODS

3.1 Substances studied

Computational studies were done on POZs derived from the conformers of chlorophenol, dihydroxybenzene and hydroxythiophenol. The names and representative structures of the compounds from which the POZs investigated in this work were derived are given in Table 1.

Table 1 Names and representative structures of the compounds from which the POZs investigated in this work were derived.

Name of compound	Representative structure
Chlorophenol	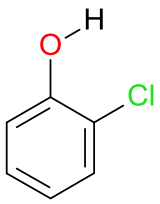
Dihydroxybenzene	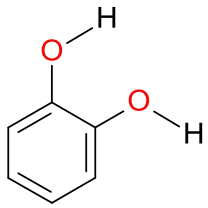
Hydroxythiophenol	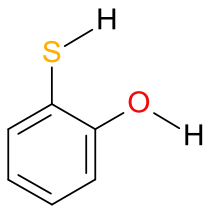

3.2 Computational methods utilized

Geometry optimizations were performed with the hybrid B3LYP functional. Initial optimizations employed the 6-31G* basis set and subsequent refinement of the geometries were done with the 6-31G** and 6-311+G(2df) basis sets. The convergence criteria for optimizations are as follows: After each iteration of the geometry optimization, the output file contains a summary of the current stage of the optimization. The first two lines of the summary contain the maximum remaining force on an atom in the system as well as the average (RMS, root mean square) force on all the atoms. Together with the actual value for the current structure appears the threshold value. The third and fourth convergence criteria are the maximum displacement, that is, the maximum structural change of one coordinate as well as the average (RMS) change over all structural parameters in the last two iterations. Once the current values of all four criteria fall below the threshold, the optimization is complete (*Electronic Structure calculations*, n.d.).

All stationary points were then characterized by frequency calculations. Energies corrected for harmonic zero-point vibrations ΔE_{zpe}, and enthalpies ΔH, and Gibbs free energies ΔG, at 298 K and 1 atm. from ideal-gas partition functions based on the rigid rotor, harmonic oscillator model were computed at the B3LYP/6-31G(d), B3LYP/6-31G(d,p) and B3LYP/6-311+G(2df) levels. The transition states were located with the reactants supplied as input. All the calculations were carried out with the Gaussian 03 suite of programs.

CHAPTER 4

RESULTS AND DISCUSSION

The addition of ozone to phenol/thiophenol can occur in many ways, but from calculations that were done on benzene by Hendrickx and Vinckier (2003) it follows that the most stable structures of the POZ are those for which the cycloaddition takes place at two neighbouring carbon atoms of the aryl ring. Our research was also confined to this type of POZs only. In this case the incoming ozone can attach at three (3) distinct places as is shown in Figure 5: an addition at positions 1 and 2, at positions 2 and 3, or at positions 3 and 4. In the following we will describe these three addition paths as modes I, II and III, respectively, i.e. we will follow the same nomenclature in naming our POZs as that that was used by Hendrickx and Vinckier (2003). Alternatively, the aforementioned modes will also be referred to as 1,2-, 2,3- or 3,4-addition, respectively.

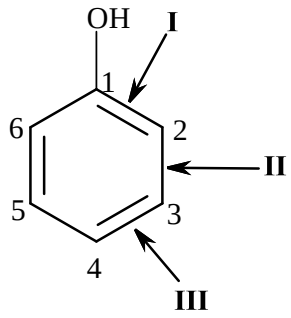

Figure 5 1,3-Cycloaddition of ozone on phenol/thiophenol: schematic representation of the three modes of addition.

4.1 Minima of conformers studied: Best 5 isomers per group and globally

4.1.1 Chlorophenol POZs

The naming of the chlorophenol POZs was done in the following way:

The first digit or number in the name refers to the position of the carbon atom to which the substituent, Cℓ (i.e. the chlorine atom in this case), is attached to the parent compound (phenol). The same numbering as in Figure 5 is used to number the carbon ring of the parent compound. The H (standing for hydrogen) refers to the hydrogen atom of the hydroxyl group of the parent compound (phenol). If the H is preceded by an *endo*- prefix, it means that the hydrogen atom is oriented towards the ozone moiety of the POZ and if the H is preceded by an *exo*- prefix, it means that the hydrogen atom is oriented away from the ozone moiety of the POZ. The O (standing for oxygen) refers to the middle oxygen atom of the ozone moiety of the POZ. If the O is preceded by an *endo*- prefix, it means that the middle oxygen atom is oriented towards the aryl ring and if O is preceded by an *exo*- prefix, it means that the middle oxygen atom is oriented away from the aryl ring. The last two digits before poz refer to the mode of addition of ozone to the aryl ring according to Figure 5. For example, the name 2_Cℓ_*endo*_H_*exo*_O_1,2_poz means the following:

2_Cℓ: means the chlorine atom is attached to carbon number 2 in the aryl ring of phenol,

*endo*_H: means the hydrogen atom of the hydroxyl group of phenol is oriented towards the ozone moiety of the POZ,

*exo*_O: means that the middle oxygen atom of the ozone moiety is oriented away from the aryl ring, and

1,2_poz: means that the addition of the incoming ozone will be on carbons number 1 and 2 on the phenol, i.e. a 1,2-addition or mode I type of addition.

4.1.1.1 The 1,2-POZs of chlorophenol

The table below shows the relative energies and thermochemical properties of the minima of the five (5) most stable products of chlorophenol 1,2-POZs that are expected to be formed from the reaction between ozone and chlorophenol at the B3LYP/6-31G(d) level of theory.

Table 2 Relative energies and thermochemical properties of the minima of the five (5) most stable chlorophenol 1,2-POZs at the B3LYP/6-31G(d) level.

Chlorophenol 1,2-POZs	**Relative Energies and Thermochemical Properties**				
	ΔE^{el}	$\Delta E^{el} + ZPE$	ΔH_r^o	ΔG_r^o	ΔS_{univ}
B3LYP/6-31G(d) level	**(kcal/mol)**				**(kcal/mol.K)**
Ozone + Chlorophenol	0.0	0.0	0.0	0.0	0.0000
2_Cℓ_*endo*_H_*exo*_O_1,2_poz	-26.6	-24.6	-25.4	-12.2	0.0410
6_Cℓ_*exo*_H_*exo*_O_1,2_poz	-26.0	-23.3	-24.2	-10.9	0.0367
4_Cℓ_*endo*_H_*exo*_O_1,2_poz	-25.6	-23.3	-24.1	-11.2	0.0376
4_Cℓ_*exo*_H_*exo*_O_1,2_poz	-25.7	-23.2	-24.1	-11.0	0.0370
5_Cℓ_*exo*_H_*exo*_O_1,2_poz	-25.6	-23.2	-24.0	-11.0	0.0369

The most stable structure of the 1,2-POZs of chlorophenol at the B3LYP/6-31G(d) level of theory was found to be 2-Cℓ-*endo*-H-*exo*-O-1,2-poz. At the B3LYP/6-31G(d) level, the energy difference ($\Delta E^{el} + ZPE$) between the reactants, i.e. ozone and 2-chlorophenol, and 2-Cℓ-*endo*-H-*exo*-O-1,2-poz, is 24.6 kcal/mol. The results in Table 2 indicate that 2-Cℓ-*endo*-H-*exo*-O-1,2-poz is positioned energetically way below the

reactants than any of the other structures in that table. The energy ordering of the different isomers is depicted in Figure 6 below. A similar trend in energy ordering is obtained at the 6-31G(d,p) level.

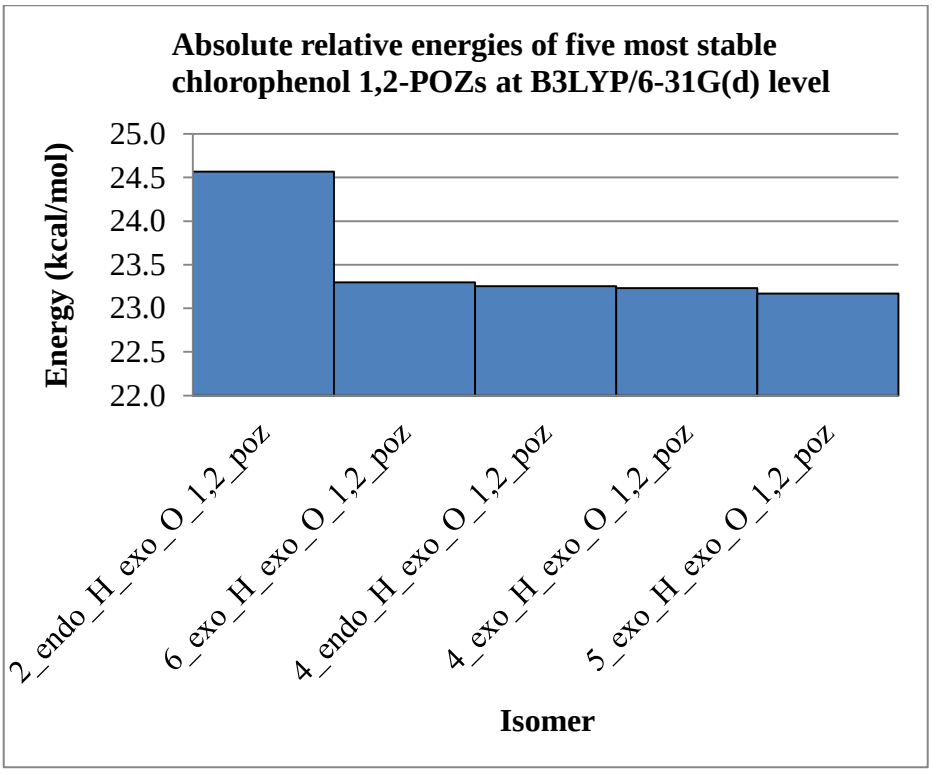

Figure 6 Absolute relative electronic energies (+ZPE) of the five (5) most stable chlorophenol 1,2-POZs at the B3LYP/6-31G(d) level.

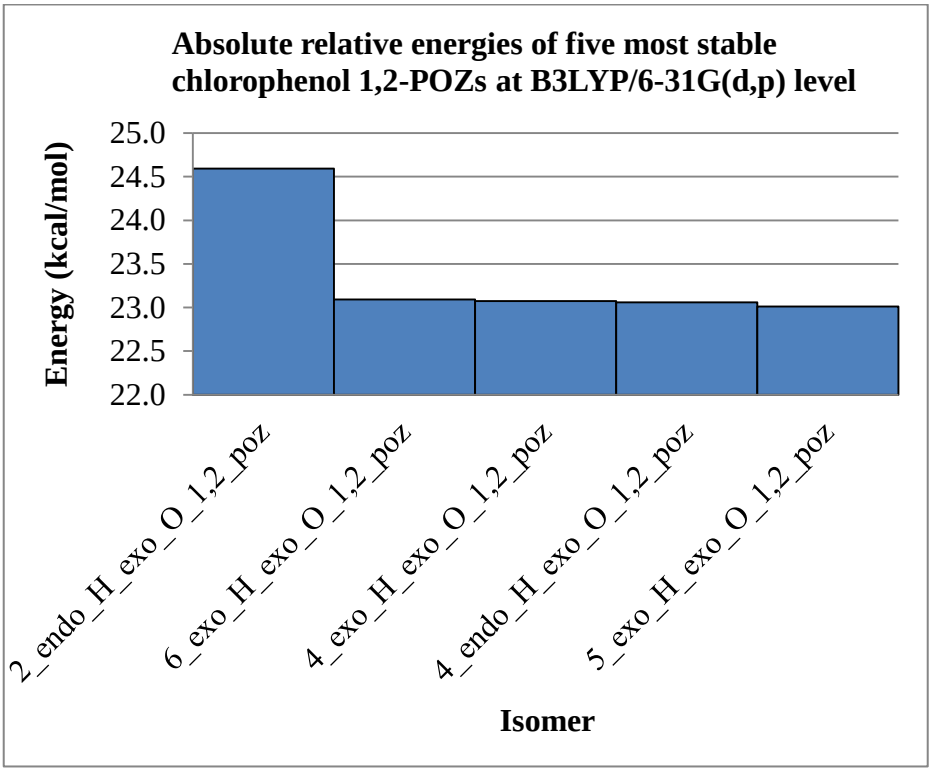

Figure 7 Absolute relative electronic energies (+ZPE) of the five (5) most stable chlorophenol 1,2-POZs at the B3LYP/6-31G(d,p) level.

The enthalpy of the reaction, ΔH_r^o, of the most stable structure of 1,2-POZs of chlorophenol at the B3LYP/6-31G(d) level is -25.4 kcal/mol. The result shows that the reaction is more exothermic than any other reaction in Table 2. For this reaction the Gibbs Free energy, ΔG_r^o, of -12.2 kcal/mol is the lowest value and the negative sign means that the reaction will be the most spontaneous at 298.15 K than any of the other reactions in Table 2. The corresponding total entropy of the system and its surroundings, ΔS_{univ}, for the reaction resulting in the most stable structure of the 1,2-POZs of chlorophenol at the B3LYP/6-31G(d) level was calculated as 0.0410 kcal/mol.K. Since this is the most positive quantity, it implies that the reaction will be the most

spontaneous at 298.15 K (Chang, 1998). This is just a confirmation of what was deduced from the Gibbs Free energy of the reaction.

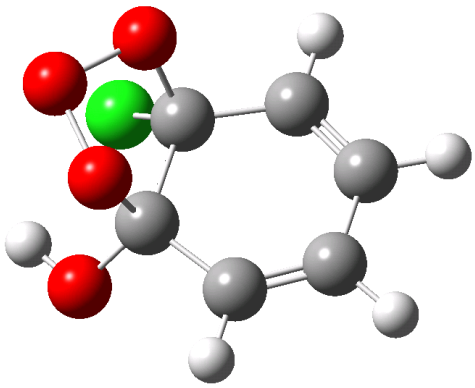

Figure 8 Structure of 2-Cℓ-*endo*-H-*exo*-O-1,2-poz.

4.1.1.2 The 2,3-POZs of chlorophenol

The table below shows the relative energies and thermochemical properties of the minima of the five (5) most stable products of chlorophenol 2,3-POZs that are expected to form from the reaction between ozone and chlorophenol at the B3LYP/6-31G(d) level of theory.

Table 3 Relative energies and thermochemical properties of the minima of the five (5) most stable chlorophenol 2,3-POZs at the B3LYP/6-31G(d) level.

Chlorophenol 2,3-POZs	**Relative Energies and Thermochemical Properties**				
	ΔE^{el}	ΔE^{el} + ZPE	ΔH_r^o	ΔG_r^o	ΔS_{univ}
B3LYP/6-31G(d) level	**(kcal/mol)**				**(kcal/mol.K)**
Ozone + Chlorophenol	0.0	0.0	0.0	0.0	0.0000
2_Cℓ_*endo*_H_*exo*_O_2,3_poz	-25.9	-23.4	-24.2	-11.1	0.0373
3_Cℓ_*endo*_H_*exo*_O_2,3_poz	-25.3	-22.8	-23.6	-10.7	0.0359
5_Cℓ_*endo*_H_*exo*_O_2,3_poz	-25.0	-22.1	-23.0	-9.9	0.0332
2_Cℓ_*exo*_H_*exo*_O_2,3_poz	-24.2	-21.6	-22.4	-9.2	0.0307
6_Cℓ_*exo*_H_*endo*_O_2,3_poz	-24.6	-21.5	-22.4	-9.5	0.0318

The most stable structure of the 2,3-POZs of chlorophenol at the B3LYP/6-31G(d) level of theory was found to be 2-Cℓ-*endo*-H-*exo*-O-2,3-poz. At the B3LYP/6-31G(d) level, the energy difference ($\Delta E^{el} + ZPE$) between the reactants, i.e. ozone and 2-chlorophenol, and 2-Cℓ-*endo*-H-*exo*-O-2,3-poz, is 23.4 kcal/mol. The results in Table 3 indicate that 2-Cℓ-*endo*-H-*exo*-O-2,3-poz is positioned energetically way below the reactants than any of the other structures in that table. The energy ordering of the different isomers is depicted in Figure 9 below. A similar trend in energy ordering is obtained at the 6-31G(d,p) level.

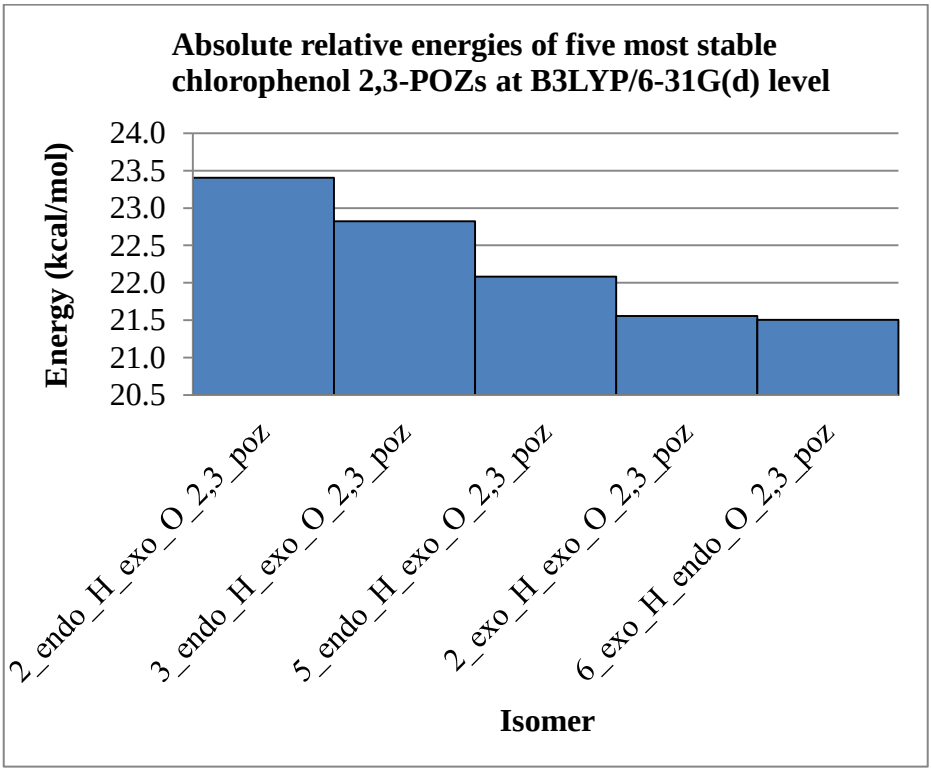

Figure 9 Absolute relative electronic energies (+ZPE) of the five (5) most stable chlorophenol 2,3-POZs at the B3LYP/6-31G(d) level.

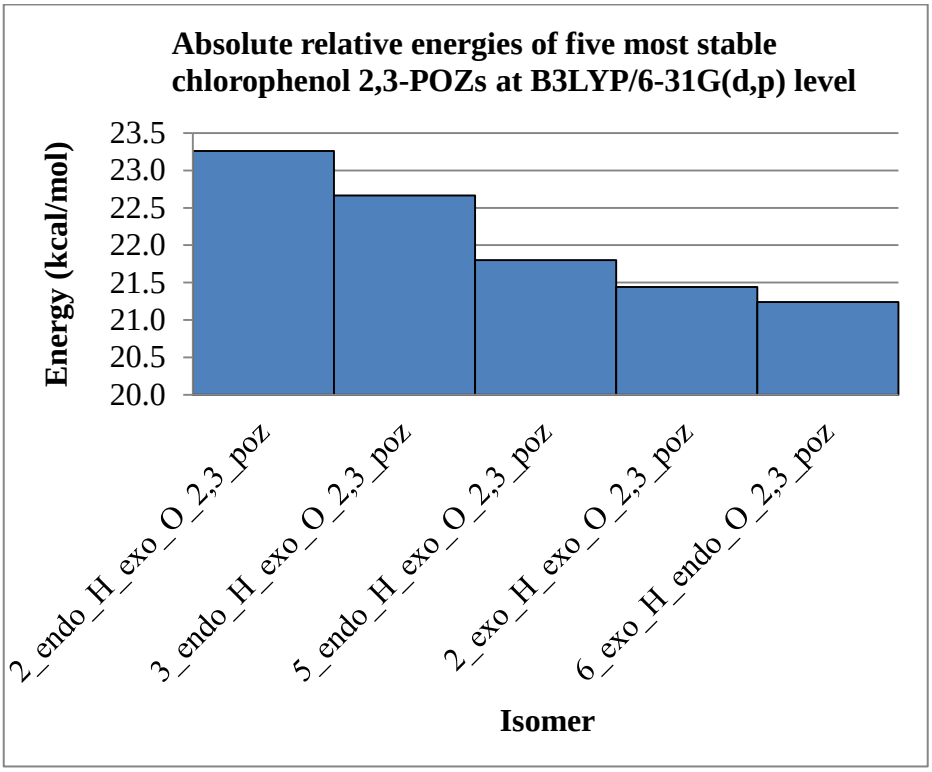

Figure 10 Absolute relative electronic energies (+ZPE) of the five (5) most stable chlorophenol 2,3-POZs at the B3LYP/6-31G(d,p) level.

The enthalpy of the reaction, ΔH_r^o, of the most stable structure of 2,3-POZs of chlorophenol at the B3LYP/6-31G(d) level is -24.2 kcal/mol. The result shows that the reaction is more exothermic than any other reaction in Table 3. For this reaction the Gibbs Free energy, ΔG_r^o, of -11.1 kcal/mol is the lowest value and the negative sign means that the reaction will be the most spontaneous at 298.15 K than any of the other reactions in Table 3. The corresponding total entropy of the system and its surroundings, ΔS_{univ}, for the reaction resulting in the most stable structure of the 2,3-POZs of chlorophenol at the B3LYP/6-31G(d) level was calculated as 0.0373 kcal/mol.K. Since this is the most positive quantity, it implies that the reaction will be the most

spontaneous at 298.15 K (Chang, 1998). This is just a confirmation of what was deduced from the Gibbs Free energy of the reaction.

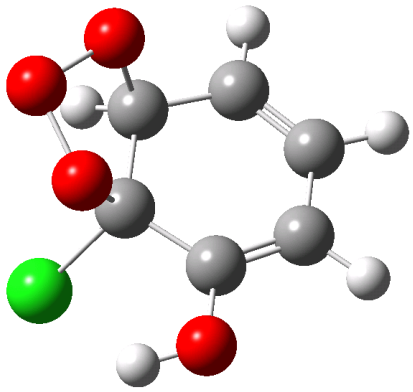

Figure 11 Structure of 2-Cℓ-*endo*-H-*exo*-O-2,3-poz.

4.1.1.3 The 3,4-POZs of chlorophenol

The table below shows the relative energies and thermochemical properties of the minima of the five (5) most stable products of chlorophenol 3,4-POZs that are expected to be formed from the reaction between ozone and chlorophenol at the B3LYP/6-31G(d) level of theory.

Table 4 Relative energies and thermochemical properties of the minima of the five (5) most stable chlorophenol 3,4-POZs at the B3LYP/6-31G(d) level.

Chlorophenol 3,4-POZs	**Relative Energies and Thermochemical Properties**				
B3LYP/6-31G(d) level	ΔE^{el}	ΔE^{el} + *ZPE*	ΔH_r^o	ΔG_r^o	ΔS_{univ}
	(kcal/mol)				**(kcal/mol.K)**
Ozone + Chlorophenol	0.0	0.0	0.0	0.0	0.0000
4_Cℓ_*endo*_H_*exo*_O_3,4_poz	-27.3	-24.6	-25.5	-12.3	0.0413
3_Cℓ_*endo*_H_*exo*_O_3,4_poz	-26.8	-24.2	-25.1	-12.0	0.0402
4_Cℓ_*exo*_H_*exo*_O_3,4_poz	-25.1	-22.7	-23.5	-10.5	0.0353
2_Cℓ_*endo*_H_*endo*_O_3,4_poz	-25.4	-22.2	-23.1	-10.1	0.0340
3_Cℓ_*exo*_H_*exo*_O_3,4_poz	-24.3	-22.0	-22.7	-9.9	0.0333

The most stable structure of the 3,4-POZs of chlorophenol at the B3LYP/6-31G(d) level of theory was found to be 4-Cℓ-*endo*-H-*exo*-O-3,4-poz. At the B3LYP/6-31G(d) level, the energy difference ($\Delta E^{el} + ZPE$) between the reactants, i.e. ozone and 4-chlorophenol, and 4-Cℓ-*endo*-H-*exo*-O-3,4-poz, is 24.6 kcal/mol. The results in Table 4 indicate that 4-Cℓ-*endo*-H-*exo*-O-3,4-poz is positioned energetically below the reactants than any of the other structures in that table. The energy ordering of the different isomers is depicted in Figure 12 below. A similar trend in energy ordering is obtained at the 6-31G(d,p) level.

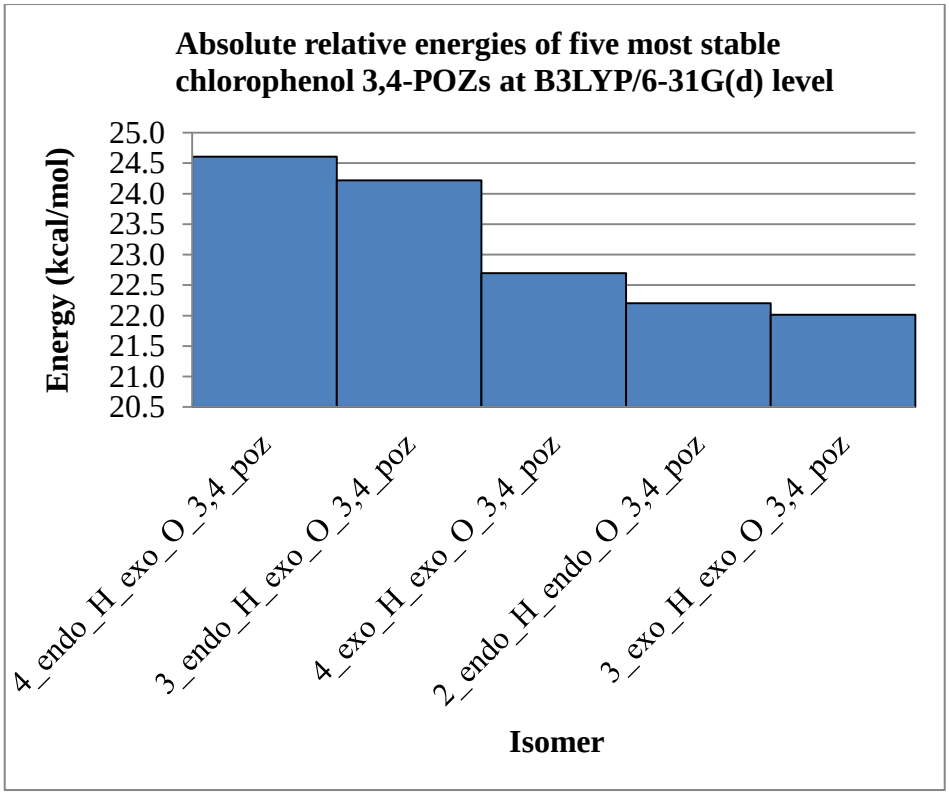

Figure 12 Absolute relative electronic energies (+ZPE) of the five (5) most stable chlorophenol 3,4-POZs at the B3LYP/6-31G(d) level.

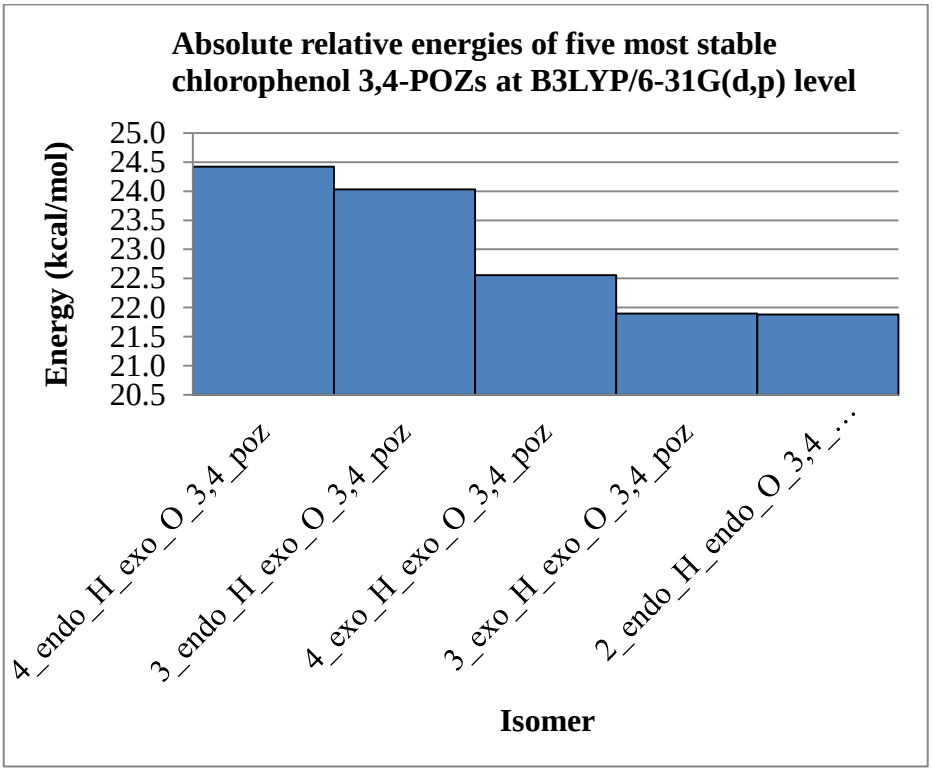

Figure 13 Absolute relative electronic energies (+ZPE) of the five (5) most stable chlorophenol 3,4-POZs at the B3LYP/6-31G(d,p) level.

The enthalpy of the reaction, ΔH_r^o, of the most stable structure of 3,4-POZs of chlorophenol at the B3LYP/6-31G(d) level is -25.5 kcal/mol. The result shows that the reaction is more exothermic than any other reaction in Table 4. For this reaction the Gibbs Free energy, ΔG_r^o, of -12.3 kcal/mol is the lowest value and the negative sign means that the reaction will be the most spontaneous at 298.15 K than any of the other reactions in Table 4. The corresponding total entropy of the system and its surroundings, ΔS_{univ}, for the reaction resulting in the most stable structure of the 3,4-POZs of chlorophenol at the B3LYP/6-31G(d) level was calculated as 0.0413 kcal/mol.K. Since this is the most positive quantity, it implies that the reaction will be the most

spontaneous at 298.15 K (Chang, 1998). This is just a confirmation of what was deduced from the Gibbs Free energy of the reaction.

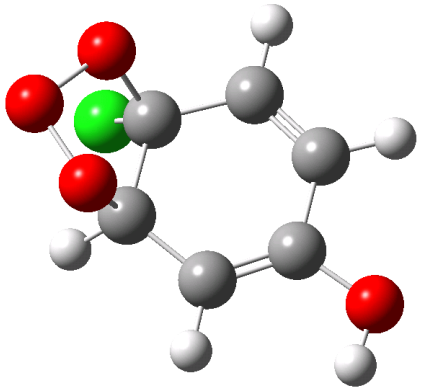

Figure 14 Structure of 4-Cℓ-*endo*-H-*exo*-O-3,4-poz.

The table below shows the relative energies and thermochemical properties of the minima of the five (5) most stable chlorophenol POZs (globally) that are expected to form from the reaction between ozone and chlorophenol at the B3LYP/6-31G(d), B3LYP/6-31G(d,p) and B3LYP/6-311+G(2df) levels of theory.

Table 5 Relative energies and thermochemical properties of the minima of the five (5) most stable chlorophenol POZs at the B3LYP/6-31G(d), B3LYP/6-31G(d,p) and B3LYP/6-311+G(2df) levels.

Chlorophenol POZs	**Relative Energies and Thermochemical Properties**				
	ΔE^{el}	$\Delta E^{el} + ZPE$	ΔH_r^o	ΔG_r^o	ΔS_{univ}
	(kcal/mol)				**(kcal/mol.K)**
B3LYP/6-31G(d) level					
Ozone + Chlorophenol	0.0	0.0	0.0	0.0	0.0000
4_Cℓ_*endo*_H_*exo*_O_3,4_poz	-27.3	-24.6	-25.5	-12.3	0.0413
2_Cℓ_*endo*_H_*exo*_O_1,2_poz	-26.6	-24.6	-25.4	-12.2	0.0410
3_Cℓ_*endo*_H_*exo*_O_3,4_poz	-26.8	-24.2	-25.1	-12.0	0.0402
2_Cℓ_*endo*_H_*exo*_O_2,3_poz	-25.9	-23.4	-24.2	-11.1	0.0373
6_Cℓ_exo_H_exo_O_1,2_poz	-26.0	-23.3	-24.2	-10.9	0.0367
B3LYP/6-31G(d,p) level					
Ozone + Chlorophenol	0.0	0.0	0.0	0.0	0.0000
2_Cℓ_*endo*_H_*exo*_O_1,2_poz	-26.6	-24.6	-25.4	-12.3	0.0412
4_Cℓ_*endo*_H_*exo*_O_3,4_poz	-27.0	-24.4	-25.3	-12.1	0.0407
3_Cℓ_*endo*_H_*exo*_O_3,4_poz	-26.6	-24.0	-24.9	-11.8	0.0396
2_Cℓ_*endo*_H_*exo*_O_2,3_poz	-25.7	-23.3	-24.0	-11.0	0.0369
6_Cℓ_*exo*_H_*exo*_O_1,2_poz	-25.8	-23.1	-24.0	-10.7	0.0360
B3LYP/6-311+G(2df) level					
Ozone + Chlorophenol	0.0	0.0	0.0	0.0	0.0000
4_Cℓ_*endo*_H_*exo*_O_3,4_poz	-21.7	-19.1	-20.0	-6.8	0.0227
3_Cℓ_*endo*_H_*exo*_O_3,4_poz	-21.3	-18.7	-19.6	-6.5	0.0217
4_Cℓ_*exo*_H_*exo*_O_1,2_poz	-20.8	-18.3	-19.1	-6.0	0.0203
5_Cℓ_*exo*_H_*exo*_O_1,2_poz	-20.7	-18.2	-19.1	-6.0	0.0202
4_Cℓ_*endo*_H_*exo*_O_1,2_poz	-20.5	-18.0	-18.9	-5.9	0.0199

At both the B3LYP/6-31G(d) and B3LYP/6-311+G(2df) levels of theory 4-Cℓ-*endo*-H-*exo*-O-3,4-poz is the most stable chlorophenol POZ structure. The reason why it is the most stable structure of the POZs of chlorophenol at the aforementioned two levels of theory is because it is the structure in which the hydrogen atom of the hydroxyl group is the furthest away from the chlorine atom and ozone. Thus there will be less steric hindrance in the 4-Cℓ-*endo*-H-*exo*-O-3,4-poz structure. And that will stabilize this structure compared to the other conformers in Table 5. However, when the B3LYP/6-31G(d,p) model is used, the 2-Cℓ-*endo*-H-*exo*-O-1,2-poz structure is lower in energy than the 4-Cℓ-*endo*-H-*exo*-O-3,4-poz structure. The reason why 2-Cℓ-*endo*-H-*exo*-O-1,2-poz is the most stable structure of the POZs of chlorophenol at the B3LYP/6-31G(d,p) level is because there is an interaction between the hydrogen atom of the hydroxyl group and the chlorine atom towards which the hydrogen atom is pointing. Further, there is also an interaction between the hydrogen atom of the hydroxyl group and the middle oxygen atom of the ozone moiety of the POZ. This will result into hydrogen bonding that will stabilize the 2-Cℓ-*endo*-H-*exo*-O-1,2-poz structure compared to the other conformers at that level of theory.

The largest model used, B3LYP/6-311+G(2df), takes priority over the smaller models that were used. When the largest model was used it was found that 4-Cℓ-*endo*-H-*exo*-O-3,4-poz is the most stable chlorophenol POZ structure. Thus, thermodynamically 4-Cℓ-*endo*-H-*exo*-O-3,4-poz structure is expected to be more favored among the chlorophenol POZs overall. The 4-Cℓ-*endo*-H-*exo*-O-3,4-poz structure possesses a planar carbon ring structure. From the bond distances between the

four carbon atoms that are not bound to oxygen atoms of ozone, a 1,3-butadiene-like moiety can be deduced, which explains the planar arrangement of the carbon ring (Hendrickx & Vinckier, 2003). Indeed, two double CC bonds exhibiting bond distances of about 1.34 Å enclose a single CC bond with a bond length of 1.458 Å. The remaining three CC bonds are single bonds with a bond length of about 1.5 Å or larger. In comparison with the chlorophenol geometry, the C-C distances in the carbon ring of 4-Cℓ-*endo*-H-*exo*-O-3,4-poz are either significantly shorter or significantly larger. This indicates the destruction of the aromaticity and the presence of two double bonds separated by single C-C bonds (Hendrickx & Vinckier, 2003).

4.1.2 Dihydroxybenzene POZs

The naming of the dihydroxybenzene POZs was done in the following way: The first digit or number in the name refers to the position of the carbon atom to which the substituent, OH (i.e. the second hydroxyl group in this case), is attached to the parent compound (phenol). The same numbering as in Figure 5 is used to number the carbon ring of the parent compound. The first H (standing for hydrogen) after the OH refers to the hydrogen atom of the hydroxyl group of the parent compound (phenol). If the H is preceded by an *endo*- prefix, it means that the hydrogen atom is oriented towards the ozone moiety of the POZ and if the H is preceded by an *exo*- prefix, it means that the hydrogen atom is oriented away from the ozone moiety of the POZ. The O (standing for oxygen) that is between the two H's refers to the middle oxygen atom of the ozone moiety of the POZ. If the O is preceded by an *endo*- prefix, it means that the middle

oxygen atom is oriented towards the aryl ring and if O is preceded by an *exo*- prefix, it means that the middle oxygen atom is oriented away from the aryl ring. The last H (also standing for hydrogen) refers to the hydrogen atom of the substituent hydroxyl group. The last two digits before poz refer to the mode of addition of ozone to the aryl ring according to Figure 5.

4.1.2.1 The 1,2-POZs of dihydroxybenzene

The table below shows the relative energies and thermochemical properties of the minima of the five (5) most stable products of dihydroxybenzene 1,2-POZs that are expected to be formed from the reaction between ozone and dihydroxybenzene at the B3LYP/6-31G(d) level of theory.

Table 6 Relative energies and thermochemical properties of the minima of the five (5) most stable dihydroxybenzene 1,2-POZs at the B3LYP/6-31G(d) level.

Dihydroxybenzene 1,2-POZs	**Relative Energies and Thermochemical Properties**				
	ΔE^{el}	ΔE^{el} + ZPE	ΔH_r^o	ΔG_r^o	ΔS_{univ}
B3LYP/6-31G(d) level	**(kcal/mol)**				**(kcal/mol.K)**
Ozone + Dihydroxybenzene	0.0	0.0	0.0	0.0	0.0000
2_OH_*endo*_H_*exo*_O_*endo*_H_1,2_poz	-31.1	-28.7	-29.7	-16.3	0.0547
4_OH_*endo*_H_*exo*_O_*endo*_H_1,2_poz	-29.3	-26.5	-27.5	-14.3	0.0478
4_OH_*exo*_H_*exo*_O_*endo*_H_1,2_poz	-29.3	-26.5	-27.4	-14.1	0.0474
3_OH_*endo*_H_*exo*_O_*endo*_H_1,2_poz	-29.1	-26.4	-27.4	-14.0	0.0470
2_OH_*endo*_H_*endo*_O_*endo*_H_1,2_poz	-28.7	-26.3	-27.3	-13.7	0.0460

The most stable structure of the 1,2-POZs of dihydroxybenzene at the B3LYP/6-31G(d) level of theory was found to be 2-OH-*endo*-H-*exo*-O-*endo*-H-1,2-poz. At the B3LYP/6-31G(d) level the energy difference (ΔE^{el} + ZPE) between the reactants, i.e.

ozone and 1,2-dihydroxybenzene, and 2-OH-*endo*-H-*exo*-O-*endo*-H-1,2-poz, is 28.7 kcal/mol. The results in Table 6 indicate that 2-OH-*endo*-H-*exo*-O-*endo*-H-1,2-poz is positioned energetically way below the reactants than any of the other structures in that table. The energy ordering of the different isomers is depicted in Figure 15 below. A similar trend in energy ordering is obtained at the 6-31G(d,p) level.

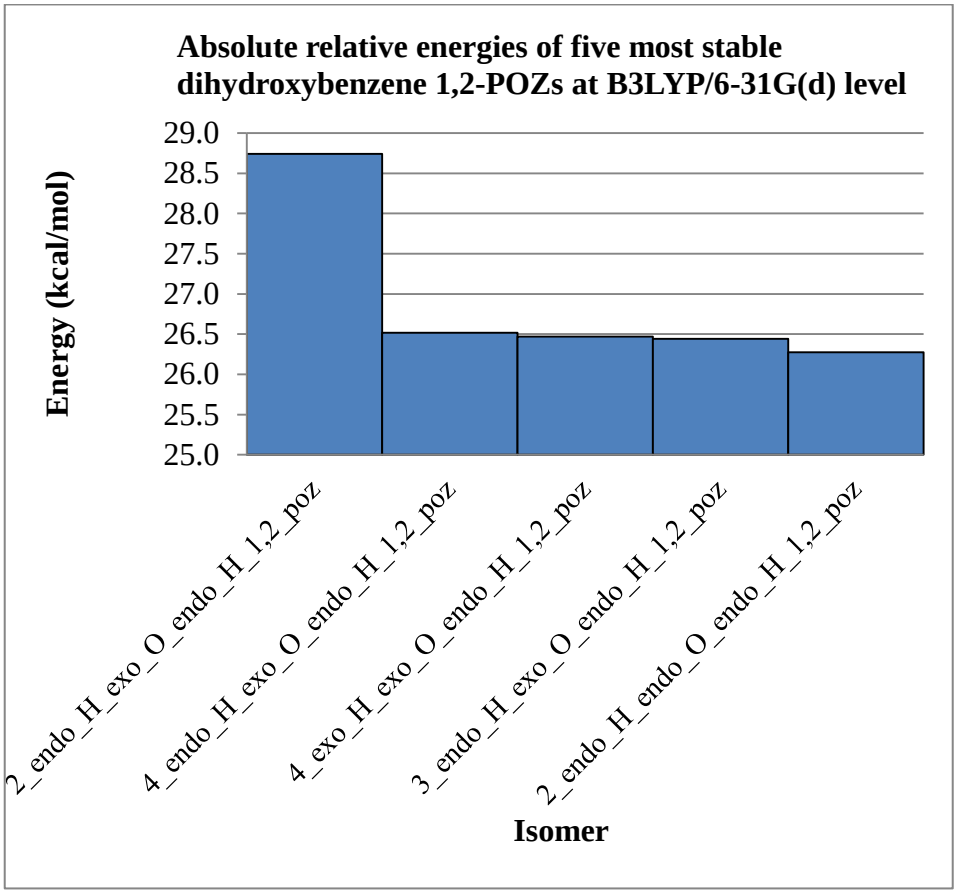

Figure 15 Absolute relative electronic energies (+ZPE) of the five (5) most stable dihydroxybenzene 1,2-POZs at the B3LYP/6-31G(d) level.

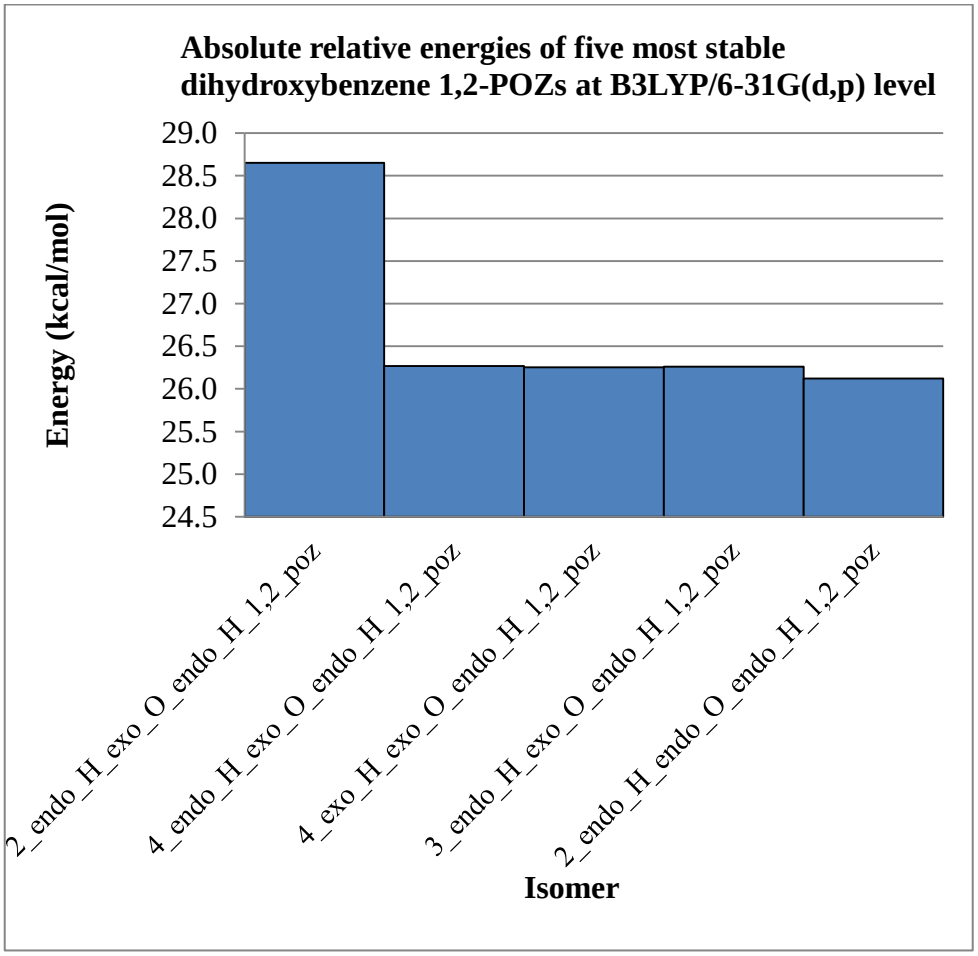

Figure 16 Absolute relative electronic energies (+ZPE) of the five (5) most stable dihydroxybenzene 1,2-POZs at the B3LYP/6-31G(d,p) level.

The enthalpy of the reaction, ΔH_r^o, resulting in the most stable structure of 1,2-POZs of dihydroxybenzene at the B3LYP/6-31G(d) level is -29.7 kcal/mol. The result shows that the reaction is more exothermic than any other reaction in Table 6. For this reaction the Gibbs Free energy, ΔG_r^o, of -16.3 kcal/mol is the lowest value and the negative sign means that the reaction will be the most spontaneous at 298.15 K than any of the other reactions in Table 6. The corresponding total entropy of the system and its

surroundings, ΔS_{univ}, for the reaction resulting in the most stable structure of the 1,2-POZs of dihydroxybenzene at the B3LYP/6-31G(d) level was calculated as 0.0547 kcal/mol.K. Since this is the most positive quantity, it implies that the reaction will be the most spontaneous at 298.15 K (Chang, 1998). This is just a confirmation of what was deduced from the Gibbs Free energy of the reaction.

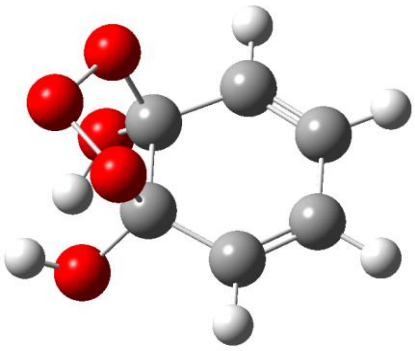

Figure 17 Structure of 2-OH-*endo*-H-*exo*-O-*endo*-H-1,2-poz.

4.1.2.2 The 2,3-POZs of dihydroxybenzene

The table below shows the relative energies and thermochemical properties of the minima of the five (5) most stable products of dihydroxybenzene 2,3-POZs that are expected to be formed from the reaction between ozone and dihydroxybenzene at the B3LYP/6-31G(d) level of theory.

Table 7 Relative energies and thermochemical properties of the minima of the five (5) most stable dihydroxybenzene 2,3-POZs at the B3LYP/6-31G(d) level.

Dihydroxybenzene 2,3-POZs	**Relative Energies and Thermochemical Properties**				
	ΔE^{el}	$\Delta E^{el} + ZPE$	ΔH_r^o	ΔG_r^o	ΔS_{univ}
B3LYP/6-31G(d) level	**(kcal/mol)**				**(kcal/mol.K)**
Ozone + Dihydroxybenzene	0.0	0.0	0.0	0.0	0.0000
2_OH_*endo*_H_*exo*_O_*endo*_H_2,3_poz	-29.8	-26.9	-27.9	-14.6	0.0489
3_OH_*endo*_H_*exo*_O_*endo*_H_2,3_poz	-29.1	-26.4	-27.4	-14.0	0.0470
4_OH_*endo*_H_*exo*_O_*endo*_H_2,3_poz	-22.8	-26.4	-27.4	-14.0	0.0470
2_OH_*endo*_H_*endo*_O_*endo*_H_2,3_poz	-29.1	-26.2	-27.2	-13.9	0.0467
2_OH_*exo*_H_*exo*_O_*exo*_H_2,3_poz	-29.0	-26.1	-27.1	-13.6	0.0456

The most stable structure of the 2,3-POZs of dihydroxybenzene at the B3LYP/6-31G(d) level of theory was found to be 2-OH-*endo*-H-*exo*-O-*endo*-H-2,3-poz. At the B3LYP/6-31G(d) level the energy difference ($\Delta E^{el} + ZPE$) between the reactants, i.e. ozone and 1,2-dihydroxybenzene, and 2-OH-*endo*-H-*exo*-O-*endo*-H-2,3-poz, is 26.9 kcal/mol. The results in Table 7 indicate that 2-OH-*endo*-H-*exo*-O-*endo*-H-2,3-poz is positioned energetically way below the reactants than any of the other structures in that table. The energy ordering of the different isomers is depicted in Figure 18 below. A similar trend in energy ordering is obtained at the 6-31G(d,p) level.

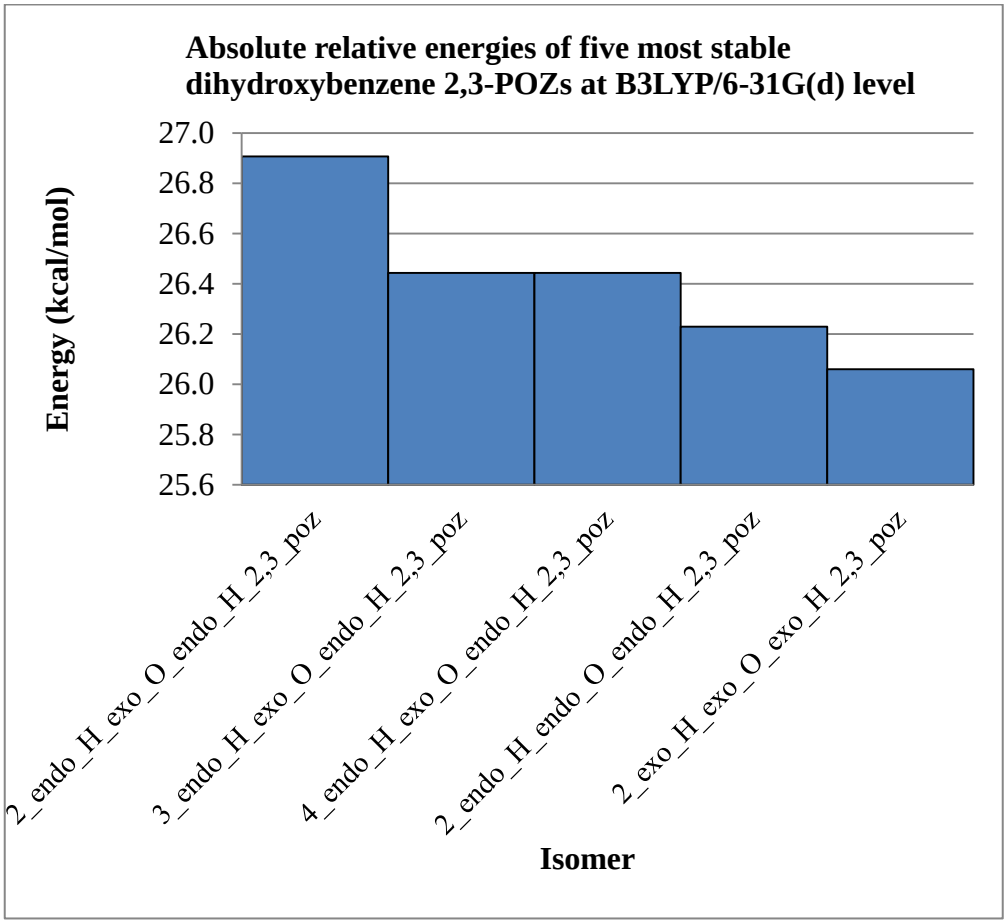

Figure 18 Absolute relative electronic energies (+ZPE) of the five (5) most stable dihydroxybenzene 2,3-POZs at the B3LYP/6-31G(d) level.

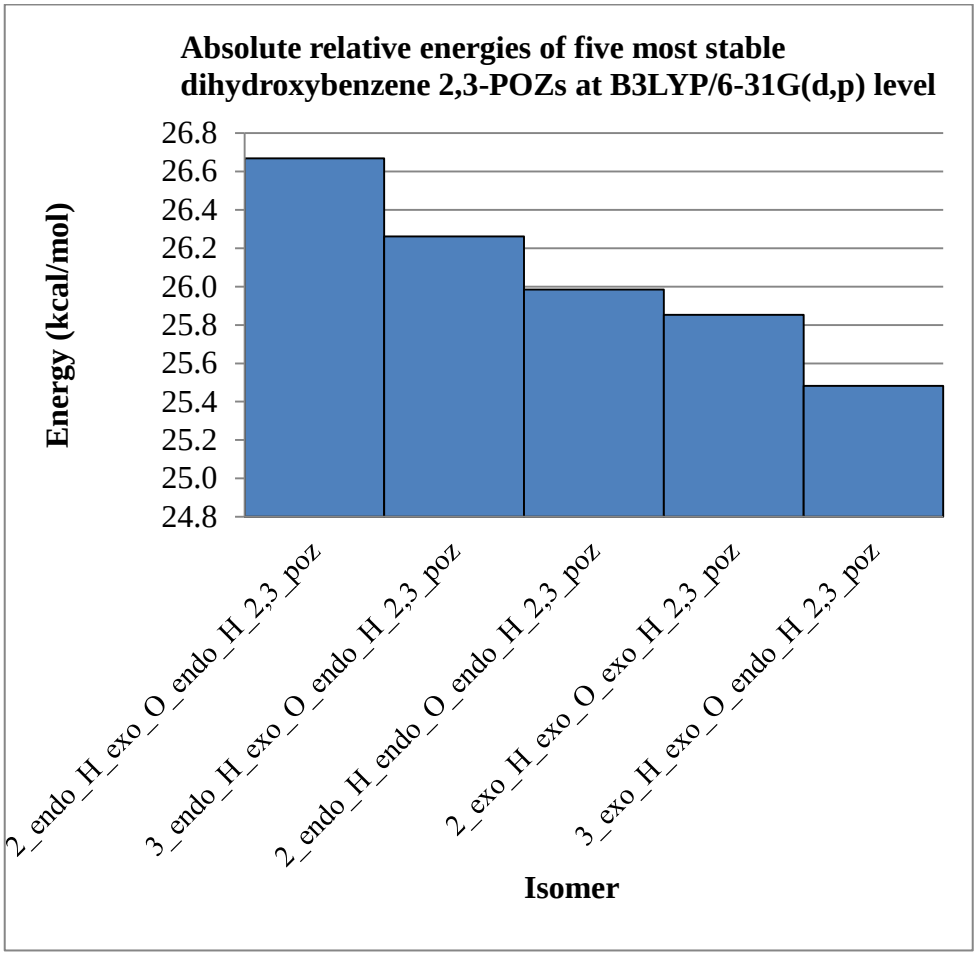

Figure 19 Absolute relative electronic energies (+ZPE) of the five (5) most stable dihydroxybenzene 2,3-POZs at the B3LYP/6-31G(d,p) level.

The enthalpy of the reaction, ΔH_r^o, resulting in the most stable structure of 2,3-POZs of dihydroxybenzene at the B3LYP/6-31G(d) level is -27.9 kcal/mol. The result shows that the reaction is more exothermic than any other reaction in Table 7. For this reaction the Gibbs Free energy, ΔG_r^o, of -14.6 kcal/mol is the lowest value and the negative sign means that the reaction will be the most spontaneous at 298.15 K than any of the other reactions in Table 7. The corresponding total entropy of the system and its

surroundings, ΔS_{univ}, for the reaction resulting in the most stable structure of the 2,3-POZs of dihydroxybenzene at the B3LYP/6-31G(d) level was calculated as 0.0489 kcal/mol.K. Since this is the most positive quantity, it implies that the reaction will be the most spontaneous at 298.15 K (Chang, 1998). This is just a confirmation of what was deduced from the Gibbs Free energy of the reaction.

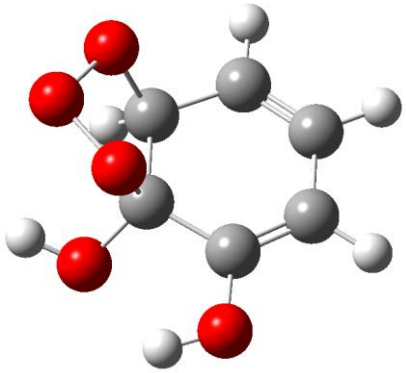

Figure 20 Structure of 2-OH-*endo*-H-*exo*-O-*endo*-H-2,3-poz.

4.1.2.3 The 3,4-POZs of dihydroxybenzene

The table below shows the relative energies and thermochemical properties of the minima of the five (5) most stable products of dihydroxybenzene 3,4-POZs that are expected to be formed from the reaction between ozone and dihydroxybenzene at the B3LYP/6-31G(d) level of theory.

Table 8 Relative energies and thermochemical properties of the minima of the five (5) most stable dihydroxybenzene 3,4-POZs at the B3LYP/6-31G(d) level.

Dihydroxybenzene 3,4-POZs	**Relative Energies and Thermochemical Properties**				
	ΔE^{el}	$\Delta E^{el} + ZPE$	ΔH_r^o	ΔG_r^o	ΔS_{univ}
B3LYP/6-31G(d) level	**(kcal/mol)**				**(kcal/mol.K)**
Ozone + Dihydroxybenzene	0.0	0.0	0.0	0.0	0.0000
3_OH_*endo*_H_*exo*_O_*endo*_H_3,4_poz	-29.4	-26.7	-27.7	-14.5	0.0486
4_OH_*endo*_H_*exo*_O_*endo*_H_3,4_poz	-29.3	-26.5	-27.5	-14.3	0.0478
4_OH_*endo*_H_*exo*_O_*exo*_H_3,4_poz	-29.3	-26.5	-27.4	-14.1	0.0474
3_OH_*endo*_H_*exo*_O_*exo*_H_3,4_poz	-28.7	-26.0	-26.9	-13.7	0.0459
3_OH_*endo*_H_*endo*_O_*endo*_H_3,4_poz	-27.8	-25.2	-26.1	-13.0	0.0437

The most stable structure of the 3,4-POZs of dihydroxybenzene at the B3LYP/6-31G(d) level of theory was found to be 3-OH-*endo*-H-*exo*-O-*endo*-H-3,4-poz. At the B3LYP/6-31G(d) level the energy difference ($\Delta E^{el} + ZPE$) between the reactants, i.e. ozone and 1,3-dihydroxybenzene, and 3-OH-*endo*-H-*exo*-O-*endo*-H-3,4-poz, is 26.7 kcal/mol. The results in Table 8 indicate that 3-OH-*endo*-H-*exo*-O-*endo*-H-3,4-poz is positioned energetically below the reactants than any of the other structures in that table. The energy ordering of the different isomers is depicted in Figure 21 below. A similar trend in energy ordering is obtained at the 6-31G(d,p) level.

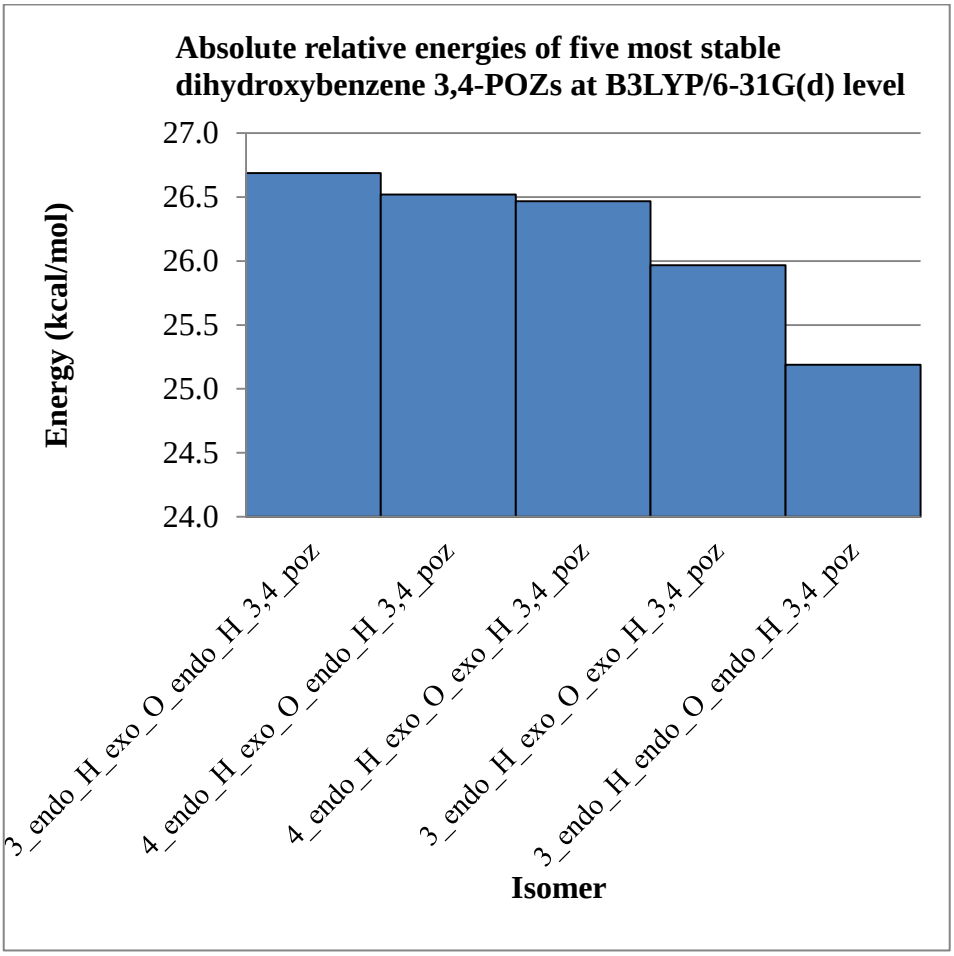

Figure 21 Absolute relative electronic energies (+ZPE) of the five (5) most stable dihydroxybenzene 3,4-POZs at the B3LYP/6-31G(d) level.

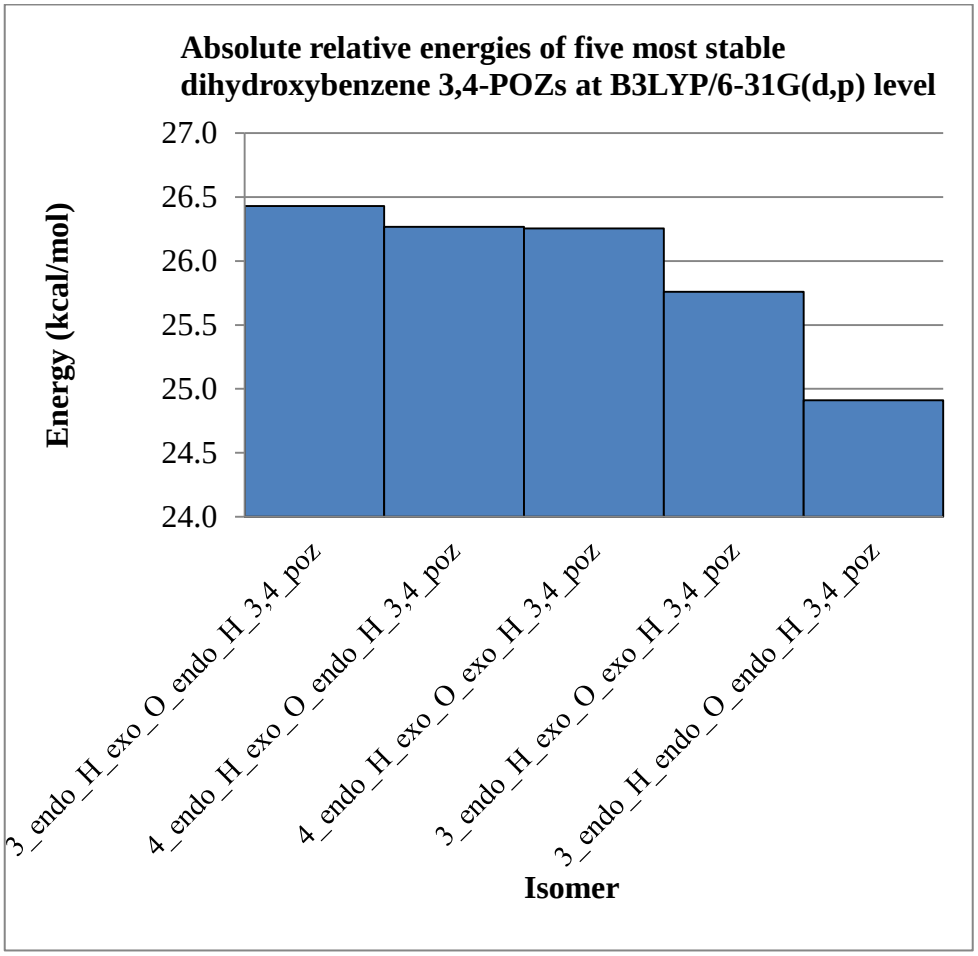

Figure 22 Absolute relative electronic energies (+ZPE) of the five (5) most stable dihydroxybenzene 3,4-POZs at the B3LYP/6-31G(d,p) level.

The enthalpy of the reaction, ΔH_r^o, resulting in the most stable structure of 3,4-POZs of dihydroxybenzene at the B3LYP/6-31G(d) level is -27.7 kcal/mol. The result shows that the reaction is more exothermic than any other reaction in Table 8. For this reaction the Gibbs Free energy, ΔG_r^o, of -14.5 kcal/mol is the lowest value and the negative sign means that the reaction will be the most spontaneous at 298.15 K than any of the other reactions in Table 8. The corresponding total entropy of the system and its

surroundings, ΔS_{univ}, for the reaction resulting in the most stable structure of the 3,4-POZs of dihydroxybenzene at the B3LYP/6-31G(d) level was calculated as 0.0486 kcal/mol.K. Since this is the most positive quantity, it implies that the reaction will be the most spontaneous at 298.15 K (Chang, 1998). This is just a confirmation of what was deduced from the Gibbs Free energy of the reaction.

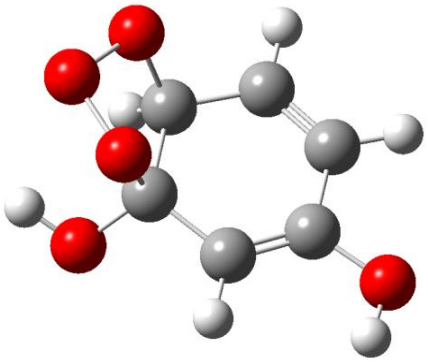

Figure 23 Structure of 3-OH-*endo*-H-*exo*-O-*endo*-H-3,4-poz.

The table below shows the relative energies and thermochemical properties of the minima of the five (5) most stable dihydroxybenzene POZs (globally) that are expected to form from the reaction between ozone and dihydroxybenzene at the B3LYP/6-31G(d), B3LYP/6-31G(d,p) and B3LYP/6-311+G(2df) levels of theory.

Table 9 Relative energies and thermochemical properties of the minima of the five (5) most stable dihydroxybenzene POZs at the B3LYP/6-31G(d), B3LYP/6-31G(d,p) and B3LYP/6-311+G(2df) levels.

Dihydroxybenzene POZs	**Relative Energies and Thermochemical Properties**				
	ΔE^{el}	ΔE^{el} + ZPE	ΔH_r^o	ΔG_r^o	ΔS_{univ}
	(kcal/mol)				**(kcal/mol.K)**
B3LYP/6-31G(d) level					
Ozone + Dihydroxybenzene	0.0	0.0	0.0	0.0	0.0000
2_OH_*endo*_H_*exo*_O_*endo*_H_1,2_poz	-31.1	-28.7	-29.7	-16.3	0.0547
2_OH_*endo*_H_*exo*_O_*endo*_H_2,3_poz	-29.8	-26.9	-27.9	-14.6	0.0489
3_OH_*endo*_H_*exo*_O_*endo*_H_3,4_poz	-29.4	-26.7	-27.7	-14.5	0.0486
4_OH_*endo*_H_*exo*_O_*endo*_H_1,2_poz	-29.3	-26.5	-27.5	-14.3	0.0478
4_OH_*exo*_H_*exo*_O_*endo*_H_1,2_poz	-29.3	-26.5	-27.4	-14.1	0.0474
B3LYP/6-31G(d,p) level					
Ozone + Dihydroxybenzene	0.0	0.0	0.0	0.0	0.0000
2_OH_*endo*_H_*exo*_O_*endo*_H_1,2_poz	-31.1	-28.7	-29.7	-16.2	0.0542
2_OH_*endo*_H_*exo*_O_*endo*_H_2,3_poz	-29.6	-26.7	-27.8	-14.2	0.0478
3_OH_*endo*_H_*exo*_O_*endo*_H_3,4_poz	-29.2	-26.4	-27.5	-14.1	0.0474
4_OH_*endo*_H_*exo*_O_*endo*_H_1,2_poz	-29.1	-26.3	-27.3	-13.9	0.0467
4_OH_*exo*_H_*exo*_O_*endo*_H_1,2_poz	-29.1	-26.3	-27.3	-13.8	0.0463
B3LYP/6-311+G(2df) level					
Ozone + Dihydroxybenzene	0.0	0.0	0.0	0.0	0.0000
2_OH_*endo*_H_*exo*_O_*endo*_H_1,2_poz	-24.4	-22.1	-23.1	-9.9	0.0333
4_OH_*exo*_H_*exo*_O_*endo*_H_1,2_poz	-24.0	-21.0	-22.1	-8.5	0.0286
3_OH_*endo*_H_*exo*_O_*endo*_H_3,4_poz	-23.8	-21.0	-22.0	-8.6	0.0289
4_OH_*endo*_H_*exo*_O_*endo*_H_1,2_poz	-23.8	-20.9	-22.0	-8.5	0.0283
3_OH_*endo*_H_*exo*_O_*exo*_H_3,4_poz	-23.5	-20.6	-21.6	-8.2	0.0274

At all the levels of theory that were used, 2-OH-*endo*-H-*exo*-O-*endo*-H-1,2-poz is the most stable dihydroxybenzene POZ structure. The reason why it is the most stable structure of the POZs of dihydroxybenzene at all the levels of theory that were used is because there will be an interaction between the hydrogen atoms of the hydroxyl groups and the central oxygen atom of the ozone moiety of the POZ. This will result into hydrogen bonding that will stabilize the 2-OH-*endo*-H-*exo*-O-*endo*-H-1,2-poz structure compared to the other conformers in Table 9.

As mentioned before, the largest model used, B3LYP/6-311+G(2df), takes priority over the smaller models that were used. Since 2-OH-*endo*-H-*exo*-O-*endo*-H-1,2-poz is the most stable dihydroxybenzene POZ structure at all the levels of theory, including the highest level that was used, it is expected to be the structure that is thermodynamically more favored among the dihydroxybenzene POZs overall. The 2-OH-*endo*-H-*exo*-O-*endo*-H-1,2-poz structure possesses a planar carbon ring structure. From the bond distances between the four carbon atoms that are not bound to oxygen atoms of ozone, a 1,3-butadiene-like moiety can be deduced, which explains the planar arrangement of the carbon ring (Hendrickx & Vinckier, 2003). Indeed, two double CC bonds exhibiting bond distances of about 1.33 Å enclose a single CC bond with a bond length of 1.457 Å. The remaining three CC bonds are single bonds with a bond length of about 1.5 Å or larger. In comparison with the dihydroxybenzene geometry, the C-C distances in the carbon ring of 2-OH-*endo*-H-*exo*-O-*endo*-H-1,2-poz are either significantly shorter or significantly larger. This indicates the destruction of the

aromaticity and the presence of two double bonds separated by single C-C bonds (Hendrickx & Vinckier, 2003).

4.1.3 Hydroxythiophenol POZs

The naming of the hydroxythiophenol POZs was done in the following way: The first digit or number in the name refers to the position of the carbon atom to which the substituent, OH (i.e. the hydroxyl group in this case), is attached to the parent compound (thiophenol). The same numbering as in Figure 5 is used to number the carbon ring of the parent compound. The first H (standing for hydrogen) after the OH refers to the hydrogen atom of the substituent hydroxyl group. If the H is preceded by an *endo*- prefix, it means that the hydrogen atom is oriented towards the ozone moiety of the POZ and if the H is preceded by an *exo*- prefix, it means that the hydrogen atom is oriented away from the ozone moiety of the POZ. The O (standing for oxygen) that is between the two H's refers to the middle oxygen atom of the ozone moiety of the POZ. If the O is preceded by an *endo*- prefix, it means that the middle oxygen atom is oriented towards the aryl ring and if O is preceded by an *exo*- prefix, it means that the middle oxygen atom is oriented away from the aryl ring. The last H (also standing for hydrogen) refers to the hydrogen atom of the sulfhydryl group of the parent compound (thiophenol). The last two digits before poz refer to the mode of addition of ozone to the aryl ring according to Figure 5.

4.1.3.1 The 1,2-POZs of hydroxythiophenol

The table below shows the relative energies and thermochemical properties of the minima of the five (5) most stable products of hydroxythiophenol 1,2-POZs that are expected to be formed from the reaction between ozone and hydroxythiophenol at the B3LYP/6-31G(d) level of theory.

Table 10 Relative energies and thermochemical properties of the minima of the five (5) most stable hydroxythiophenol 1,2-POZs at the B3LYP/6-31G(d) level.

Hydroxythiophenol 1,2-POZs	**Relative Energies and Thermochemical Properties**				
	ΔE^{el}	$\Delta E^{el} + ZPE$	ΔH_r^o	ΔG_r^o	ΔS_{univ}
B3LYP/6-31G(d) level	**(kcal/mol)**				**(kcal/mol.K)**
Ozone + Hydroxythiophenol	0.0	0.0	0.0	0.0	0.0000
2_OH_*endo*_H_*exo*_O_*exo*_H_1,2_poz	-24.2	-22.0	-22.9	-9.4	0.0317
4_OH_*endo*_H_*exo*_O_*exo*_H_1,2_poz	-23.4	-21.0	-21.8	-8.7	0.0292
2_OH_*exo*_H_*exo*_O_*endo*_H_1,2_poz	-22.8	-20.9	-21.8	-8.4	0.0283
4_OH_*endo*_H_*exo*_O_*endo*_H_1,2_poz	-23.1	-20.7	-21.5	-8.5	0.0286
5_OH_*endo*_H_*exo*_O_*endo*_H_1,2_poz	-22.8	-20.3	-21.1	-8.2	0.0276

The most stable structure of the 1,2-POZs of hydroxythiophenol at the B3LYP/6-31G(d) level of theory was found to be 2-OH-*endo*-H-*exo*-O-*exo*-H-1,2-poz. At the B3LYP/6-31G(d) level, the energy difference ($\Delta E^{el} + ZPE$) between the reactants, i.e. ozone and 2-hydroxythiophenol, and 2-OH-*endo*-H-*exo*-O-*exo*-H-1,2-poz, is 22.0 kcal/mol. The results in Table 10 indicate that 2-OH-*endo*-H-*exo*-O-*exo*-H-1,2-poz is positioned energetically way below the reactants than any of the other structures in that table. The energy ordering of the different isomers is depicted in Figure 24 below. A similar trend in energy ordering is obtained at the 6-31G(d,p) level.

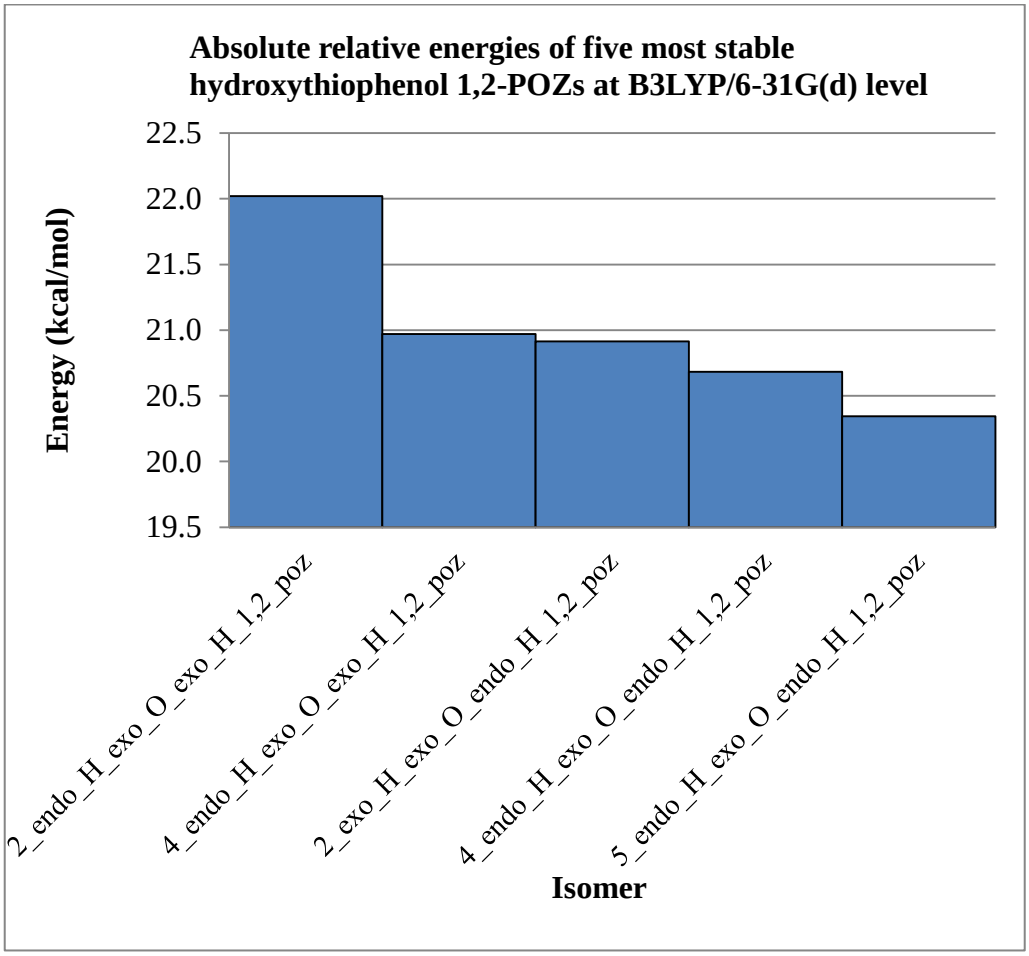

Figure 24 Absolute relative electronic energies (+ZPE) of the five (5) most stable hydroxythiophenol 1,2-POZs at the B3LYP/6-31G(d) level.

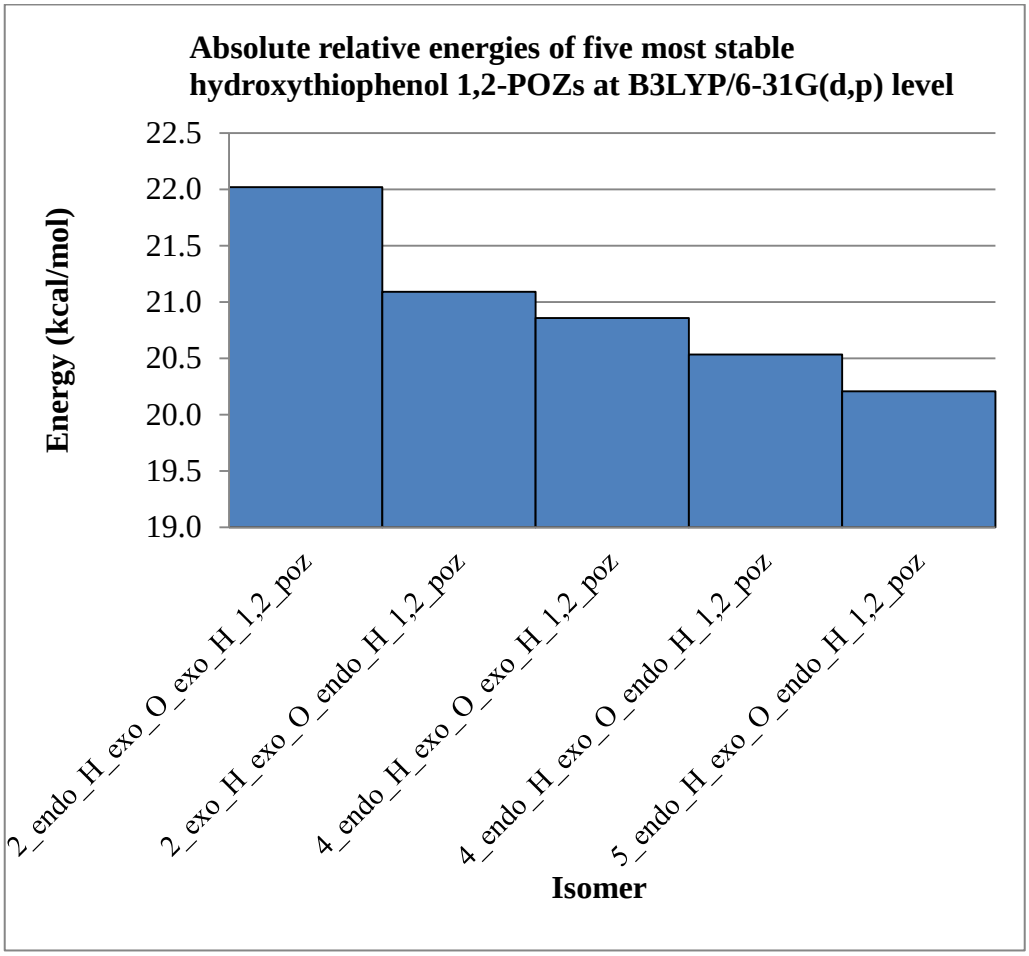

Figure 25 Absolute relative electronic energies (+ZPE) of the five (5) most stable hydroxythiophenol 1,2-POZs at the B3LYP/6-31G(d,p) level.

The enthalpy of the reaction, ΔH_r^o, of the most stable structure of 1,2-POZs of hydroxythiophenol at the B3LYP/6-31G(d) level is -22.9 kcal/mol. The result shows that the reaction is more exothermic than any other reaction in Table 10. For this reaction the Gibbs Free energy, ΔG_r^o, of -9.4 kcal/mol is the lowest value and the negative sign means that the reaction will be the most spontaneous at 298.15 K than any of the other reactions in Table 10. The corresponding total entropy of the system and its

surroundings, ΔS_{univ}, for the reaction resulting in the most stable structure of the 1,2-POZs of hydroxythiophenol at the B3LYP/6-31G(d) level was calculated as 0.0317 kcal/mol.K. Since this is the most positive quantity, it implies that the reaction will be the most spontaneous at 298.15 K (Chang, 1998). This is just a confirmation of what was deduced from the Gibbs Free energy of the reaction.

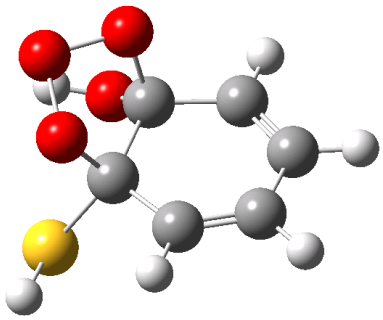

Figure 26 Structure of 2-OH-*endo*-H-*exo*-O-*exo*-H-1,2-poz.

4.1.3.2 The 2,3-POZs of hydroxythiophenol

The table below shows the relative energies and thermochemical properties of the minima of the five (5) most stable products of hydroxythiophenol 2,3-POZs that are expected to be formed from the reaction between ozone and hydroxythiophenol at the B3LYP/6-31G(d) level of theory.

Table 11 Relative energies and thermochemical properties of the minima of the five (5) most stable hydroxythiophenol 2,3-POZs at the B3LYP/6-31G(d) level.

Hydroxythiophenol 2,3-POZs	**Relative Energies and Thermochemical Properties**				
	ΔE^{el}	$\Delta E^{el} + ZPE$	ΔH_r^o	ΔG_r^o	ΔS_{univ}
B3LYP/6-31G(d) level	**(kcal/mol)**				**(kcal/mol.K)**
Ozone + Hydroxythiophenol	0.0	0.0	0.0	0.0	0.0000
2_OH_*exo*_H_*exo*_O_*endo*_H_2,3_poz	-27.3	-24.5	-25.5	-12.1	0.0407
6_OH_*exo*_H_*endo*_O_*endo*_H_2,3_poz	-27.7	-24.5	-25.4	-12.4	0.0416
6_OH_*exo*_H_*exo*_O_*endo*_H_2,3_poz	-27.4	-24.2	-25.1	-12.1	0.0407
3_OH_*endo*_H_*exo*_O_*endo*_H_2,3_poz	-26.3	-23.9	-24.6	-12.0	0.0401
3_OH_*exo*_H_*exo*_O_*endo*_H_2,3_poz	-26.1	-23.6	-24.4	-11.5	0.0385

The most stable structure of the 2,3-POZs of hydroxythiophenol at the B3LYP/6-31G(d) level of theory was found to be 2-OH-*exo*-H-*exo*-O-*endo*-H-2,3-poz. At the B3LYP/6-31G(d) level, the energy difference ($\Delta E^{el} + ZPE$) between the reactants, i.e. ozone and 2-hydroxythiophenol, and 2-OH-*exo*-H-*exo*-O-*endo*-H-2,3-poz, is 24.5 kcal/mol. Even though it seems as if 2-OH-*exo*-H-*exo*-O-*endo*-H-2,3-poz and 6-OH-*exo*-H-*endo*-O-*endo*-H-2,3-poz structures have the same energy difference after rounding off was done, the 2-OH-*exo*-H-*exo*-O-*endo*-H-2,3-poz structure has got a slightly lower energy difference than the 6-OH-*exo*-H-*endo*-O-*endo*-H-2,3-poz structure. This is clearly evident in Figure 27. The results in Table 10 indicate that 2-OH-*exo*-H-*exo*-O-

endo-H-2,3-poz is positioned energetically below the reactants than any of the other structures in that table. The energy ordering of the different isomers is depicted in Figure 27 below. A similar trend in energy ordering is obtained at the 6-31G(d,p) level.

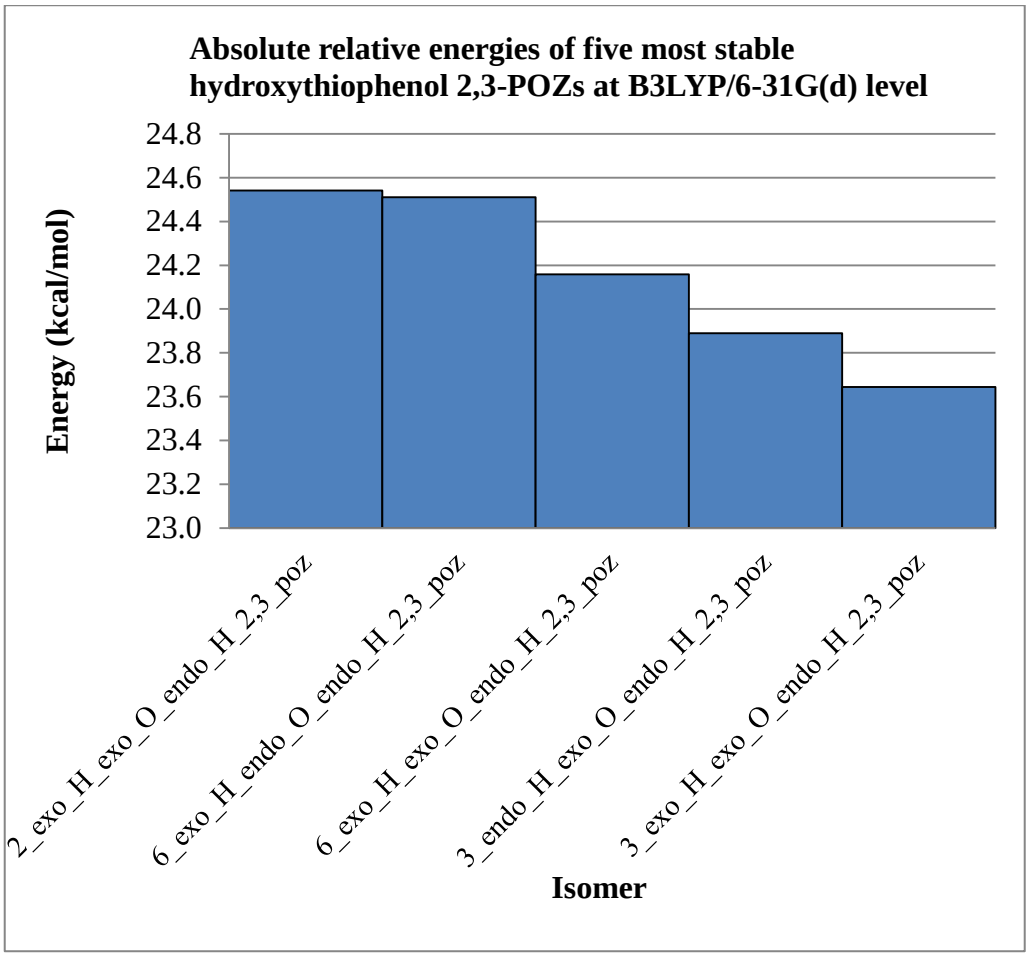

Figure 27 Absolute relative electronic energies (+ZPE) of the five (5) most stable hydroxythiophenol 2,3-POZs at the B3LYP/6-31G(d) level.

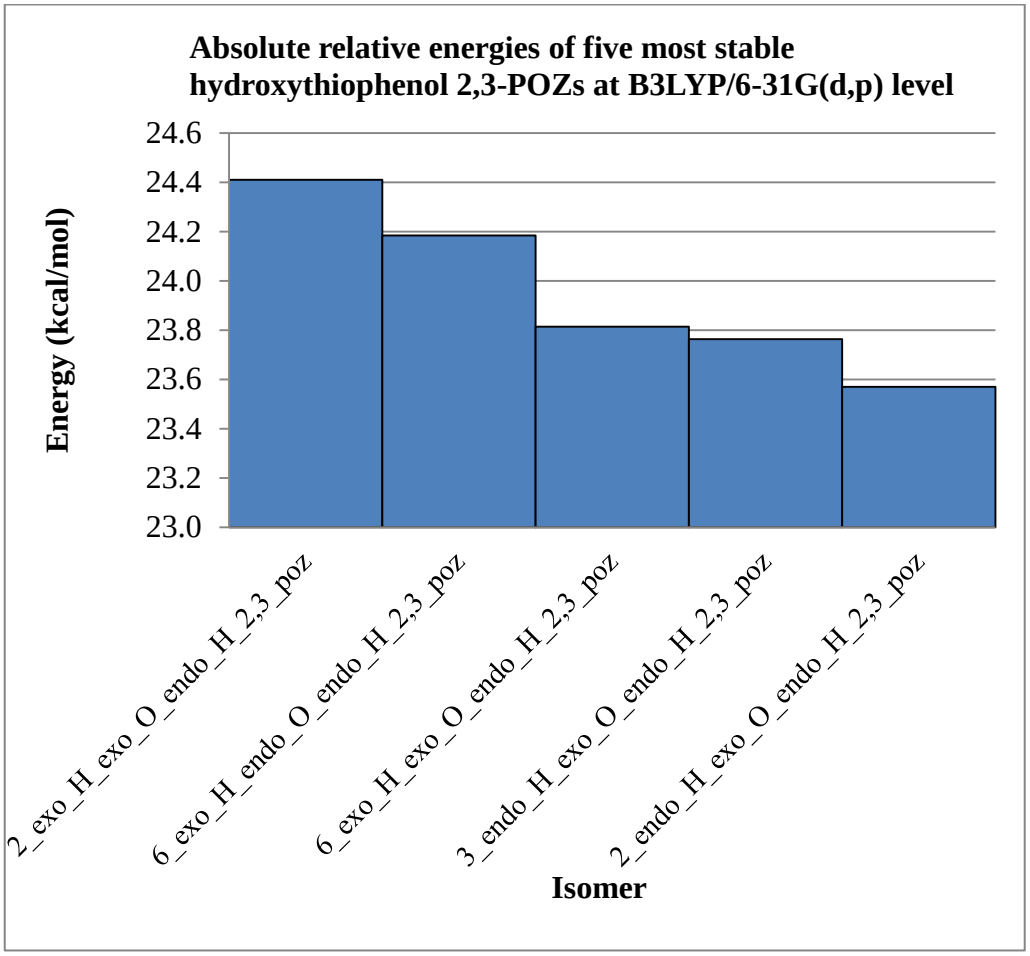

Figure 28 Absolute relative electronic energies (+ZPE) of the five (5) most stable hydroxythiophenol 2,3-POZs at the B3LYP/6-31G(d,p) level.

The enthalpy of the reaction, ΔH_r^o, of the most stable structure of 2,3-POZs of hydroxythiophenol at the B3LYP/6-31G(d) level is -25.5 kcal/mol. The result shows that the reaction is more exothermic than any other reaction in Table 11. For this reaction the Gibbs Free energy, ΔG_r^o, of -12.1 kcal/mol is among the lowest values and the negative sign means that the reaction will more spontaneous at 298.15 K than some of the other reactions in Table 10. The corresponding total entropy of the system and its

surroundings, ΔS_{univ}, for the reaction resulting in the most stable structure of the 2,3-POZs of hydroxythiophenol at the B3LYP/6-31G(d) level was calculated as 0.0407 kcal/mol.K. Since this is one of the most positive quantities, it implies that the reaction will be more spontaneous than some of the other reactions at 298.15 K (Chang, 1998). This is just a confirmation of what was deduced from the Gibbs Free energy of the reaction.

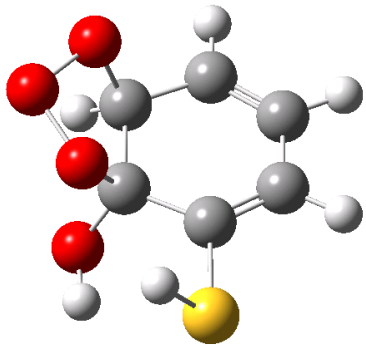

Figure 29 Structure of 2-OH-*exo*-H-*exo*-O-*endo*-H-2,3-poz.

4.1.3.3 The 3,4-POZs of hydroxythiophenol

The table below shows the relative energies and thermochemical properties of the minima of the five (5) most stable products of hydroxythiophenol 3,4-POZs that are expected to be formed from the reaction between ozone and hydroxythiophenol at the B3LYP/6-31G(d) level of theory.

Table 12 Relative energies and thermochemical properties of the minima of the five (5) most stable hydroxythiophenol 3,4-POZs at the B3LYP/6-31G(d) level.

Hydroxythiophenol 3,4-POZs	**Relative Energies and Thermochemical Properties**				
	ΔE^{el}	$\Delta E^{el} + ZPE$	ΔH_r^o	ΔG_r^o	ΔS_{univ}
B3LYP/6-31G(d) level	**(kcal/mol)**				**(kcal/mol.K)**
Ozone + Hydroxythiophenol	0.0	0.0	0.0	0.0	0.0000
3_OH_*endo*_H_*exo*_O_*exo*_H_3,4_poz	-25.2	-22.9	-23.7	-10.9	0.0365
4_OH_*exo*_H_*exo*_O_*exo*_H_3,4_poz	-25.2	-22.8	-23.5	-10.6	0.0357
3_OH_*exo*_H_*exo*_O_*exo*_H_3,4_poz	-24.8	-22.5	-23.2	-10.4	0.0349
2_OH_*exo*_H_*endo*_O_*endo*_H_3,4_poz	-25.4	-22.3	-23.2	-10.3	0.0344
4_OH_*endo*_H_*exo*_O_*endo*_H_3,4_poz	-24.5	-22.3	-23.0	-10.4	0.0347

The most stable structure of the 3,4-POZs of hydroxythiophenol at the B3LYP/6-31G(d) level of theory was found to be 3-OH-*endo*-H-*exo*-O-*exo*-H-3,4-poz. At the B3LYP/6-31G(d) level, the energy difference ($\Delta E^{el} + ZPE$) between the reactants, i.e. ozone and 3-hydroxythiophenol, and 3-OH-*endo*-H-*exo*-O-*exo*-H-3,4-poz, is 22.9 kcal/mol. The results in Table 12 indicate that 3-OH-*endo*-H-*exo*-O-*exo*-H-3,4-poz is positioned energetically below the reactants than any of the other structures in that table. The energy ordering of the different isomers is depicted in Figure 30 below. A similar trend in energy ordering is obtained at the 6-31G(d,p) level.

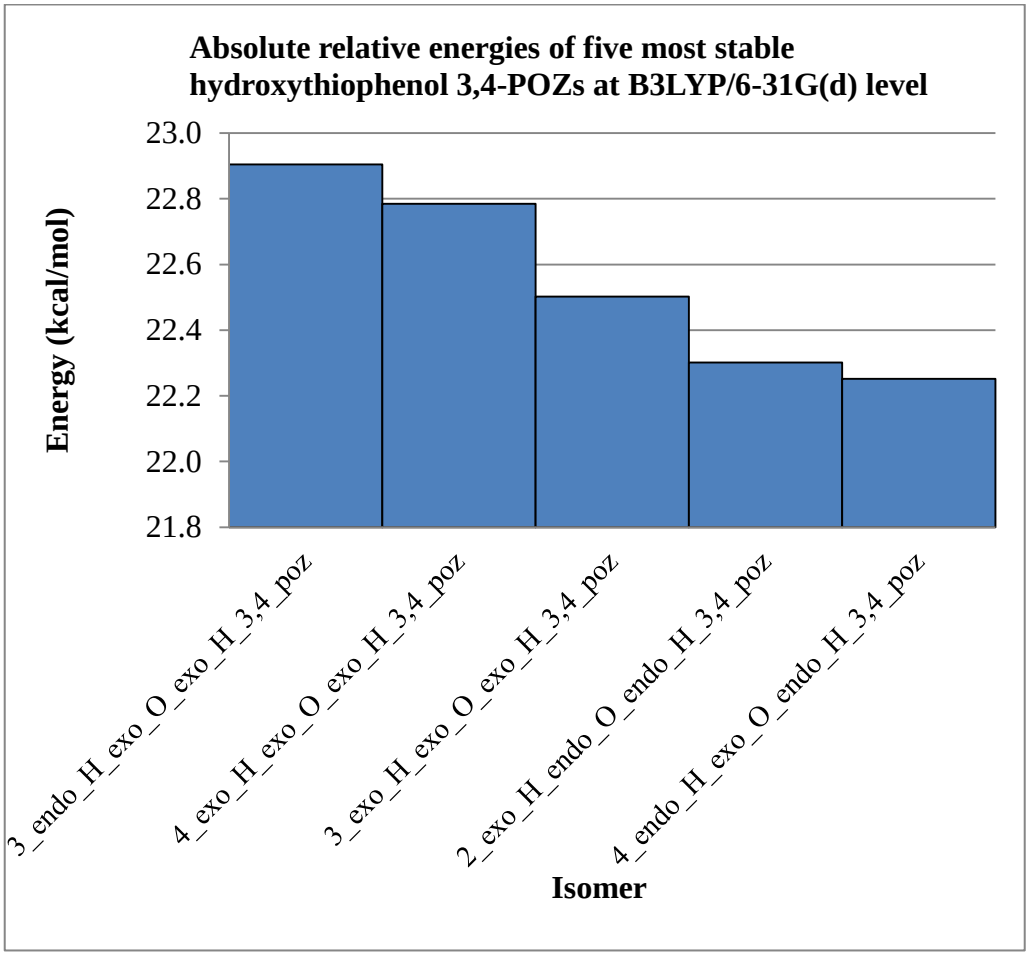

Figure 30 Absolute relative electronic energies (+ZPE) of the five (5) most stable hydroxythiophenol 3,4-POZs at the B3LYP/6-31G(d) level.

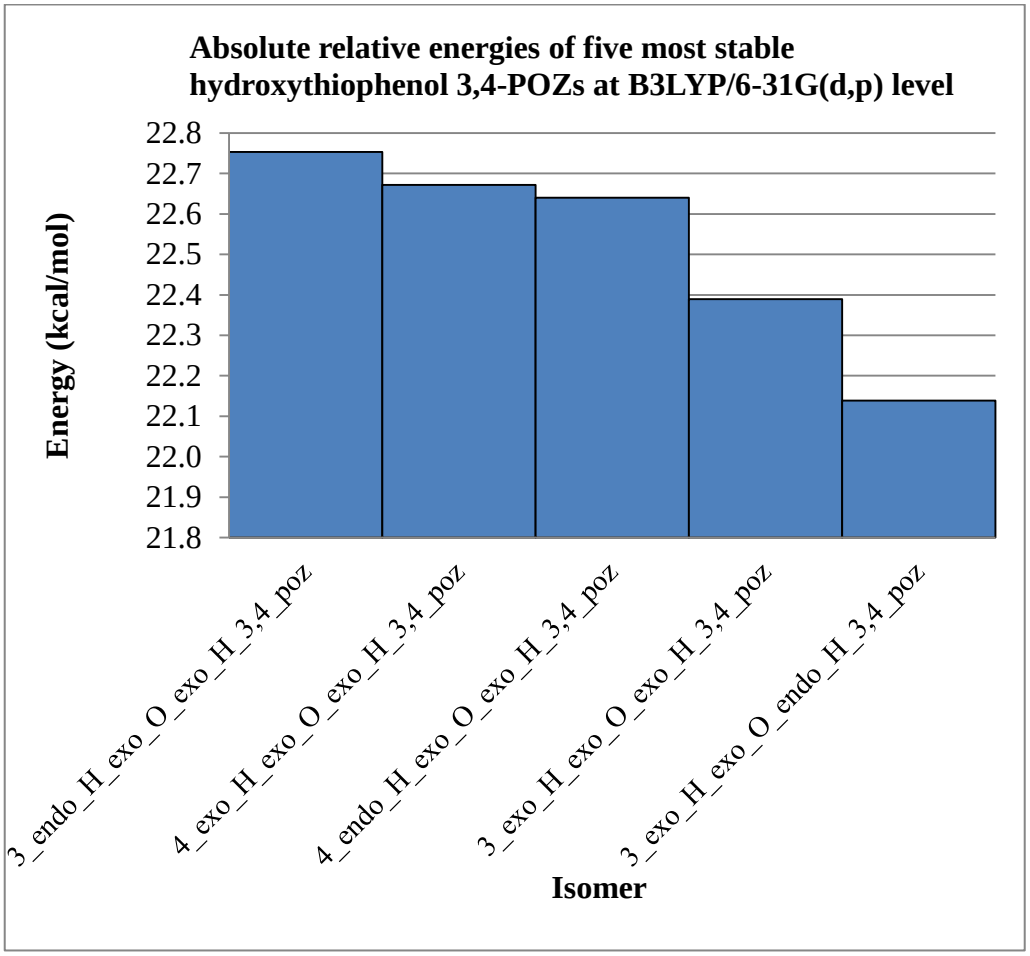

Figure 31 Absolute relative electronic energies (+ZPE) of the five (5) most stable hydroxythiophenol 3,4-POZs at the B3LYP/6-31G(d,p) level.

The enthalpy of the reaction, ΔH_r^o, of the most stable structure of 3,4-POZs of hydroxythiophenol at the B3LYP/6-31G(d) level is -23.7 kcal/mol. The result shows that the reaction is more exothermic than any other reaction in Table 12. For this reaction the Gibbs Free energy, ΔG_r^o, of -10.9 kcal/mol is the lowest value and the negative sign means that the reaction will be the most spontaneous at 298.15 K than any of the other reactions in Table 12. The corresponding total entropy of the system and its

surroundings, ΔS_{univ}, for the reaction resulting in the most stable structure of the 3,4-POZs of hydroxythiophenol at the B3LYP/6-31G(d) level was calculated as 0.0365 kcal/mol.K. Since this is the most positive quantity, it implies that the reaction will be the most spontaneous at 298.15 K (Chang, 1998). This is just a confirmation of what was deduced from the Gibbs Free energy of the reaction.

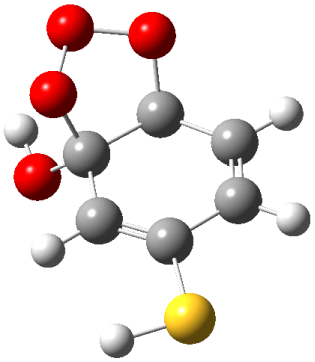

Figure 32 Structure of 3-OH-*endo*-H-*exo*-O-*exo*-H-3,4-poz.

The table below shows the relative energies and thermochemical properties of the minima of the five (5) most stable hydroxythiophenol POZs (globally) that are expected to form from the reaction between ozone and hydroxythiophenol at the B3LYP/6-31G(d), B3LYP/6-31G(d,p) and B3LYP/6-311+G(2df) levels of theory.

Table 13 Relative energies and thermochemical properties of the minima of the five (5) most stable hydroxythiophenol POZs at the B3LYP/6-31G(d), B3LYP/6-31G(d,p) and B3LYP/6-311+G(2df) levels.

Hydroxythiophenol POZs	**Relative Energies and Thermochemical Properties**				
	ΔE^{el}	$\Delta E^{el} + ZPE$	ΔH_r^o	ΔG_r^o	ΔS_{univ}
	(kcal/mol)				**(kcal/mol.K)**
B3LYP/6-31G(d) level					
Ozone + Hydroxythiophenol	0.0	0.0	0.0	0.0	0.0000
2_OH_*exo*_H_*exo*_O_*endo*_H_2,3_poz	-27.3	-24.5	-25.5	-12.1	0.0407
6_OH_*exo*_H_*endo*_O_*endo*_H_2,3_poz	-27.7	-24.5	-25.4	-12.4	0.0416
6_OH_*exo*_H_*exo*_O_*endo*_H_2,3_poz	-27.4	-24.2	-25.1	-12.1	0.0407
3_OH_*endo*_H_*exo*_O_*endo*_H_2,3_poz	-26.3	-23.9	-24.6	-12.0	0.0401
3_OH_*exo*_H_*exo*_O_*endo*_H_2,3_poz	-26.1	-23.6	-24.4	-11.5	0.0385
B3LYP/6-31G(d,p) level					
Ozone + Hydroxythiophenol	0.0	0.0	0.0	0.0	0.0000
2_OH_*exo*_H_*exo*_O_*endo*_H_2,3_poz	-27.1	-24.4	-25.3	-12.0	0.0403
6_OH_*exo*_H_*endo*_O_*endo*_H_2,3_poz	-27.3	-24.2	-25.1	-12.1	0.0405
6_OH_*exo*_H_*exo*_O_*endo*_H_2,3_poz	-27.0	-23.8	-24.7	-11.8	0.0396
3_OH_*endo*_H_*exo*_O_*endo*_H_2,3_poz	-26.1	-23.8	-24.5	-11.9	0.0398
2_OH_*endo*_H_*exo*_O_*endo*_H_2,3_poz	-26.1	-23.6	-24.4	-11.4	0.0381
B3LYP/6-311+G(2df) level					
Ozone + Hydroxythiophenol	0.0	0.0	0.0	0.0	0.0000
2_OH_*exo*_H_*exo*_O_*endo*_H_2,3_poz	-22.2	-19.4	-20.3	-6.9	0.0231
3_OH_*exo*_H_*exo*_O_*endo*_H_2,3_poz	-21.5	-18.9	-19.7	-6.7	0.0225
6_OH_*exo*_H_*endo*_O_*endo*_H_2,3_poz	-22.0	-18.8	-19.8	-6.7	0.0224
3_OH_*endo*_H_*exo*_O_*endo*_H_2,3_poz	-21.3	-18.8	-19.6	-6.7	0.0224
6_OH_*exo*_H_*exo*_O_*endo*_H_2,3_poz	-22.0	-18.7	-19.7	-6.7	0.0224

At all the levels of theory that were used, 2-OH-*exo*-H-*exo*-O-*endo*-H-2,3-poz is the most stable hydroxythiophenol POZ structure. The reason why it is the most stable structure of the POZs of hydroxythiophenol at all the levels of theory that were used is because there will be an interaction between the hydrogen atom of the hydroxyl group and the sulfur atom of the sulfhydryl group. Moreover, there will also be interactions between the hydrogen atom of the sulfhydryl group and the terminal oxygen atom of the ozone moiety of the POZ that is nearest to it as well as the oxygen atom of the hydroxyl group. This will result into hydrogen bonding that will stabilize the 2-OH-*exo*-H-*exo*-O-*endo*-H-2,3-poz structure compared to the other conformers in Table 13.

As mentioned before, the largest model used, B3LYP/6-311+G(2df), takes priority over the smaller models that were used. Since 2-OH-*exo*-H-*exo*-O-*endo*-H-2,3-poz is the most stable hydroxythiophenol POZ structure at all the levels of theory, including the highest level that was used, it is expected to be the structure that is thermodynamically more favored among the hydroxythiophenol POZs overall. The 2-OH-*exo*-H-*exo*-O-*endo*-H-2,3-poz structure possesses a planar carbon ring structure. From the bond distances between the four carbon atoms that are not bound to oxygen atoms of ozone, a 1,3-butadiene-like moiety can be deduced, which explains the planar arrangement of the carbon ring (Hendrickx & Vinckier, 2003). Indeed, two double CC bonds exhibiting bond distances of about 1.34 Å enclose a single CC bond with a bond length of 1.455 Å. The remaining three CC bonds are single bonds with a bond length of about 1.5 Å or larger. In comparison with the hydroxythiophenol geometry, the C-C distances in the carbon ring of 2-OH-*exo*-H-*exo*-O-*endo*-H-2,3-poz are either

significantly shorter or significantly larger. This indicates the destruction of the aromaticity and the presence of two double bonds separated by single C-C bonds (Hendrickx & Vinckier, 2003).

4.3 General Discussion

4.3.1 Reaction of Ozone with Chlorophenol

In total, 60 chlorophenol POZ isomers were computed. Seventeen (17) of the most stable isomers are just within 3 kcal/mol of each other on the energy scale. Computational errors at the level of theory that was used suggest that these isomers are nearly isoenergetic.

Table 14 Relative energies and thermochemical properties of the minima of the three (3) most stable chlorophenol POZs at the B3LYP/6-311+G(2df) level.

Chlorophenol POZs	**Structure**	$E^{el} + ZPE$ (kcal/mol)	ΔH_r^o (kcal/mol)	ΔG_r^o (kcal/mol)
4-Cℓ-*endo*-H-*exo*-O-3,4-poz	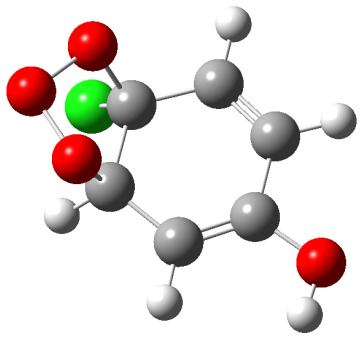	-19.1	-20.0	-6.8

3-Cℓ-*endo*-H-*exo*-O-3,4-poz	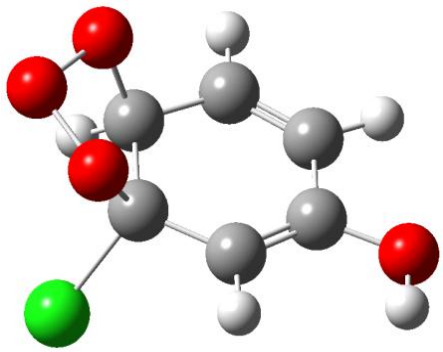	-18.7	-19.6	-6.5
4-Cℓ-*exo*-H-*exo*-O-1,2-poz	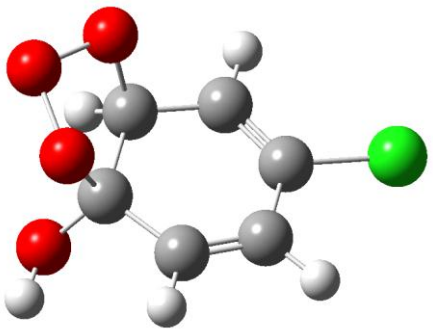	-18.3	-19.1	-6.0

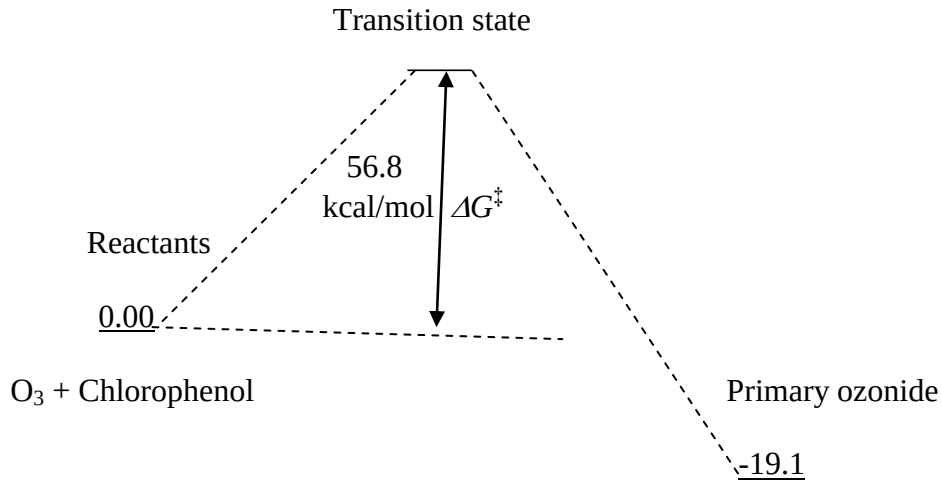

Figure 33 Activation barrier (kcal/mol) and exothermicity (kcal/mol) of 4-Cℓ-*endo*-H-*exo*-O-3,4-poz.

The transition state leading to the most stable chlorophenol POZ has an activated Gibbs free energy of 56.8 kcal/mol, while the POZ, i.e. 4-Cℓ-*endo*-H-*exo*-O-3,4-poz, is located at 19.1 kcal/mol below the reactants (Figure 33). The calculated reaction enthalpy (ΔH_r^o) and Gibbs free energy (ΔG_r^o) for 4-Cℓ-*endo*-H-*exo*-O-3,4-poz are 20.0 kcal/mol and 6.8 kcal/mol below those of the reactants, respectively (Table 14). Further calculation shows that the rate constant, *k*, for the formation of 4-Cℓ-*endo*-H-*exo*-O-3,4-poz is 1.48 x 10^{-29} $atm^{-1}.s^{-1}$. Kinetically 4-Cℓ-*exo*-H-*exo*-O-1,2-poz is more favored because the TS leading to its formation has an activated Gibbs free energy of 8.1 kcal/mol which is lower than that of 4-Cℓ-*endo*-H-*exo*-O-3,4-poz (56.8 kcal/mol). Thermodynamically 4-Cℓ-*endo*-H-*exo*-O-3,4-poz appears to be more favored (Figure 34).

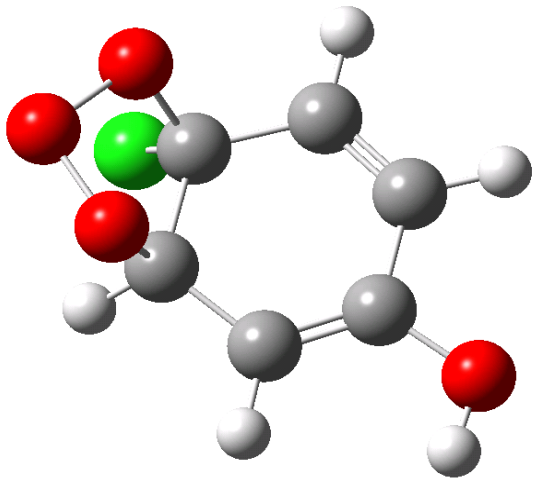

Figure 34 Geometry of most stable chlorophenol POZ intermediate (4-Cℓ-*endo*-H-*exo*-O-3,4-poz).

The calculations suggest that mode III (3,4-addition) appears to be energetically most favorable for chlorophenol POZs (Note that for phenol and thiophenol POZs the mode of addition is 1,2- and 2,3-addition, respectively). Therefore, this is expected to be the major reaction path at room temperature (rt) for chlorophenol POZs.

In addition, the Mulliken population analysis clearly shows that the terminal oxygen atoms of ozone carry a charge of -0.13 e^-. The electron-withdrawing capacity of the chlorine atom of 4-chlorophenol causes the carbon atom bound to this atom to have a Mulliken charge that is positive by as much as +0.87 e^-, whereas the other carbon atoms of 4-chlorophenol remain negatively charged (~-0.37 e^-). The attractive electrostatic forces between C_4 (following the same numbering of C atoms as in Fig. 5) and the terminal oxygen atoms of ozone make addition mode III the most favorable.

4.3.2 Reaction of Ozone with Dihydroxybenzene

In total, 72 dihydroxybenzene POZ isomers were computed. Twenty-five (25) most stable of these isomers are just within 3 kcal/mol of each other on the energy scale. Again, as was the case for the 17 most stable isomers of chlorophenol POZ, the computational errors at the level of theory that was used suggest that these isomers are nearly isoenergetic.

Table 15 Relative energies and thermochemical properties of the minima of the three (3) most stable dihydroxybenzene POZs at the B3LYP/6-311+G(2df) level.

Dihydroxybenzene POZs	**Structure**	E^{el} + ZPE (kcal/mol)	ΔH_r^o (kcal/mol)	ΔG_r^o (kcal/mol)
2-OH-*endo*-H-*exo*-O-*endo*-H-1,2-poz	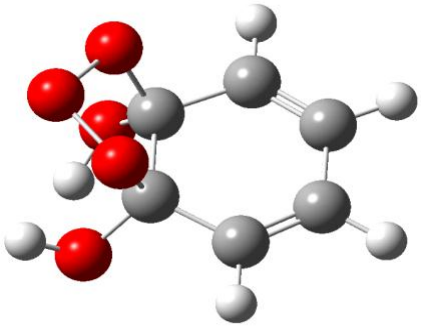	-22.1	-23.1	-9.9
3-OH-*endo*-H-*exo*-O-*endo*-H-3,4-poz	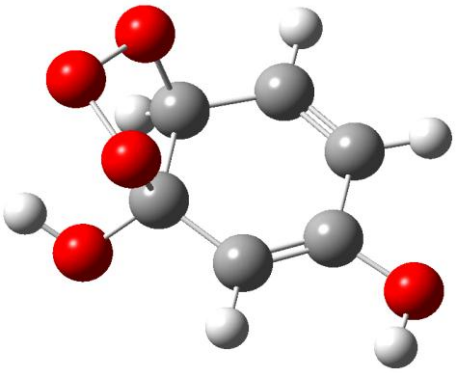	-21.0	-22.0	-8.6
4-OH-*exo*-H-*exo*-O-*endo*-H-1,2-poz	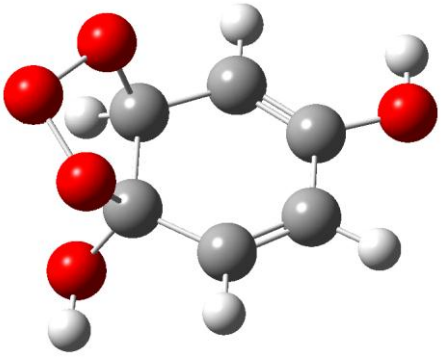	-21.0	-22.1	-8.5

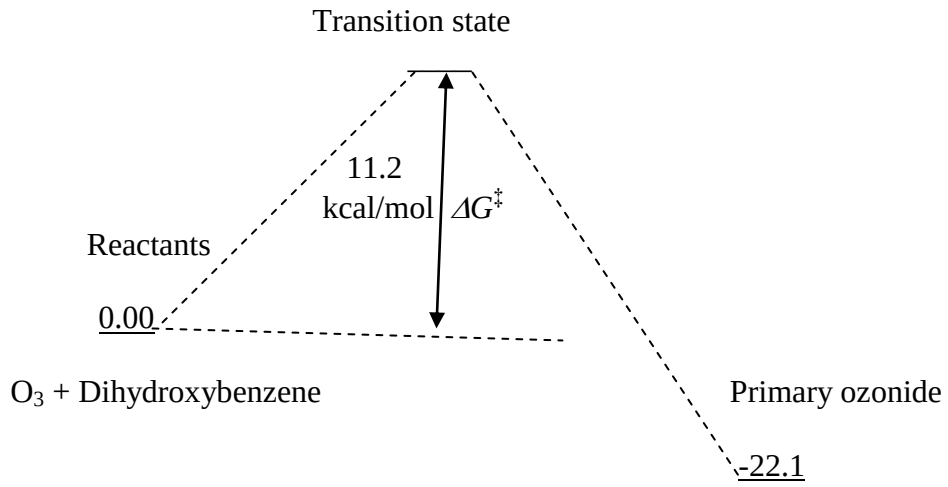

Figure 35 Activation barrier (kcal/mol) and exothermicity (kcal/mol) of 2-OH-*endo*-H-*exo*-O-*endo*-H-1,2-poz.

The transition state leading to the most stable dihydroxybenzene POZ has an activated Gibbs free energy of 11.2 kcal/mol, while the POZ, i.e. 2-OH-*endo*-H-*exo*-O-*endo*-H-1,2-poz, is located at 22.1 kcal/mol below the reactants (Figure 35). The calculated reaction enthalpy (ΔH_r^o) and Gibbs free energy (ΔG_r^o) for 2-OH-*endo*-H-*exo*-O-*endo*-H-1,2-poz are 23.1 kcal/mol and 9.9 kcal/mol below those of the reactants, respectively (Table 15). Further calculation shows that the rate constant, *k*, for the formation of 2-OH-*endo*-H-*exo*-O-*endo*-H-1,2-poz is 3.85 x 10^4 $atm^{-1}.s^{-1}$. Kinetically 3-OH-*endo*-H-*exo*-O-*endo*-H-3,4-poz is more favored because the TS leading to its formation has an activated Gibbs free energy of 8.3 kcal/mol which is lower than that of 2-OH-*endo*-H-*exo*-O-*endo*-H-1,2-poz (11.2 kcal/mol). Thermodynamically 2-OH-*endo*-H-*exo*-O-*endo*-H-1,2-poz appears to be more favored (Figure 36).

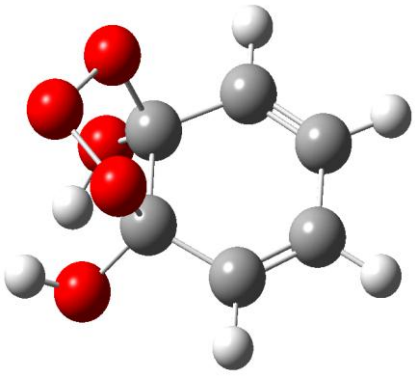

Figure 36 Geometry of most stable dihydroxybenzene POZ intermediate (2-OH-*endo*-H-*exo*-O-*endo*-H-1,2-poz).

The calculations suggest that mode I (1,2-addition) appears to be energetically most favorable for dihydroxybenzene POZs (Note that for chlorophenol, phenol and thiophenol POZs the mode of addition is 3,4-, 1,2- and 2,3-addition, respectively). Therefore, this is expected to be the major reaction path at rt for dihydroxybenzene POZs.

In addition, the Mulliken population analysis clearly shows that the terminal oxygen atoms of ozone carry a charge of -0.13 e^-. The carbon atoms (C_1 and C_2 (following the same numbering of C atoms as in Fig. 5)) bound to the hydroxyl groups of 1,2-dihydroxybenzene have a negative Mulliken charge (-0.198). It seems as if the electron-withdrawing capacities of the hydroxyl groups of 1,2-dihydroxybenzene have a little or no significant effect on the Mulliken charges of the carbon atoms bound to them. If they had a significant effect, the Mulliken charges of the carbon atoms bound to them would have been positive rather than being negative. The other carbon atoms of 1,2-dihydroxybenzene remain slightly negatively charged (~-0.08 e^-). It seems as if the need

for hydrogen bonding rather than the electrostatic forces between carbon atoms (C_1 and C_2) and the terminal oxygen atoms of ozone is the driving force behind the most favorable mode. This results in addition mode I being the most favorable.

4.3.3 Reaction of Ozone with Hydroxythiophenol

In total, 120 hydroxythiophenol POZ isomers were computed. Twenty-nine (29) most stable of these isomers are just within 3 kcal/mol of each other on the energy scale. Once again, as was the case for the 17 and 25 most stable isomers of the chlorophenol and dihydroxybenzene POZs, respectively, the computational errors at the level of theory that was used suggest that these isomers are nearly isoenergetic.

Table 16 Relative energies and thermochemical properties of the minima of the three (3) most stable hydroxythiophenol POZs at the B3LYP/6-311+G(2df) level.

Hydroxythiophenol POZs	**Structure**	$E^{el} + ZPE$	ΔH_r^o	ΔG_r^o
		(kcal/mol)		
2-OH-*exo*-H-*exo*-O-*endo*-H-2,3-poz	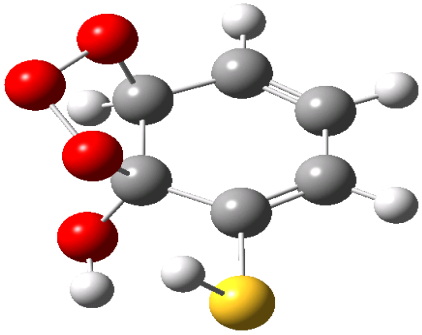	-19.4	-20.3	-6.9

3-OH-*exo*-H-*exo*-O-*endo*-H-2,3-poz	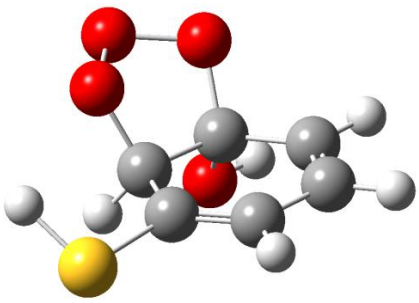	-18.9	-19.7	-6.7
6-OH-*exo*-H-*endo*-O-*endo*-H-2,3-poz	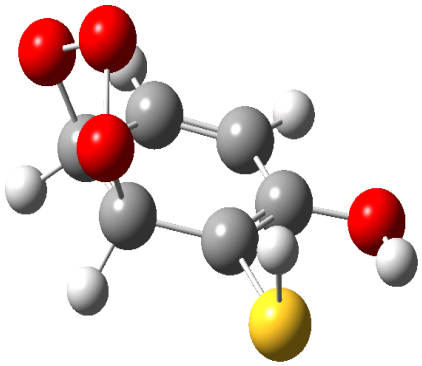	-18.8	-19.8	-6.7

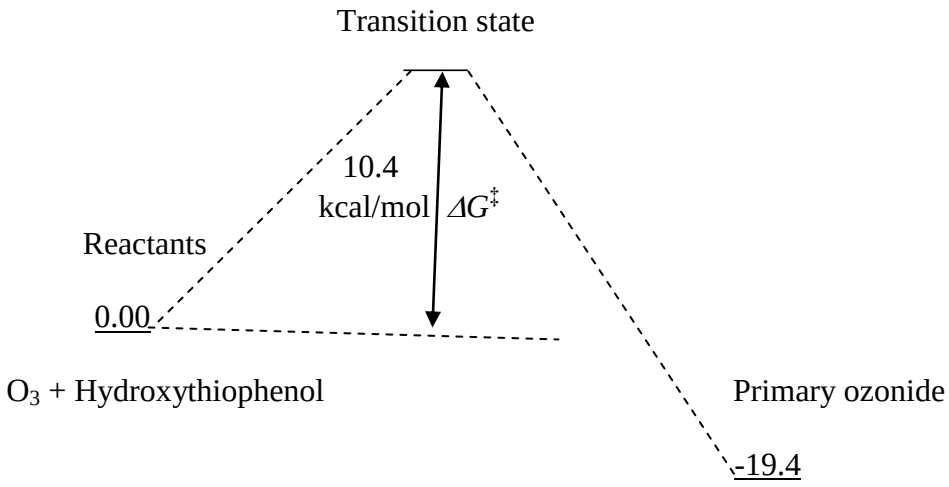

Figure 37 Activation barrier (kcal/mol) and exothermicity (kcal/mol) of 2-OH-*exo*-H-*exo*-O-*endo*-H-2,3-poz.

The transition state leading to the most stable hydroxythiophenol POZ has an activated Gibbs free energy of 10.4 kcal/mol, while the POZ, i.e. 2-OH-*exo*-H-*exo*-O-*endo*-H-2,3-poz, is located at 19.4 kcal/mol below the reactants (Figure 37). The calculated reaction enthalpy (ΔH_r^o) and Gibbs free energy (ΔG_r^o) for 2-OH-*exo*-H-*exo*-O-*endo*-H-2,3-poz are 20.3 kcal/mol and 6.9 kcal/mol below those of the reactants, respectively (Table 16). Further calculation shows that the rate constant, *k*, for the formation of 2-OH-*exo*-H-*exo*-O-*endo*-H-2,3-poz is 1.56 x 10^5 $atm^{-1}.s^{-1}$. Kinetically 6-OH-*exo*-H-*endo*-O-*endo*-H-2,3-poz is more favored because the TS leading to its formation has an activated Gibbs free energy of 9.4 kcal/mol which is lower than that of 2-OH-*exo*-H-*exo*-O-*endo*-H-2,3-poz (10.4 kcal/mol). Thermodynamically 2-OH-*exo*-H-*exo*-O-*endo*-H-2,3-poz appears to be more favored (Figure 38).

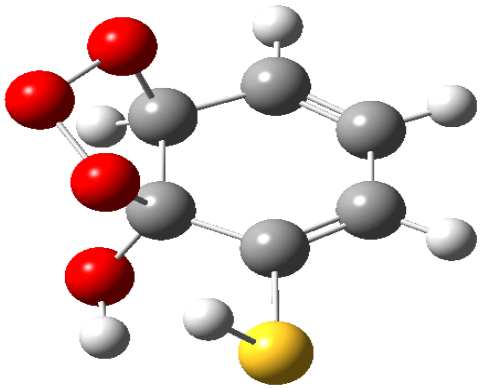

Figure 38 Geometry of most stable hydroxythiophenol POZ intermediate (2-OH-*exo*-H-*exo*-O-*endo*-H-2,3-poz).

The calculations suggest that mode II (2,3-addition) apopears to be energetically most favorable for hydroxythiophenol POZs (Note that for chlorophenol, dihydroxybenzene, phenol and thiophenol POZs the mode of addition is 3,4-, 1,2-, 1,2-

and 2,3-addition, respectively). Therefore, this is expected to be the major reaction path at rt for hydroxythiophenol POZs.

In addition, the Mulliken population analysis clearly shows that the terminal oxygen atoms of ozone carry a charge of -0.13 e^-. The electron-withdrawing capacity of the sulfhydryl group of 2-hydroxythiophenol causes the carbon atom bound to this group to have a Mulliken charge that is positive by as much as +1.56 e^-, whereas the other carbon atoms of 2-hydroxythiophenol (except C_3 (following the same numbering of C atoms as in Fig. 5)) remain negatively charged (~-0.63 e^-). It seems as if the electron-withdrawing capacity of the hydroxyl group of 2-hydroxythiophenol has a little or no significant effect on the Mulliken charge of the carbon atom (C_2) bound to it. If it had a significant effect, the Mulliken charge of C_2 would have been positive rather than being negative (-1.15 e^-). The hydrogen atom of the sulfhydryl group of 2-hydroxythiophenol being perpendicular to the benzene ring makes it very difficult for C_1 to bind to any of the terminal oxygen atoms of ozone, since this would result into steric hindrance and hence an unstable product. The attractive electrostatic forces between the next most positive carbon atom on the benzene ring (in this case C_3 with a Mulliken charge of 0.37 e^-) and the terminal oxygen atoms of ozone make addition mode II the most favorable.

When it comes to the stability of a molecule or species, it can easily be checked by verifying whether there exists imaginary (negative) frequencies by running a frequency calculation. Negative frequencies indicate the stability of a molecule or species. A stable molecule has no negative frequencies. It was, however, observed that

transition states have one negative frequency which is in line with the theory (Tomberg, n.d.). This means that a transition state is not a stable species because it has one (1^{st}-order saddle point) negative frequency. In fact, a transition state is a structure in which the reactant moieties are loosely bound and still needs to become a product in order for it to be stable. It is an intermediate between the reactant(s) and the product(s).

There is a quantity known as the force constant of a vibrational mode which is a measure of the 'stiffness' of the molecule towards the vibrational mode – the harder it is to stretch or bend the molecule in the manner of that mode, the bigger is that force constant. Going from the transition state to the product(s) along the reaction coordinate, the surface slopes downwards. This implies that the force constant for this mode is negative. Since a frequency calculation involves taking the square root of a force constant, and the square root of a negative number is an imaginary number, a transition state has one imaginary (negative) frequency, corresponding to the reaction coordinate.

In terms of enthalpies of reactions (ΔH_r^o), the ozonolysis of dihydroxybenzene will evolve the most heat followed by that of hydroxythiophenol and then that of chlorophenol. In terms of Gibbs free energies (ΔG_r^o), the order of the decrease in spontaneity of the ozonolysis reactions will be the same as that of the decrease in enthalpies of the reactions. However, in terms of the Gibbs free energies of activation ($\Delta G^{\ddagger}$), the barrier in getting from the reactants to the products increase in the following order: Hydroxythiophenol < Dihydroxybenzene < Chlorophenol

This means that the ozonolysis reaction of hydroxythiophenol will be the fastest followed by that of dihydroxybenzene and then that of chlorophenol.

Theory suggests that the chlorophenol ring would be expected to be less reactive than the dihydroxybenzene and hydroxythiophenol rings. The reason for this is that the chlorine atom in the chlorophenol ring is a deactivating atom meaning that the chlorine atom will cause the chlorophenol ring to undergo ozonolysis much slower than the dihydroxybenzene or hydroxythiophenol rings. This is in agreement with what is deduced from the calculations that were done. Theory also suggests that the dihydroxybenzene ring should be more reactive than that of the hydroxythiophenol, because the dihydroxybenzene ring contains two strongly activating hydroxyl groups, whereas the hydroxythiophenol ring contains one strongly activating hydroxyl group and one sulfhydryl group that is not as strongly activating as that of the hydroxyl group because of the sulfhydryl group being less polar compared to the hydroxyl group (Solomons & Fryhle, 2000). However, the order in which the calculated Gibbs free energies of activation arrange these compounds (dihydroxybenzene and hydroxythiophenol) differ from this expectation. This could suggest that the level of theory (B3LYP) at which the calculations were carried out might not be as good as was expected, but is nevertheless still decent. All in all, in order to obtain more precise and reliable results the use of CCSD(T) might be a necessity.

CHAPTER 5

CONCLUSIONS

The 1,3-cycloaddition of ozone to phenol and thiophenol derivatives was computationally modeled. Specifically, the stability, bonding and thermochemical properties of the primary ozonides resulting from the ozonolysis of chlorophenol, dihydroxybenzene and hydroxythiophenol were computationally investigated.

For the chlorophenol POZs, the 4-Cℓ-*endo*-H-*exo*-O-3,4-poz appears to be the most stable POZ. The transition state that leads to the aforementioned chlorophenol POZ has a barrier of 56.8 kcal/mol while the POZ is located at 19.1 kcal/mol below the reactants. The calculated reaction enthalpy (ΔH_r^o) and Gibbs free energy (ΔG_r^o) are 20.0 kcal/mol and 6.8 kcal/mol below those of the reactants, respectively. The calculations suggest that mode III (3,4-addition) is energetically most favorable for chlorophenol POZs. Therefore addition to the 3,4 position is expected to be the major reaction path at room temperature for chlorophenol POZs.

For the dihydroxybenzene POZs, the 2-OH-*endo*-H-*exo*-O-*endo*-H-1,2-poz appears to be the most stable POZ. The transition state leading to the most stable dihydroxybenzene POZ has a barrier of 11.2 kcal/mol while the POZ is located at 22.1 kcal/mol below the reactants. The calculated reaction enthalpy (ΔH_r^o) and Gibbs free energy (ΔG_r^o) are 23.1 kcal/mol and 9.9. kcal/mol below those of the reactants, respectively. The calculations suggest that mode I (1,2-addition) is energetically most favorable for dihydroxybenzene POZs. Therefore addition to the 1,2 position is expected to be the major reaction path at room temperature for dihydroxybenzene POZs.

For the hydroxythiophenol POZs, the 2-OH-*exo*-H-*exo*-O-*endo*-H-2,3-poz appears to be the most stable POZ. The transition state leading to the most stable hydroxythiophenol POZ has a barrier of 10.4 kcal/mol while the POZ is located at 19.4 kcal/mol below the reactants. The calculated reaction enthalpy (ΔH_r^o) and Gibbs free energy (ΔG_r^o) are 20.3 kcal/mol and 6.9 kcal/mol below those of the reactants, respectively. The calculations suggest that mode II (2,3-addition) is energetically most favorable for hydroxythiophenol POZs. Therefore addition to the 2,3 position is expected to be the major reaction path at room temperature for hydroxythiophenol POZs.

The aforementioned results imply that hydroxythiophenol ozonolysis is more favored. This is based on the barriers of the transition states or the Gibbs free energies of activation. The calculations show that hydroxythiophenol should react slightly faster than dihydroxybenzene followed by chlorophenol. Thermodynamic stability of the POZs also follow the same order. This is due to the -SH group being less polar compared to the -OH group.

The results here are obtained at a decent level of theory, however, the energy separation of isomers can be improved at a higher level of theory. The thermochemical properties obtained here are the first for this set of compounds computationally or experimentally.

Experimentally, the results discussed in this thesis would have been more difficult to obtain as these compounds enjoy only a transient existence. The data

produced in this work will help and complement future experimental investigations involving the ozonolysis of substituted phenol and thiophenol.

The limitation of this study was that the computational resources at UNAM are very much limited and that made it impossible for this research to be conducted at the highest level of theory. In future, with more and advanced computational resources at UNAM, the calculations can be sophisticated by using coupled cluster (CCSD(T)) approach and very large one-particle basis set.

CHAPTER 6

REFERENCES

Archibong, E. F. (2007, April 16). *Basis Sets*. Unpublished lecture notes, University of Namibia, Windhoek, Namibia.

Bailey, P. S. (1978). *Ozonation in organic chemistry*. New York: Academic Press.

Ball, P. (n.d.). *Column: The crucible*. Retrieved March 17, 2011, from http://www.rsc.org/chemistryworld/Issues/2011/March/ColumnThecrucible.asp

Carey, F. A. (2000). *Organic Chemistry* (4th ed.). USA: The McGraw-Hill Companies. Retrieved September 30, 2009, from http://www.mhhe.com/physsci/chemistry/carey/student/olc/ch24 phenolpreparations.html

Chang, R. (1998). *Chemistry* (6th ed.). USA: James M. Smith.

Chemical Heritage Foundation. (2001). *Making and Destroying Ozone*. Philadelphia: Author.

Cramer, C. J. (2004). *Essentials of Computational Chemistry: Theories and Models* (2nd ed.).West Sussex, England: Wiley.

Curtiss, L. A., & Pople, J. A. (1999). *Recent Advances in Computational Thermochemistry and Challenges for the future*. Washington, D. C., USA: US Department of Energy.

Davidson, E. R., & Feller, D. (1986). Basis Set Selection for Molecular Calculations. *Chemical Reviews*, *86*(4), 681-696.

Density-Functional Theory. (n.d.). Retrieved August 26, 2009, from http://dissertations.ub.rug.nl/FILES/ faculties/science/2006/j.a.berger/01_c1.pdf

Drees, M. (2008, September 12). *Introduction to Computational Chemistry for Experimental Chemists…(Part 1/2)*. Paper presented at the 11th Seminar, Garching, Germany.

Electronic Structure calculations in Gaussian. (n.d.). Retrieved January 21, 2013, from http://collum.chem.cornell.edu/documents/Gaussian_optimization.pdf

European Commission. (2003). *Ozone-climate interactions – Air pollution research report No. 81*. Luxembourg: Office for Official Publications of the European Communities. Retrieved January 17, 2013, from http://xweb.geos.ed.ac.uk/~dstevens/publications/isaksen_ozone_climate_ec03.pdf

Franken, L. (2005). The Application of Ozone Technology for Public Health and Industry. p. 1-16. Retrieved January 15, 2013, from http://www.emo3.com/files/Laurence%20Franken,%20Kansas%20State%20University.pdf

Freudenrich, C. (2001). Ozone Reactions. *The Chemical Ozone*. Retrieved September 09, 2009, from http://www.howstuffworks.com/ozone-pollution.htm

Gotwals, R. R., & Sendlinger, S. C. (2007). Chapter 15: Thermochemistry. *Guide to Molecular Modeling*. Retrieved August 19, 2009, from http://chemistry.ncssm.edu/book/Chap15Thermo.pdf

Harrison, K. (2007). *Phenol*. Retrieved August 19, 2009, from http://www.3dchem.com/molecules. asp?ID=100

Hay, P. J., & Goddard III, W. A. (1972). Theoretical results for the excited states of ozone. *Chemical Physics Letters*, *14*(1), 46-48.

Hendrickx, M. F. A., & Vinckier, C. (2003). 1,3-Cycloaddition of Ozone to Ethylene, Benzene, and Phenol: A Comparative ab Initio Study. *Journal of Physical Chemistry A*, *107*, 7574-7580.

Industries. (n.d.). Retrieved January 15, 2013, from http://www.oxyzone.com.au/industries_retail_fruit-veg.php

Koch, W., & Holthausen, M. C. (2000). *A Chemist's Guide to Density Functional Theory* (2nd ed.). Germany: Wiley-VCH.

Labanowski, J. K. (1996). *Simplified Introduction to Ab Inition Basis Sets: Terms and Notation*. Retrieved September 28, 2009, from http://www.ccl.net/cca/documents/basis-sets/basis.html

Lenntech Water treatment & purification Holding B. V. (2009). *Ozone applications in Drinking Water*. Retrieved February 19, 2010, from http://www.lenntech.com/library/ozone/drinking/ozone-applications-drinking-water.htm#ixzz0gMpgsFk0

Leuckart Thiophenol Reaction. (n.d.). Retrieved September 30, 2009, from http://www.organic-chemistry.org/namedreactions/leuckart-thiophenol-reaction.shtm

Marinelli, L., & Worth, W. (1994). Global Warming: A White Paper on the Science, Policies and Control Technologies that impact the U.S. Semiconductor Industry. Retrieved January 16, 2013, from http://www.sematech.org/docubase/document/2074atr.pdf

Matta, C. F., & Boyd, R. J. (2007). *An Introduction to the Quantum Theory of Atoms in Molecules*. Retrieved January 12, 2011, from http://media.wiley.com/product_data/excerpt/86/35273074/3527307486.pdf

Murphy, J. (2003). *Speaking out to a wall of silence*. Retrieved March 17, 2011, from http://www.scientific-computing.com/features/feature.php?feature_id=114

Mvula, E., & Von Sonntag, C. (2003). Ozonolysis of phenols in aqueous solution. *Organic and Biomolecular Chemistry, 1,* 1749-1756.

Mvula, E. N. (2002). *The Reactions of Ozone with Compounds Relevant to Drinking-Water Processing: Phenol and its Derivatives*. Unpublished doctoral dissertation, University of Namibia, Windhoek, Namibia.

Mvula, E. N., Kandawa-Schulz, M., & Archibong, E. F. (2006). *The reaction of ozone with phenol. Part 1. Structure and Stability of the Primary Ozonide (POZ)*. Unpublished results. Department of Chemistry and Biochemistry, University of Namibia, Windhoek, Namibia.

Ochterski, J. W. (2000). *Thermochemistry in Gaussian*. Retrieved August 27, 2009, from http://www.gaussian.com/g_whitepap/thermo.htm

The Ozone. (n.d.). Retrieved August 12, 2009, from http://www.tesisenxarxa.net/TESIS_UB/AVAILABLE/TDX-0311103-135423//TOL167B.pdf

Production of Thiophenols. (2009). Retrieved October 01, 2009, from http://www.freepatentsonline.com/ 4088698.html

Reactions of alkenes (II). (n.d.). Retrieved October 03, 2009, from www.science.ru.nl/chemistry/onderwijs/ oc1b/College%20H09.ppt

Razumovskii, S. D., & Zaikov, G. E. (n.d.). Kinetics and Mechanism of the Reaction of Ozone with Aromatic Hydrocarbons. 2524-2529.

Samuni, U., Fraenkel, R., Haas, Y., Fajgar, R., & Pola, J. (1996). Environmental Effects on the Formation of Primary and Secondary Ozonides of Ethylene at Cryogenic Temperatures. *Journal of American Chemical Society, 118*, 3687-3697.

Scannell, C., Hurtmans, D., Boynard, A., Hadji-Lazaro, J., George, M., Delcloo, A., etal. (2001). A review of the ozone hole from 2008 to 2010 as observed by IASI. Atmospheric Measurement Techniques, 4717-4752. doi: 10.5194/amtd-4-4717-2011

Sciencelab. (2008). *Thiophenol Material Safety Data Sheet*. Houston, Texas: Author.

Session 2: Basis Sets. (2008). Retrieved September 03, 2009, from http://www.computationalscience.org/ccce/Lesson2/Notebook%202%20Lecture.pdf

Simons, J. (1991). An Experimental Chemists Guide to *ab Initio* Quantum Chemistry. *Journal of Physical Chemistry, 95*, 1017-1029

Solomons, F. & Fryhle, C. (2000). *Organic Chemistry* (7th ed.). USA: John Wiley & Sons, Inc.

Stattersfield, E. (2001a). Ozone Reactions. *The Chemical Ozone*. Retrieved September 09, 2009, from http://www.chm.bris.ac.uk/motm/ozone/CHEM.htm

Stattersfield, E. (2001b). *High Level Ozone*. Retrieved September 24, 2009, from http://www.chm. bris.ac. uk/motm/ozone/high.htm

Stattersfield, E. (2001c). *Low Level Ozone*. Retrieved September 24, 2009, from http://www.chm.bris.ac. uk/motm/ozone/Low.htm

Thiophenol. (2007). Retrieved September 30, 2009, from http://www.orgsyn.org/orgsyn/prep.asp?prep= cv1p0504

Thiophenol. (2008). Retrieved August 19, 2009, from http://chemicalland21.com/lifescience/phar /THIOPHENOL.htm

Tomas, A., Olariu, R., Barnes, I., Bejan, I., Geiger, H., & Mocanu, R. (2001). *Atmospheric Chemistry of Benzenediols: Reaction with Ozone*. Retrieved January 06, 2010, from http://imk-aida.fzk.de /CMD /AR2001/AR01Barnes.pdf

Tomberg, A. (n.d.). *Gaussian 09W Tutorial*. Retrieved January 16, 2013, from http://barrett-group.mcgill.ca/tutorials/Gaussian%20tutorial.pdf

Tropospheric Ozone, the Polluter. (n.d.). Retrieved September 09, 2009, from http://www.ucar.edu/learn/1_7_1.htm

Velders, G. J. M., Slaper, H., Pearce, D. W., & Howarth, A. (n.d.). *Technical Report on Stratospheric Ozone Depletion*. (Tech. Rep. No. 481505011). Bilthoven: Environment Directorate-General of the European Commission.

World Bank Group. (1998). *Pulp and Paper Mills*. Retrieved January 18, 2013, from http://www.ifc.org/ifcext/enviro.nsf/attachmentsbytitle/gui_pulp_wb/$file/pulp_ppah.pdf

APPENDICES

APPENDIX A Structures of POZs.

Chlorophenol POZs

1,2-Addition POZs

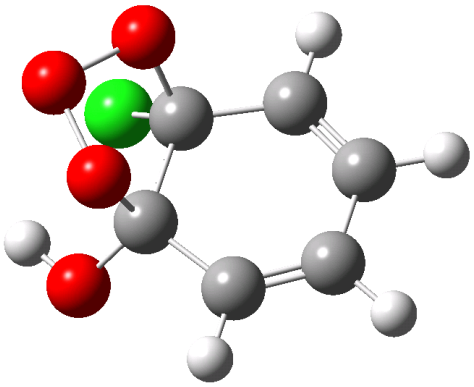

Figure 1A: 2-endo-H-exo-O-1,2-poz

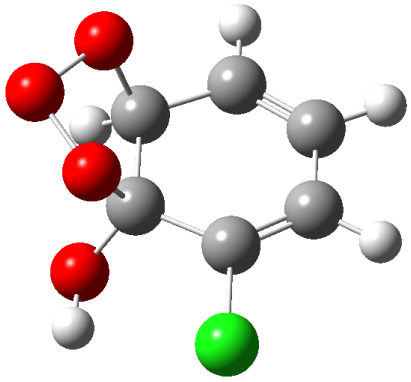

Figure 1B: 6-exo-H-exo-O-1,2-poz

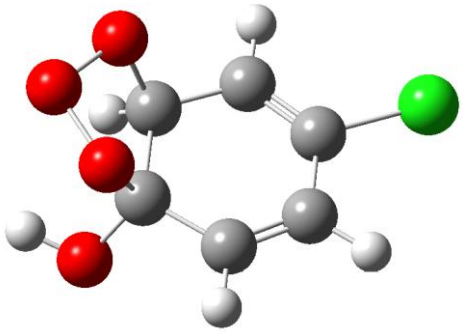

Figure 1C: 4-endo-H-exo-O-1,2-poz

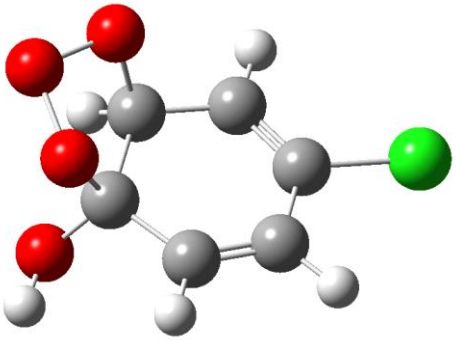

Figure 1D: 4-exo-H-exo-O-1,2-poz

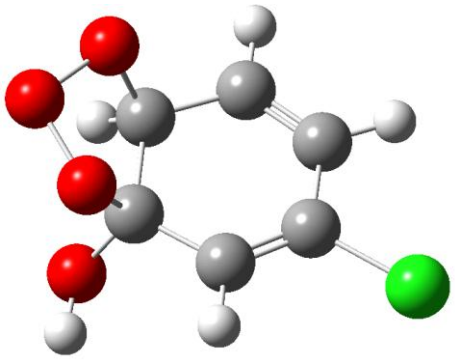

Figure 1E: 5-exo-H-exo-O-1,2-poz

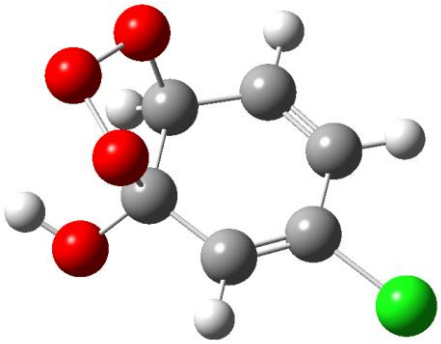

Figure 1F: 5-endo-H-exo-O-1,2-poz

2,3-Addition POZs

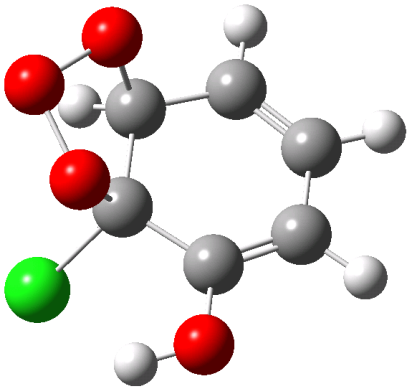

Figure 2A: 2-endo-H-exo-O-2,3-poz

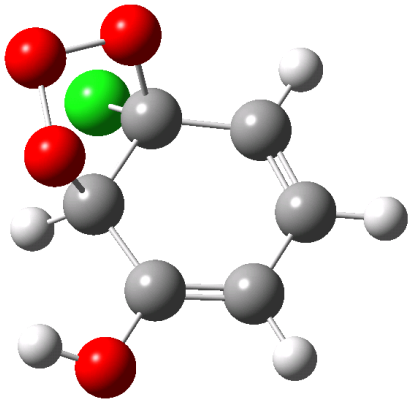

Figure 2B: 3-endo-H-exo-O-2,3-poz

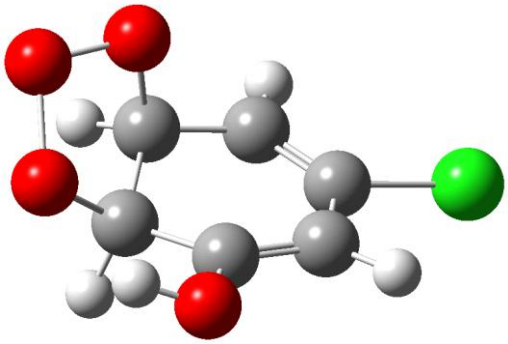

Figure 2C: 5-endo-H-exo-O-2,3-poz

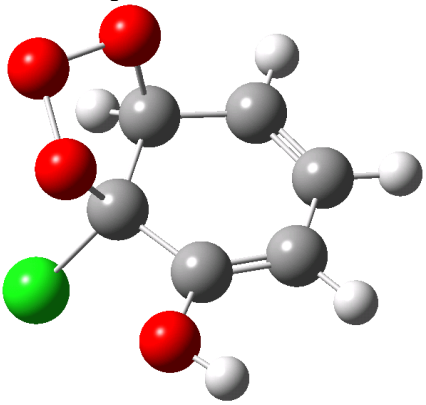

Figure 2D: 2-exo-H-exo-O-2,3-poz

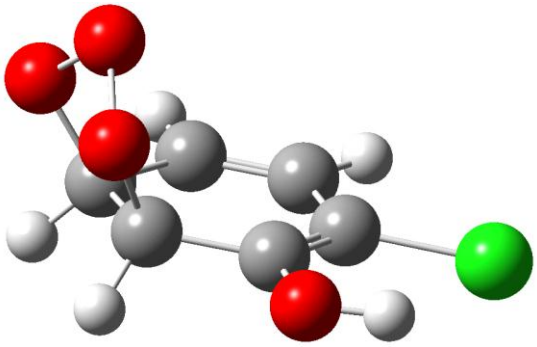

Figure 2E: 6-exo-H-endo-O-2,3-poz

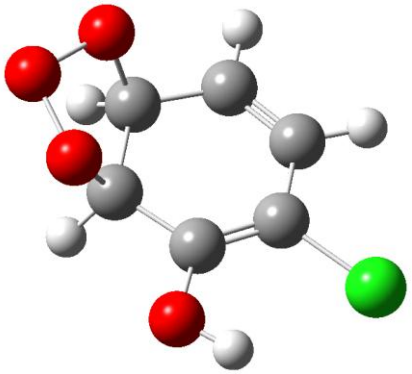

Figure 2F: 6-exo-H-exo-O-2,3-poz

3,4-Addition POZs

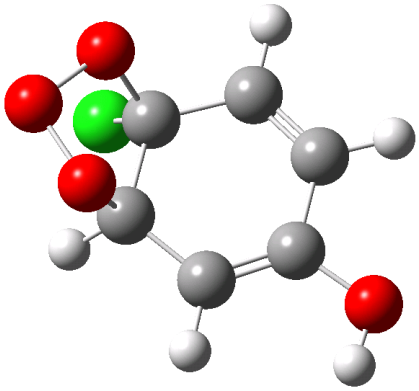

Figure 3A: 4-endo-H-exo-O-3,4-poz

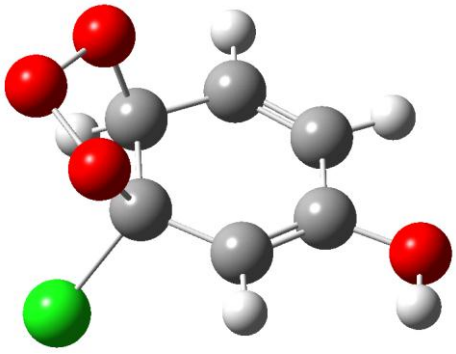

Figure 3B: 3-endo-H-exo-O-3,4-poz

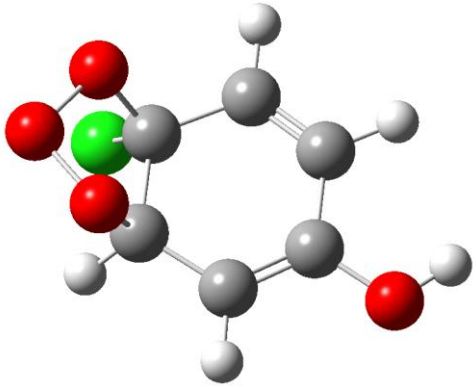

Figure 3C: 4-exo-H-exo-O-3,4-poz

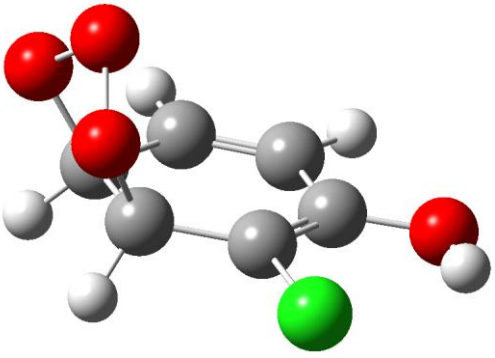

Figure 3D: 2-endo-H-endo-O-3,4-poz

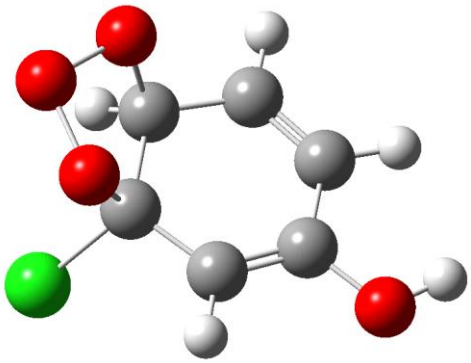

Figure 3E: 3-exo-H-exo-O-3,4-poz

Dihydroxybenzene POZs

1,2-Addition POZs

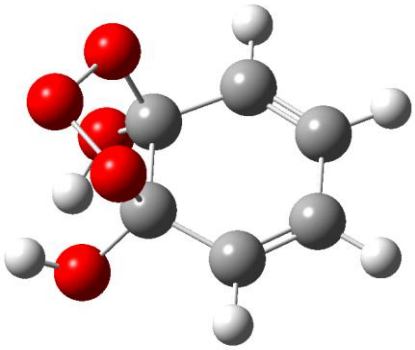

Figure 4A: 2-endo-H-exo-O-endo-H-1,2-poz

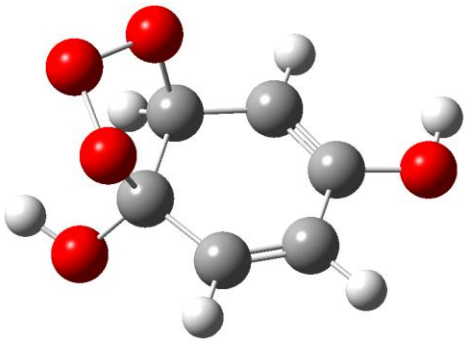

Figure 4B: 4-endo-H-exo-O-endo-H-1,2-poz

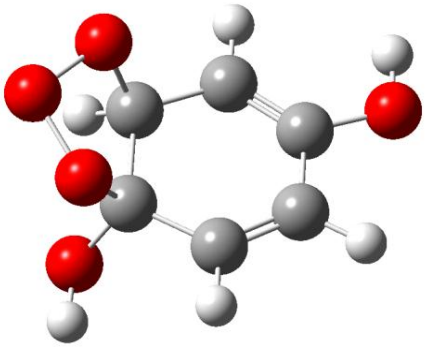

Figure 4C: 4-exo-H-exo-O-endo-H-1,2-poz

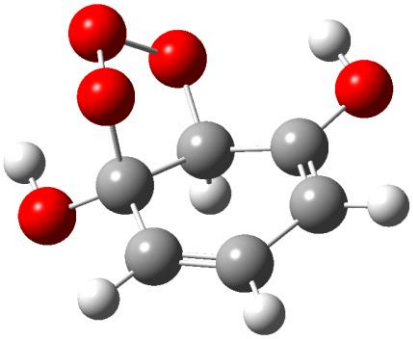

Figure 4D: 3-endo-H-exo-O-endo-H-1,2-poz

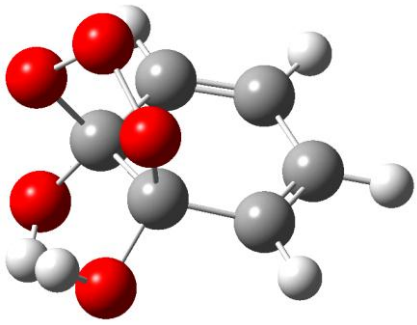

Figure 4E: 2-endo-H-endo-O-endo-H-1,2-poz

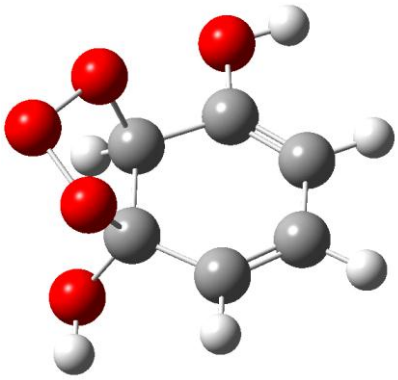

Figure 4G: 3-exo-H-exo-O-exo-H-1,2-poz

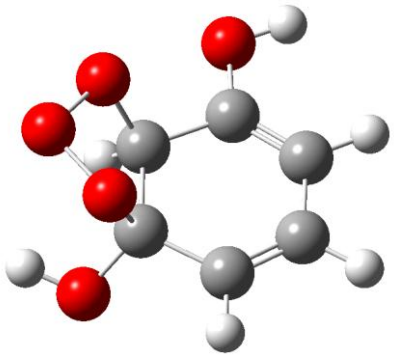

Figure 4H: 3-endo-H-exo-O-exo-H-1,2-poz

2,3-Addition POZs

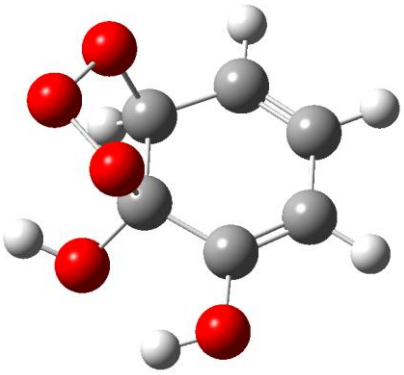

Figure 5A: 2-endo-H-exo-O-endo-H-2,3-poz

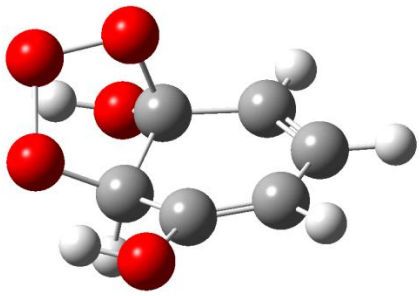

Figure 5B: 3-endo-H-exo-O-endo-H-2,3-poz

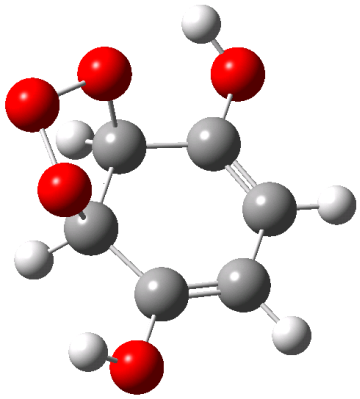

Figure 5C: 4-endo-H-exo-O-endo-H-2,3-poz

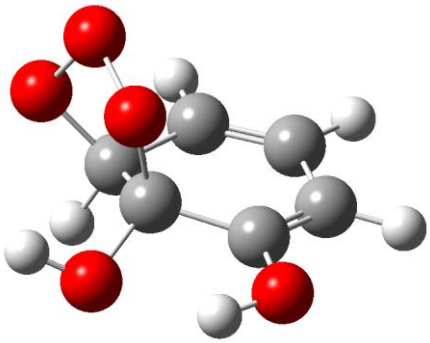

Figure 5D: 2-endo-H-endo-O-endo-H-2,3-poz

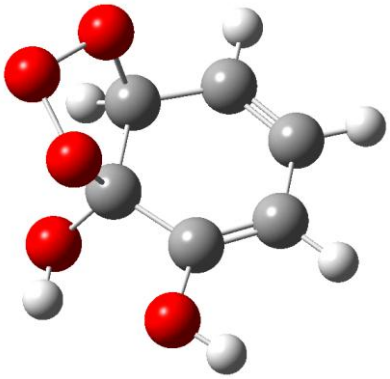

Figure 5E: 2-exo-H-exo-O-exo-H-2,3-poz

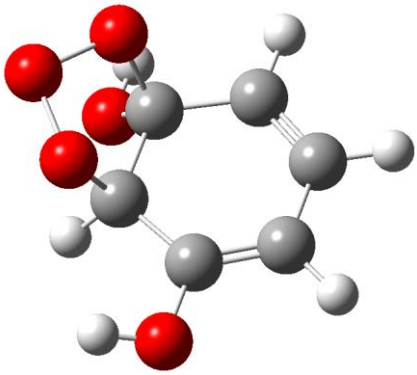

Figure 5F: 3-endo-H-exo-O-exo-H-2,3-poz

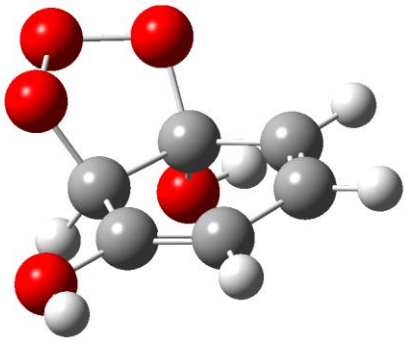

Figure 5G: 3-exo-H-exo-O-exo-H-2,3-poz

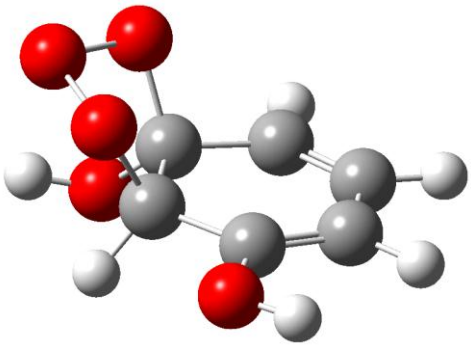

Figure 5H: 3-exo-H-exo-O-endo-H-2,3-poz

3,4-Addition POZs

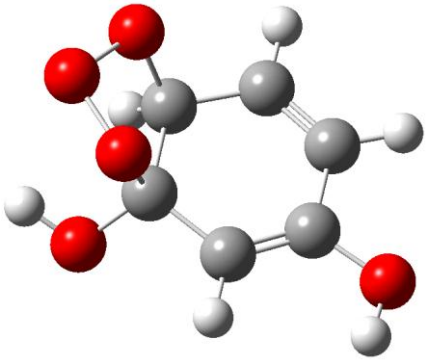

Figure 6A: 3-endo-H-exo-O-endo-H-3,4-poz

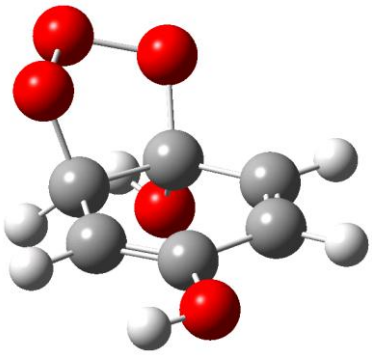

Figure 6B: 4-endo-H-exo-O-endo-H-3,4-poz

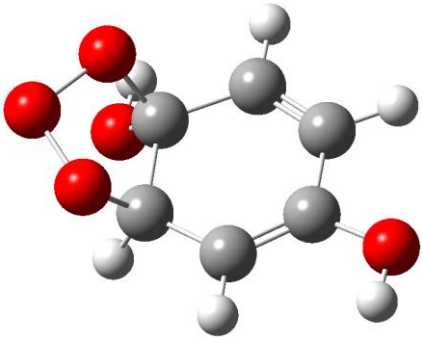

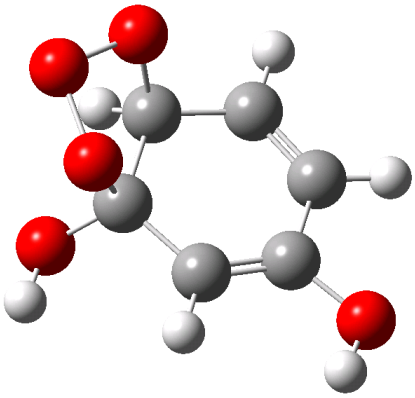

Figure 6C: 4-endo-H-exo-O-exo-H-3,4-poz Figure 6D: 3-endo-H-exo-O-exo-H-3,4-poz

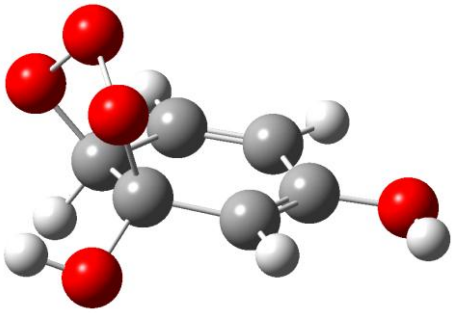

Figure 6E: 3-endo-H-endo-O-endo-H-3,4-poz

Hydroxythiophenol POZs

1,2-Addition POZs

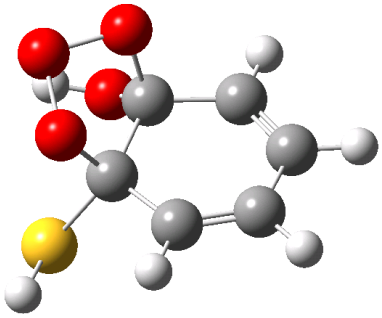

Figure 7A: 2-endo-H-exo-O-exo-H-1,2-poz

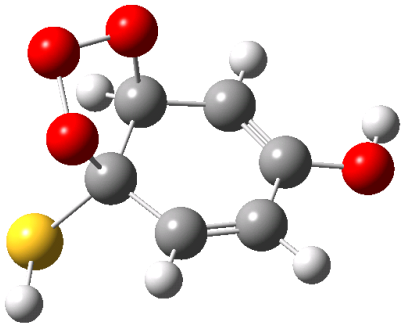

Figure 7B: 4-endo-H-exo-O-exo-H-1,2-poz

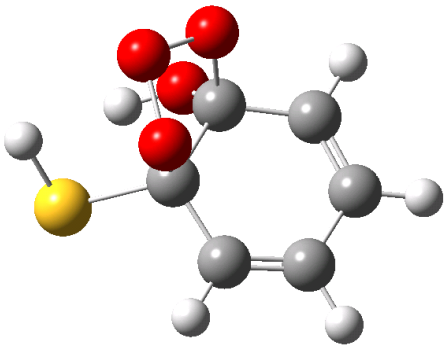

Figure 7C: 2-exo-H-exo-O-endo-H-1,2-poz

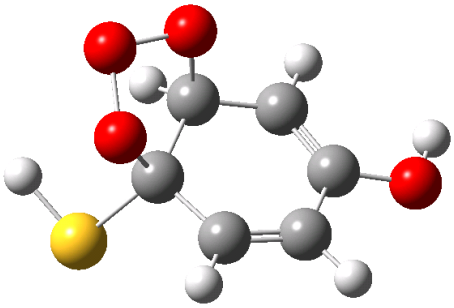

Figure 7D: 4-endo-H-exo-O-endo-H-1,2-poz

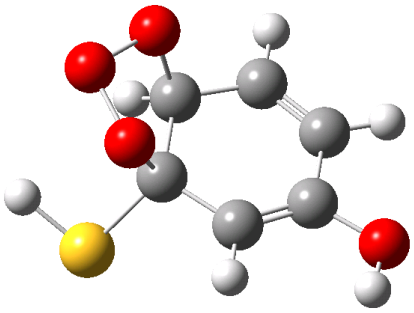

Figure 7E: 5-endo-H-exo-O-endo-H-1,2-poz

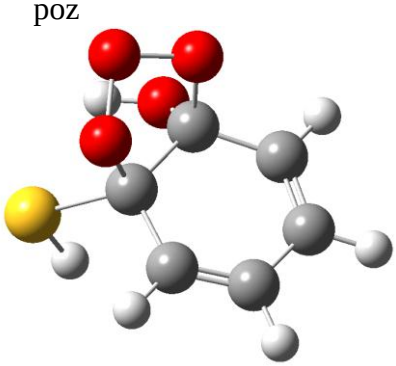

Figure 7F: 2-endo-H-exo-O-endo-H-1,2-poz

2,3-Addition POZs

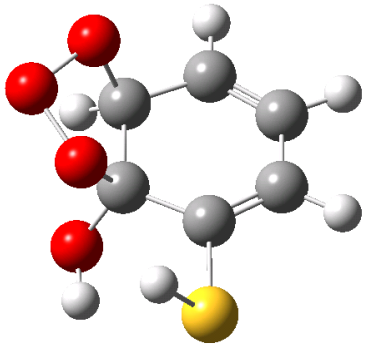

Figure 8A: 2-exo-H-exo-O-endo-H-2,3-poz

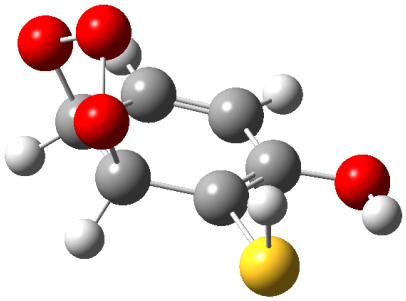

Figure 8B: 6-exo-H-endo-O-endo-H-2,3-poz

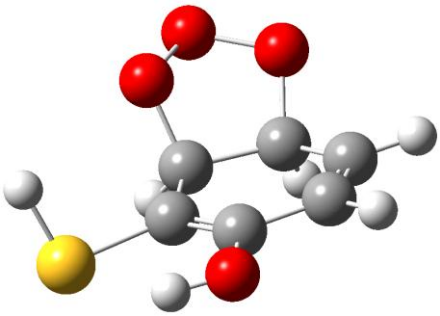

Figure 8C: 6-exo-H-exo-O-endo-H-2,3-poz

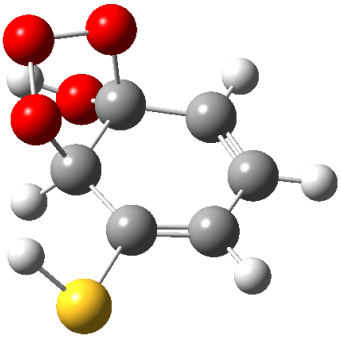

Figure 8D: 3-endo-H-exo-O-endo-H-2,3-poz

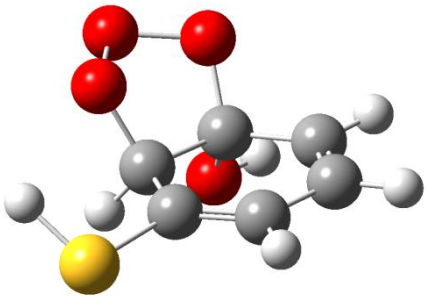

Figure 8E: 3-exo-H-exo-O-endo-H-2,3-poz

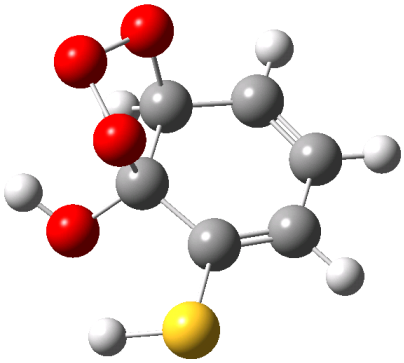

Figure 8F: 2-endo-H-exo-O-endo-H-2,3-poz

3,4-Addition POZs

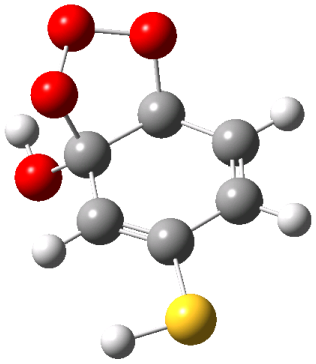

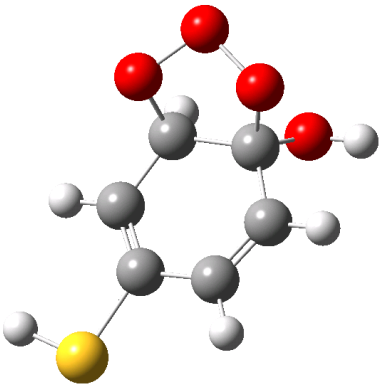

Figure 9A: 3-endo-H-exo-O-exo-H-3,4-poz Figure 9B: 4-exo-H-exo-O-exo-H-3,4-poz

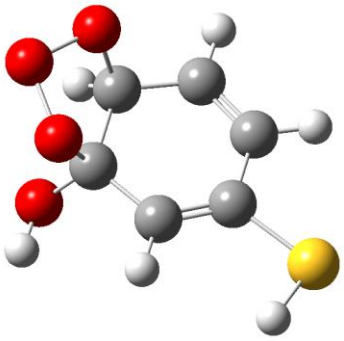

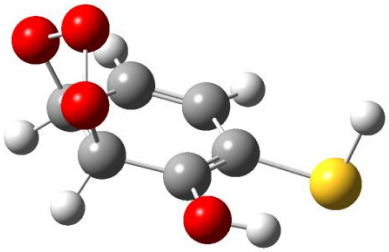

Figure 9C: 3-exo-H-exo-O-exo-H-3,4-poz Figure 9D: 2-exo-H-endo-O-endo-H-3,4-poz

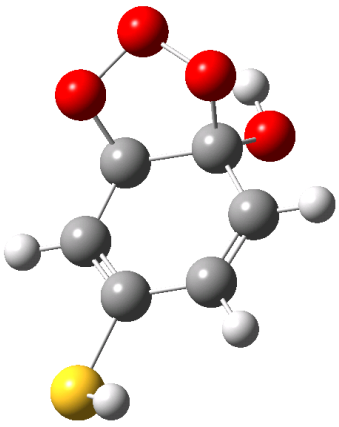

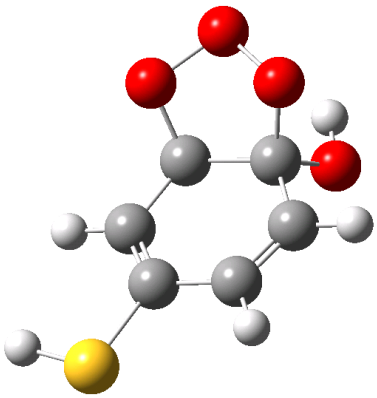

Figure 9E: 4-endo-H-exo-O-endo-H-3,4-poz Figure 9F: 4-endo-H-exo-O-exo-H-3,4-poz

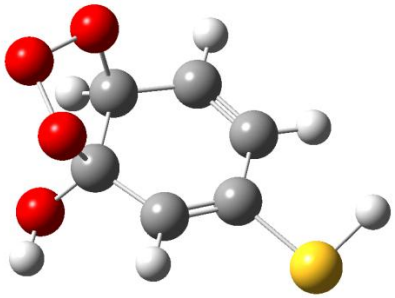

Figure 9G: 3-exo-H-exo-O-endo-H-3,4-poz

APPENDIX B Transition states.

Chlorophenol POZs TS

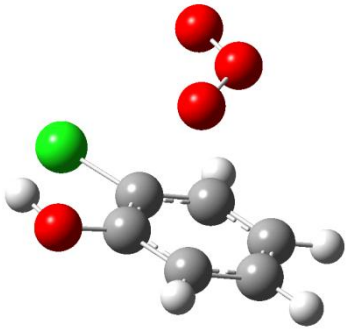

Fig 10A: 2-endo-H-exo-O-1,2-poz-ts

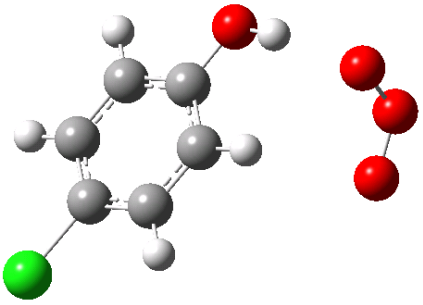

Fig 10B: 4-exo-H-exo-O-1,2-poz-ts

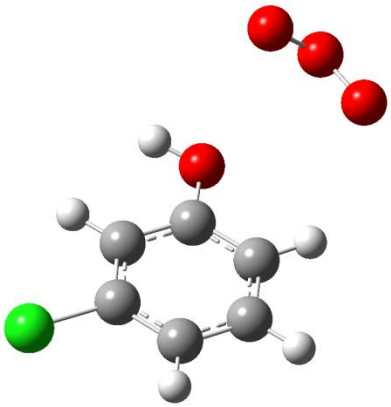

Fig 10C: 5-exo-H-exo-O-1,2-poz-ts

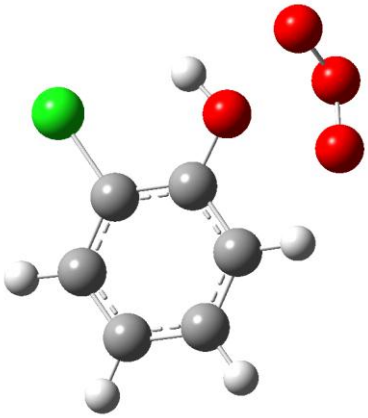

Fig 10D: 6-exo-H-exo-O-1,2-poz-ts

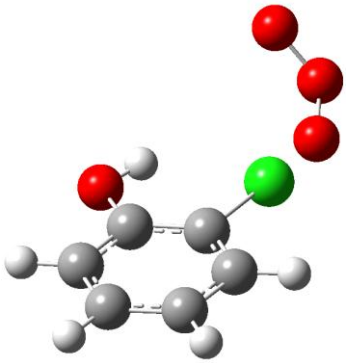

Fig 10E: 2-endo-H-exo-O-2,3-poz-ts

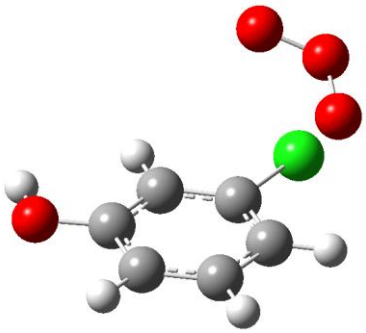

Fig 10F: 3-endo-H-exo-O-3,4-poz-ts

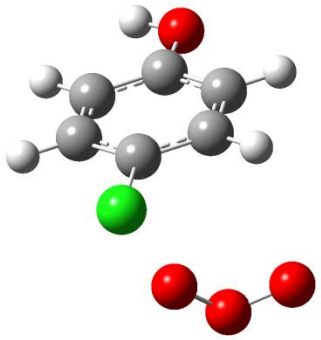

Fig 10G: 4-endo-H-exo-O-3,4-poz-ts

Dihydroxybenzene POZs TS

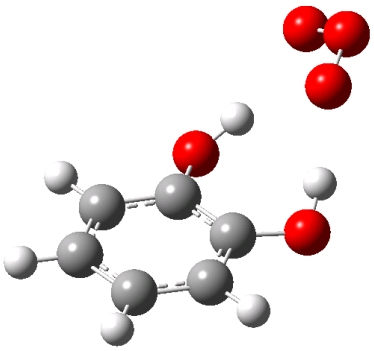

Figure 11A: 2-endo-H-exo-O-endo-O-1,2-poz-ts

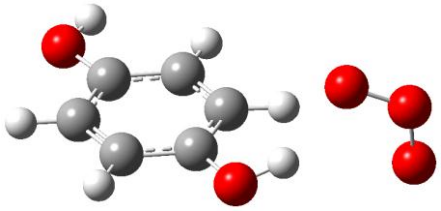

Figure 11B: 4-endo-H-exo-O-endo-O-1,2-poz-ts

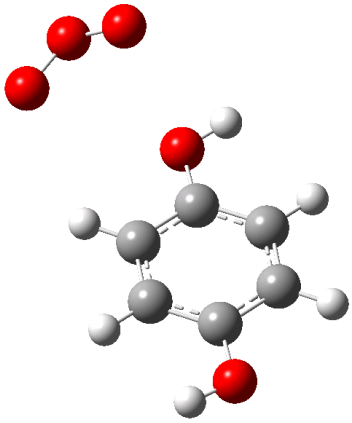

Figure 11C: 4-exo-H-exo-O-endo-O-1,2-poz-ts

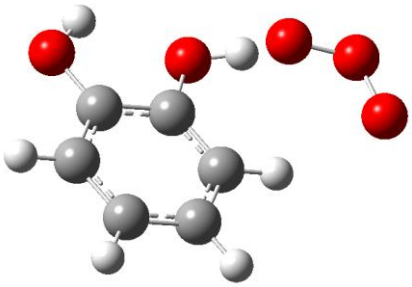

Figure 11D: 2-endo-H-exo-O-endo-O-2,3-poz-ts

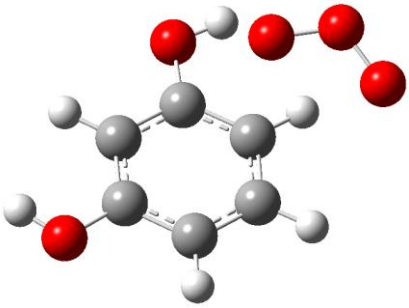

Figure 11E: 3-endo-H-exo-O-endo-O-3,4-poz-ts

Hydroxythiophenol POZs TS

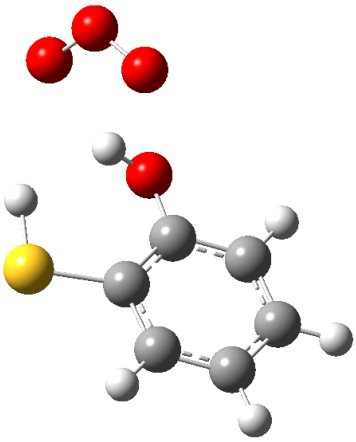

Figure 12A: 2-exo-H-exo-O-endo-O-2,3-poz-ts

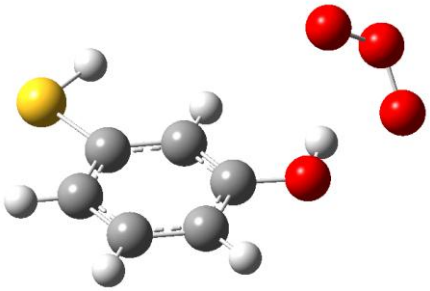

Figure 12B: 3-endo-H-exo-O-endo-O-2,3-poz-ts

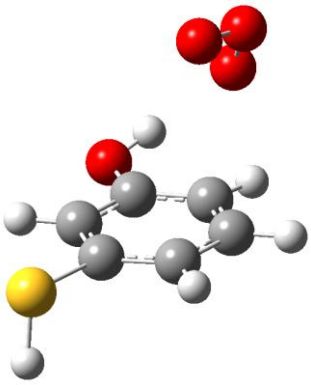

Figure 12C: 3-exo-H-exo-O-endo-O-2,3-poz-ts

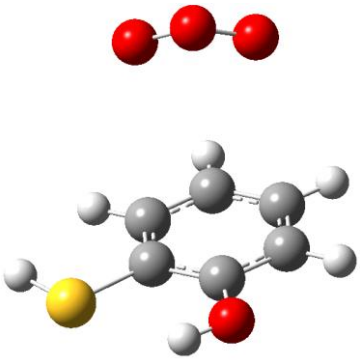

Figure 12D: 6-exo-H-endo-O-endo-O-2,3-poz-ts

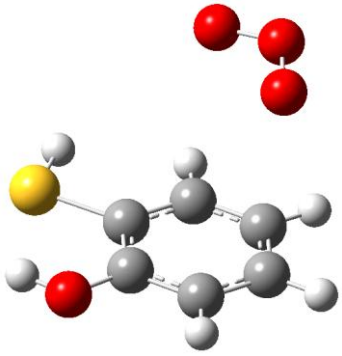

Figure 12E: 6-exo-H-exo-O-endo-O-2,3-poz-ts

APPENDIX C Group electronic energies and thermochemical properties of POZs.

Chlorophenol POZs

Chlorophenol_POZs B3LYP/6-31G(d)	**Electronic energies and thermochemical properties (a.u.)**			
	E^{el}	$E^{el} + ZPE$	$E^{el} + H^{therm}$	$E^{el} + G^{therm}$
Ozone	-225.40645	-225.39907	-225.39517	-225.4222
Chlorophenol	-767.06265	-766.96718	-766.95965	-766.99826
Ozone + Chlorophenol	-992.4691	-992.36625	-992.35482	-992.42046
1,2_POZs				
2_endo_H_endo_O_1,2_poz	-992.50475	-992.39867	-992.38855	-992.43352
3_endo_H_endo_O_1,2_poz	-992.50828	-992.40147	-992.39139	-992.43643
4_endo_H_endo_O_1,2_poz	-992.50812	-992.4015	-992.39142	-992.4365
5_endo_H_endo_O_1,2_poz	-992.50792	-992.40136	-992.39126	-992.43638
6_endo_H_endo_O_1,2_poz	-992.50524	-992.39857	-992.38844	-992.43347
2_endo_H_exo_O_1,2_poz	-992.5115	-992.4054	-992.3953	-992.43996
3_endo_H_exo_O_1,2_poz	-992.5099	-992.40305	-992.39297	-992.43801
4_endo_H_exo_O_1,2_poz	-992.50997	-992.40331	-992.39323	-992.43834
5_endo_H_exo_O_1,2_poz	-992.50977	-992.40312	-992.39305	-992.4381
6_endo_H_exo_O_1,2_poz	-992.50732	-992.40052	-992.39042	-992.43534
2_exo_H_endo_O_1,2_poz	-992.49766	-992.39195	-992.38164	-992.42692
3_exo_H_endo_O_1,2_poz	-992.50514	-992.39842	-992.38825	-992.43341
4_exo_H_endo_O_1,2_poz	-992.50504	-992.39853	-992.38834	-992.43367
5_exo_H_endo_O_1,2_poz	-992.50503	-992.39852	-992.38833	-992.43363
6_exo_H_endo_O_1,2_poz	-992.50618	-992.3993	-992.38923	-992.43407
2_exo_H_exo_O_1,2_poz	-992.50511	-992.39911	-992.38897	-992.4337
3_exo_H_exo_O_1,2_poz	-992.50976	-992.40279	-992.39272	-992.43749
4_exo_H_exo_O_1,2_poz	-992.51008	-992.40327	-992.39321	-992.43804
5_exo_H_exo_O_1,2_poz	-992.50995	-992.40317	-992.3931	-992.43798
6_exo_H_exo_O_1,2_poz	-992.51058	-992.40338	-992.39342	-992.4379
2,3_POZs				
2_endo_H_endo_O_2,3_poz	-992.5044	-992.39799	-992.38776	-992.43266
3_endo_H_endo_O_2,3_poz	-992.5063	-992.39961	-992.38936	-992.43465
4_endo_H_endo_O_2,3_poz	-992.50715	-992.39941	-992.38936	-992.43444

5_endo_H_endo_O_2,3_poz	-992.50785	-992.40024	-992.39022	-992.43528
6_endo_H_endo_O_2,3_poz	-992.50471	-992.397	-992.38695	-992.43203
2_endo_H_exo_O_2,3_poz	-992.51035	-992.40355	-992.39335	-992.4382
3_endo_H_exo_O_2,3_poz	-992.50941	-992.40262	-992.39239	-992.43751
4_endo_H_exo_O_2,3_poz	-992.50692	-992.39932	-992.38923	-992.43423
5_endo_H_exo_O_2,3_poz	-992.5089	-992.40144	-992.39141	-992.43625
6_endo_H_exo_O_2,3_poz	-992.50513	-992.3975	-992.38744	-992.43233
2_exo_H_endo_O_2,3_poz	-992.5005	-992.39389	-992.38369	-992.42914
3_exo_H_endo_O_2,3_poz	-992.50448	-992.39757	-992.38747	-992.4325
4_exo_H_endo_O_2,3_poz	-992.50624	-992.39851	-992.38847	-992.43357
5_exo_H_endo_O_2,3_poz	-992.50706	-992.39948	-992.38945	-992.43456
6_exo_H_endo_O_2,3_poz	-992.50827	-992.40052	-992.3905	-992.43557
2_exo_H_exo_O_2,3_poz	-992.50764	-992.4006	-992.39055	-992.43506
3_exo_H_exo_O_2,3_poz				
4_exo_H_exo_O_2,3_poz	-992.50544	-992.39766	-992.38758	-992.43287
5_exo_H_exo_O_2,3_poz	-992.50677	-992.39917	-992.38909	-992.43443
6_exo_H_exo_O_2,3_poz	-992.5077	-992.39992	-992.38985	-992.43522
3,4_POZs				
2_endo_H_endo_O_3,4_poz	-992.50953	-992.40163	-992.39164	-992.4366
3_endo_H_endo_O_3,4_poz	-992.50589	-992.39915	-992.38903	-992.43414
4_endo_H_endo_O_3,4_poz	-992.5053	-992.39851	-992.3884	-992.43357
5_endo_H_endo_O_3,4_poz	-992.50705	-992.39944	-992.38941	-992.43449
6_endo_H_endo_O_3,4_poz	-992.50299	-992.39544	-992.38544	-992.43053
2_endo_H_exo_O_3,4_poz	-992.50912	-992.40119	-992.39114	-992.43633
3_endo_H_exo_O_3,4_poz	-992.51183	-992.40484	-992.39478	-992.43955
4_endo_H_exo_O_3,4_poz	-992.51254	-992.40546	-992.39545	-992.44006
5_endo_H_exo_O_3,4_poz	-992.50691	-992.39931	-992.38922	-992.43458
6_endo_H_exo_O_3,4_poz	-992.50293	-992.39538	-992.38532	-992.43069
2_exo_H_endo_O_3,4_poz	-992.50164	-992.39431	-992.38406	-992.42955
3_exo_H_endo_O_3,4_poz	-992.50199	-992.39573	-992.38539	-992.43093
4_exo_H_endo_O_3,4_poz	-992.50162	-992.39536	-992.38499	-992.43072
5_exo_H_endo_O_3,4_poz	-992.50336	-992.39627	-992.38596	-992.43165

6_exo_H_endo_O_3,4_poz	-992.50482	-992.39753	-992.38744	-992.43268
2_exo_H_exo_O_3,4_poz	-992.5014	-992.39405	-992.38375	-992.42945
3_exo_H_exo_O_3,4_poz	-992.50784	-992.40133	-992.39105	-992.4363
4_exo_H_exo_O_3,4_poz	-992.50905	-992.40242	-992.39221	-992.43721
5_exo_H_exo_O_3,4_poz	-992.50338	-992.39625	-992.38592	-992.43179
6_exo_H_exo_O_3,4_poz	-992.50497	-992.39765	-992.38752	-992.43294

Chlorophenol_POZs	**Electronic energies and thermochemical properties (a.u.)**			
B3LYP/6-31G(d,p)	E^{el}	$E^{el} + ZPE$	$E^{el} + H^{therm}$	$E^{el} + G^{therm}$
Ozone	-225.40645	-225.39907	-225.39517	-225.4222
Chlorophenol	-767.07473	-766.97925	-766.97172	-767.01033
Ozone + Chlorophenol	-992.48118	-992.37832	-992.36689	-992.43253
1,2_POZs				
2_endo_H_endo_O_1,2_poz	-992.51671	-992.41068	-992.40053	-992.44563
3_endo_H_endo_O_1,2_poz	-992.51991	-992.41316	-992.40306	-992.44814
4_endo_H_endo_O_1,2_poz	-992.51979	-992.41324	-992.40314	-992.44825
5_endo_H_endo_O_1,2_poz	-992.5196	-992.4131	-992.40298	-992.44814
6_endo_H_endo_O_1,2_poz	-992.51694	-992.41032	-992.40018	-992.44524
2_endo_H_exo_O_1,2_poz	-992.52358	-992.41751	-992.4074	-992.45209
3_endo_H_exo_O_1,2_poz	-992.52158	-992.41478	-992.40469	-992.44975
4_endo_H_exo_O_1,2_poz	-992.52168	-992.41507	-992.40498	-992.45012
5_endo_H_exo_O_1,2_poz	-992.5215	-992.41489	-992.40481	-992.44987
6_endo_H_exo_O_1,2_poz	-992.51905	-992.41229	-992.40218	-992.44713
2_exo_H_endo_O_1,2_poz	-992.50977	-992.40405	-992.39373	-992.43904
3_exo_H_endo_O_1,2_poz	-992.51693	-992.41025	-992.40007	-992.44525
4_exo_H_endo_O_1,2_poz	-992.51685	-992.4104	-992.4002	-992.44555
5_exo_H_endo_O_1,2_poz	-992.51684	-992.41039	-992.40018	-992.4455
6_exo_H_endo_O_1,2_poz	-992.51792	-992.41109	-992.40102	-992.44588
2_exo_H_exo_O_1,2_poz	-992.5172	-992.4112	-992.40104	-992.44581
3_exo_H_exo_O_1,2_poz	-992.52152	-992.41458	-992.4045	-992.44929
4_exo_H_exo_O_1,2_poz	-992.52186	-992.41509	-992.40502	-992.44986
5_exo_H_exo_O_1,2_poz	-992.52172	-992.41499	-992.4049	-992.4498
6_exo_H_exo_O_1,2_poz	-992.52227	-992.41512	-992.40514	-992.44965

2,3_POZs				
2_endo_H_endo_O_2,3_poz	-992.51628	-992.40991	-992.39968	-992.44459
3_endo_H_endo_O_2,3_poz	-992.51809	-992.41144	-992.40119	-992.44649
4_endo_H_endo_O_2,3_poz	-992.51861	-992.41097	-992.40092	-992.446
5_endo_H_endo_O_2,3_poz	-992.51937	-992.41186	-992.40183	-992.4469
6_endo_H_endo_O_2,3_poz	-992.51624	-992.40862	-992.39856	-992.44366
2_endo_H_exo_O_2,3_poz	-992.52212	-992.41539	-992.40518	-992.45007
3_endo_H_exo_O_2,3_poz	-992.52117	-992.41444	-992.4042	-992.44934
4_endo_H_exo_O_2,3_poz	-992.51836	-992.41086	-992.40076	-992.44578
5_endo_H_exo_O_2,3_poz	-992.52041	-992.41306	-992.40302	-992.44787
6_endo_H_exo_O_2,3_poz	-992.51662	-992.40908	-992.39901	-992.44391
2_exo_H_endo_O_2,3_poz	-992.51236	-992.40579	-992.39559	-992.44106
3_exo_H_endo_O_2,3_poz	-992.51627	-992.40941	-992.3993	-992.44434
4_exo_H_endo_O_2,3_poz	-992.51771	-992.41008	-992.40002	-992.44514
5_exo_H_endo_O_2,3_poz	-992.51857	-992.4111	-992.40106	-992.44619
6_exo_H_endo_O_2,3_poz	-992.51982	-992.41217	-992.40214	-992.44722
2_exo_H_exo_O_2,3_poz	-992.5195	-992.41249	-992.40244	-992.44696
3_exo_H_exo_O_2,3_poz				
4_exo_H_exo_O_2,3_poz	-992.51689	-992.40921	-992.39911	-992.44442
5_exo_H_exo_O_2,3_poz	-992.51827	-992.41076	-992.40067	-992.44603
6_exo_H_exo_O_2,3_poz	-992.51923	-992.41154	-992.40146	-992.44685
3,4_POZs				
2_endo_H_endo_O_3,4_poz	-992.52097	-992.41319	-992.40318	-992.44817
3_endo_H_endo_O_3,4_poz	-992.51761	-992.41094	-992.40081	-992.44594
4_endo_H_endo_O_3,4_poz	-992.517	-992.41029	-992.40016	-992.44537
5_endo_H_endo_O_3,4_poz	-992.51847	-992.41097	-992.40093	-992.44604
6_endo_H_endo_O_3,4_poz	-992.51449	-992.40705	-992.39703	-992.44216
2_endo_H_exo_O_3,4_poz	-992.52055	-992.41273	-992.40267	-992.44787
3_endo_H_exo_O_3,4_poz	-992.52355	-992.41662	-992.40656	-992.45135
4_endo_H_exo_O_3,4_poz	-992.52425	-992.41724	-992.40722	-992.45185
5_endo_H_exo_O_3,4_poz	-992.51833	-992.41084	-992.40073	-992.44611
6_endo_H_exo_O_3,4_poz	-992.51442	-992.40698	-992.3969	-992.44229

2_exo_H_endo_O_3,4_poz	-992.51314	-992.40593	-992.39566	-992.4412
3_exo_H_endo_O_3,4_poz	-992.51379	-992.40761	-992.39726	-992.44284
4_exo_H_endo_O_3,4_poz	-992.5134	-992.40722	-992.39683	-992.44261
5_exo_H_endo_O_3,4_poz	-992.51484	-992.40788	-992.39755	-992.4433
6_exo_H_endo_O_3,4_poz	-992.51646	-992.40928	-992.39918	-992.44443
2_exo_H_exo_O_3,4_poz	-992.51289	-992.40565	-992.39533	-992.44107
3_exo_H_exo_O_3,4_poz	-992.51964	-992.41321	-992.40291	-992.4482
4_exo_H_exo_O_3,4_poz	-992.52084	-992.41427	-992.40405	-992.44908
5_exo_H_exo_O_3,4_poz	-992.51486	-992.40785	-992.39751	-992.4434
6_exo_H_exo_O_3,4_poz	-992.5166	-992.40938	-992.39924	-992.44466
Chlorophenol_POZs	**Electronic energies and thermochemical properties (a.u.)**			
B3LYP/6-311+G(2df)	E^{el}	$E^{el} + ZPE$	$E^{el} + H^{therm}$	$E^{el} + G^{therm}$
Ozone	-225.4962	-225.48887	-225.48497	-225.51197
Chlorophenol	-767.1964	-767.10136	-767.09385	-767.13243
Ozone + Chlorophenol	-992.6926	-992.59023	-992.57882	-992.6444
1,2_POZs				
2_endo_H_endo_O_1,2_poz	-992.71848	-992.613	-992.60286	-992.64779
3_endo_H_endo_O_1,2_poz	-992.72259	-992.61627	-992.60619	-992.6512
4_endo_H_endo_O_1,2_poz				
5_endo_H_endo_O_1,2_poz	-992.72266	-992.6165	-992.60642	-992.65143
6_endo_H_endo_O_1,2_poz	-992.71924	-992.61306	-992.60293	-992.64791
2_endo_H_exo_O_1,2_poz				
3_endo_H_exo_O_1,2_poz	-992.72481	-992.61841	-992.60836	-992.65321
4_endo_H_exo_O_1,2_poz	-992.72527	-992.61898	-992.60894	-992.65384
5_endo_H_exo_O_1,2_poz	-992.72498	-992.61881	-992.60873	-992.65373
6_endo_H_exo_O_1,2_poz	-992.72192	-992.61566	-992.60555	-992.65042
2_exo_H_endo_O_1,2_poz	-992.71254	-992.60728	-992.597	-992.6421
3_exo_H_endo_O_1,2_poz	-992.72056	-992.61429	-992.60414	-992.64919
4_exo_H_endo_O_1,2_poz	-992.72075	-992.6146	-992.60445	-992.64962
5_exo_H_endo_O_1,2_poz	-992.72075	-992.61463	-992.60447	-992.64963
6_exo_H_endo_O_1,2_poz	-992.7211	-992.61466	-992.60463	-992.64931
2_exo_H_exo_O_1,2_poz				
3_exo_H_exo_O_1,2_poz	-992.72516	-992.61865	-992.60861	-992.65328

4_exo_H_exo_O_1,2_poz	-992.72573	-992.61934	-992.60931	-992.65404
5_exo_H_exo_O_1,2_poz	-992.72557	-992.61924	-992.60919	-992.65398
6_exo_H_exo_O_1,2_poz	-992.72558	-992.61886	-992.60892	-992.65331
2,3_POZs				
2_endo_H_endo_O_2,3_poz	-992.71773	-992.61189	-992.60164	-992.64688
3_endo_H_endo_O_2,3_poz				
4_endo_H_endo_O_2,3_poz	-992.72112	-992.614	-992.60394	-992.64903
5_endo_H_endo_O_2,3_poz	-992.72227	-992.61524	-992.60519	-992.65031
6_endo_H_endo_O_2,3_poz	-992.71895	-992.61182	-992.60174	-992.64687
2_endo_H_exo_O_2,3_poz	-992.72411	-992.61783	-992.60767	-992.65245
3_endo_H_exo_O_2,3_poz	-992.72374	-992.61752	-992.60729	-992.65236
4_endo_H_exo_O_2,3_poz	-992.72025	-992.61338	-992.60318	-992.64878
5_endo_H_exo_O_2,3_poz	-992.72253	-992.61576	-992.60564	-992.65085
6_endo_H_exo_O_2,3_poz	-992.71856	-992.61161	-992.60146	-992.64678
2_exo_H_endo_O_2,3_poz	-992.71457	-992.60842	-992.59827	-992.64332
3_exo_H_endo_O_2,3_poz	-992.71866	-992.61231	-992.60222	-992.64712
4_exo_H_endo_O_2,3_poz	-992.72042	-992.6133	-992.60325	-992.64834
5_exo_H_endo_O_2,3_poz	-992.7217	-992.61468	-992.60465	-992.64971
6_exo_H_endo_O_2,3_poz	-992.72277	-992.61552	-992.60552	-992.65048
2_exo_H_exo_O_2,3_poz	-992.72156	-992.6151	-992.60504	-992.64954
3_exo_H_exo_O_2,3_poz				
4_exo_H_exo_O_2,3_poz	-992.71996	-992.61281	-992.60272	-992.648
5_exo_H_exo_O_2,3_poz	-992.7217	-992.61462	-992.60456	-992.64978
6_exo_H_exo_O_2,3_poz	-992.72256	-992.61526	-992.60523	-992.6504
3,4_POZs				
2_endo_H_endo_O_3,4_poz	-992.7244	-992.617	-992.60704	-992.6519
3_endo_H_endo_O_3,4_poz				
4_endo_H_endo_O_3,4_poz	-992.72032	-992.61396	-992.60389	-992.64884
5_endo_H_endo_O_3,4_poz	-992.72225	-992.61514	-992.60513	-992.65013
6_endo_H_endo_O_3,4_poz	-992.71785	-992.61078	-992.6008	-992.64582
2_endo_H_exo_O_3,4_poz	-992.72424	-992.61684	-992.60682	-992.6519
3_endo_H_exo_O_3,4_poz	-992.72654	-992.62004	-992.61	-992.65469

4_endo_H_exo_O_3,4_poz	-992.72719	-992.62063	-992.61063	-992.65519
5_endo_H_exo_O_3,4_poz				
6_endo_H_exo_O_3,4_poz	-992.718	-992.61095	-992.6009	-992.64628
2_exo_H_endo_O_3,4_poz	-992.71698	-992.61015	-992.59989	-992.64538
3_exo_H_endo_O_3,4_poz	-992.71735	-992.61153	-992.6012	-992.64665
4_exo_H_endo_O_3,4_poz	-992.71707	-992.61123	-992.60088	-992.64645
5_exo_H_endo_O_3,4_poz	-992.71894	-992.61237	-992.60205	-992.64775
6_exo_H_endo_O_3,4_poz	-992.72007	-992.61323	-992.60318	-992.64832
2_exo_H_exo_O_3,4_poz	-992.71693	-992.61006	-992.59978	-992.64538
3_exo_H_exo_O_3,4_poz	-992.72303	-992.61702	-992.60671	-992.65199
4_exo_H_exo_O_3,4_poz	-992.72413	-992.61795	-992.60775	-992.6527
5_exo_H_exo_O_3,4_poz				
6_exo_H_exo_O_3,4_poz	-992.72039	-992.61351	-992.60343	-992.64872

Dihydroxybenzene POZs

Dihydroxybenzene_POZs B3LYP/6-31G(d)	**Electronic energies and thermochemical properties (a.u.)**			
	E^{el}	$E^{el} + ZPE$	$E^{el} + H^{therm}$	$E^{el} + G^{therm}$
Ozone	-225.40645	-225.39907	-225.39517	-225.4222
Dihydroxybenzene	-382.68164	-382.57273	-382.56514	-382.60316
Ozone + Dihydroxybenzene	-608.08809	-607.9718	-607.96031	-608.02536
1,2_POZs				
2_endo_H_endo_O_endo_H_1,2_poz	-608.13386	-608.01367	-608.00383	-608.0472
3_endo_H_endo_O_endo_H_1,2_poz	-608.13301	-608.01233	-608.00234	-608.04639
4_endo_H_endo_O_endo_H_1,2_poz	-608.13206	-608.01151	-608.00153	-608.04568
2_endo_H_endo_O_exo_H_1,2_poz	-608.13112	-608.01106	-608.00104	-608.04482
3_endo_H_endo_O_exo_H_1,2_poz	-608.13084	-608.0102	-608.0002	-608.04445
4_endo_H_endo_O_exo_H_1,2_poz	-608.12852	-608.0085	-607.99826	-608.04296
2_endo_H_exo_O_endo_H_1,2_poz	-608.13773	-608.0176	-608.00771	-608.05135
3_endo_H_exo_O_endo_H_1,2_poz	-608.13446	-608.01394	-608.00399	-608.04767
4_endo_H_exo_O_endo_H_1,2_poz	-608.13478	-608.01406	-608.00413	-608.04807
2_endo_H_exo_O_exo_H_1,2_poz	-608.13773	-608.0176	-608.00771	-608.05135
3_endo_H_exo_O_exo_H_1,2_poz	-608.13343	-608.01276	-608.00279	-608.04692
4_endo_H_exo_O_exo_H_1,2_poz	-608.13135	-608.01109	-608.00094	-608.04531
2_exo_H_endo_O_endo_H_1,2_poz	-608.13112	-608.01106	-608.00104	-608.04482
3_exo_H_endo_O_endo_H_1,2_poz	-608.1296	-608.00918	-607.99901	-608.04373
4_exo_H_endo_O_endo_H_1,2_poz	-608.12882	-608.00838	-607.99829	-608.04266
2_exo_H_endo_O_exo_H_1,2_poz	-608.12015	-608.00082	-607.99045	-608.03517
3_exo_H_endo_O_exo_H_1,2_poz	-608.12823	-608.00768	-607.99758	-608.04187
4_exo_H_endo_O_exo_H_1,2_poz	-608.12494	-608.0051	-607.99472	-608.03975
2_exo_H_exo_O_endo_H_1,2_poz	-608.13773	-608.0176	-608.00771	-608.05135
3_exo_H_exo_O_endo_H_1,2_poz	-608.13446	-608.01394	-608.00399	-608.04767
4_exo_H_exo_O_endo_H_1,2_poz	-608.13477	-608.01398	-608.00404	-608.04786
2_exo_H_exo_O_exo_H_1,2_poz	-608.1269	-608.00737	-607.99716	-608.04145

3_exo_H_exo_O_exo_H_1,2_poz	-608.13318	-608.01239	-608.00241	-608.0463
4_exo_H_exo_O_exo_H_1,2_poz	-608.13105	-608.01077	-608.00059	-608.04487
2,3_POZs				
2_endo_H_endo_O_endo_H_2,3_poz	-608.1344	-608.0136	-608.00366	-608.04753
3_endo_H_endo_O_endo_H_2,3_poz	-608.13301	-608.01233	-608.00234	-608.04639
4_endo_H_endo_O_endo_H_2,3_poz	-608.12667	-608.00547	-607.99537	-608.03988
2_endo_H_endo_O_exo_H_2,3_poz	-608.12891	-608.00783	-607.99797	-608.04163
3_endo_H_endo_O_exo_H_2,3_poz	-608.1296	-608.00918	-607.99901	-608.04373
4_endo_H_endo_O_exo_H_2,3_poz	-608.12752	-608.0061	-607.9961	-608.04032
2_endo_H_exo_O_endo_H_2,3_poz	-608.13563	-608.01468	-608.00481	-608.04859
3_endo_H_exo_O_endo_H_2,3_poz	-608.13446	-608.01394	-608.00399	-608.04767
4_endo_H_exo_O_endo_H_2,3_poz	-608.12447	-608.01394	-608.00399	-608.04767
2_endo_H_exo_O_exo_H_2,3_poz	-608.13025	-608.00954	-607.99954	-608.04349
3_endo_H_exo_O_exo_H_2,3_poz	-608.13294	-608.01236	-608.00223	-608.04645
4_endo_H_exo_O_exo_H_2,3_poz	-608.12664	-608.00546	-607.99537	-608.0397
2_exo_H_endo_O_endo_H_2,3_poz	-608.12742	-608.00697	-607.9969	-608.04112
3_exo_H_endo_O_endo_H_2,3_poz	-608.13084	-608.0102	-608.0002	-608.04445
4_exo_H_endo_O_endo_H_2,3_poz	-608.12752	-608.0061	-607.9961	-608.04032
2_exo_H_endo_O_exo_H_2,3_poz	-608.12742	-608.00697	-607.9969	-608.04112
3_exo_H_endo_O_exo_H_2,3_poz	-608.12823	-608.00768	-607.99758	-608.04187
4_exo_H_endo_O_exo_H_2,3_poz	-608.12607	-608.00472	-607.99469	-608.03907
2_exo_H_exo_O_endo_H_2,3_poz	-608.12998	-608.00939	-607.99936	-608.04337
3_exo_H_exo_O_endo_H_2,3_poz	-608.13343	-608.01276	-608.00279	-608.04691
4_exo_H_exo_O_endo_H_2,3_poz	-608.12664	-608.00546	-607.99537	-608.03971
2_exo_H_exo_O_exo_H_2,3_poz	-608.13437	-608.01333	-608.00345	-608.04704
3_exo_H_exo_O_exo_H_2,3_poz	-608.13318	-608.01239	-608.00241	-608.0463
4_exo_H_exo_O_exo_H_2,3_poz	-608.12569	-608.0043	-607.99423	-608.03879
3,4_POZs				

2_endo_H_endo_O_endo_H_3,4_poz	-608.12894	-608.00753	-607.99752	-608.04176
3_endo_H_endo_O_endo_H_3,4_poz	-608.13247	-608.01194	-608.00196	-608.04614
4_endo_H_endo_O_endo_H_3,4_poz				
2_endo_H_endo_O_exo_H_3,4_poz	-608.12452	-608.00356	-607.99336	-608.03808
3_endo_H_endo_O_exo_H_3,4_poz	-608.12875	-608.00833	-607.99822	-608.04259
4_endo_H_endo_O_exo_H_3,4_poz	-608.12882	-608.00838	-607.99829	-608.04266
2_endo_H_exo_O_endo_H_3,4_poz	-608.1278	-608.00651	-607.99634	-608.04153
3_endo_H_exo_O_endo_H_3,4_poz	-608.13501	-608.01433	-608.00441	-608.04844
4_endo_H_exo_O_endo_H_3,4_poz	-608.13478	-608.01406	-608.00413	-608.04807
2_endo_H_exo_O_exo_H_3,4_poz	-608.12447	-608.00341	-607.99319	-608.03812
3_endo_H_exo_O_exo_H_3,4_poz	-608.13385	-608.01318	-608.00319	-608.04718
4_endo_H_exo_O_exo_H_3,4_poz	-608.13477	-608.01398	-608.00404	-608.04786
2_exo_H_endo_O_endo_H_3,4_poz	-608.11931	-607.9987	-607.98829	-608.0335
3_exo_H_endo_O_endo_H_3,4_poz	-608.12839	-608.00842	-607.99818	-608.0429
4_exo_H_endo_O_endo_H_3,4_poz	-608.12852	-608.0085	-607.99826	-608.04296
2_exo_H_endo_O_exo_H_3,4_poz	-608.12452	-608.00356	-607.99336	-608.03808
3_exo_H_endo_O_exo_H_3,4_poz	-608.12583	-608.00587	-607.99554	-608.04032
4_exo_H_endo_O_exo_H_3,4_poz	-608.12494	-608.0051	-607.99472	-608.03975
2_exo_H_exo_O_endo_H_3,4_poz	-608.11868	-607.99807	-607.98768	-608.03271
3_exo_H_exo_O_endo_H_3,4_poz	-608.13094	-608.01079	-608.00063	-608.04516
4_exo_H_exo_O_endo_H_3,4_poz	-608.13135	-608.01109	-608.00094	-608.04531
2_exo_H_exo_O_exo_H_3,4_poz	-608.12433	-608.00336	-607.99309	-608.03813
3_exo_H_exo_O_exo_H_3,4_poz	-608.13071	-608.0105	-608.00028	-608.04474
4_exo_H_exo_O_exo_H_3,4_poz	-608.13105	-608.01077	-608.00059	-608.04488

Dihydroxybenzene_POZs B3LYP/6-31G(d,p)	**Electronic energies and thermochemical properties (a.u.)**			
	E^{el}	$E^{el} + ZPE$	$E^{el} + H^{therm}$	$E^{el} + G^{therm}$
Ozone	-225.40645	-225.39907	-225.39517	-225.4222
Dihydroxybenzene	-382.69927	-382.59035	-382.58261	-382.62093
Ozone + Dihydroxybenzene	-608.10572	-607.98942	-607.97778	-608.04313

1,2_POZs				
2_endo_H_endo_O_endo_H_1,2_poz	-608.15135	-608.03105	-608.02119	-608.06461
3_endo_H_endo_O_endo_H_1,2_poz	-608.15033	-608.02958	-608.01957	-608.06366
4_endo_H_endo_O_endo_H_1,2_poz	-608.14929	-608.02869	-608.01869	-608.06288
2_endo_H_endo_O_exo_H_1,2_poz	-608.14864	-608.02849	-608.01844	-608.06228
3_endo_H_endo_O_exo_H_1,2_poz	-608.14814	-608.02743	-608.01741	-608.06171
4_endo_H_endo_O_exo_H_1,2_poz	-608.14583	-608.02576	-608.01549	-608.06027
2_endo_H_exo_O_endo_H_1,2_poz	-608.15529	-608.03508	-608.02516	-608.06889
3_endo_H_exo_O_endo_H_1,2_poz	-608.15187	-608.03127	-608.02131	-608.06499
4_endo_H_exo_O_endo_H_1,2_poz	-608.15206	-608.03128	-608.02133	-608.06531
2_endo_H_exo_O_exo_H_1,2_poz	-608.15529	-608.03507	-608.02516	-608.06888
3_endo_H_exo_O_exo_H_1,2_poz	-608.15079	-608.03003	-608.02005	-608.06418
4_endo_H_exo_O_exo_H_1,2_poz	-608.1487	-608.02839	-608.01821	-608.06264
2_exo_H_endo_O_endo_H_1,2_poz	-608.14864	-608.02849	-608.01844	-608.06228
3_exo_H_endo_O_endo_H_1,2_poz	-608.14707	-608.02657	-608.01639	-608.06115
4_exo_H_endo_O_endo_H_1,2_poz	-608.14619	-608.02569	-608.01559	-608.06
2_exo_H_endo_O_exo_H_1,2_poz	-608.13801	-608.01853	-608.00815	-608.05291
3_exo_H_endo_O_exo_H_1,2_poz	-608.14568	-608.02504	-608.01493	-608.05925
4_exo_H_endo_O_exo_H_1,2_poz	-608.1424	-608.02251	-608.0121	-608.0572
2_exo_H_exo_O_endo_H_1,2_poz	-608.15529	-608.03508	-608.02516	-608.06889
3_exo_H_exo_O_endo_H_1,2_poz	-608.15187	-608.03127	-608.02131	-608.06499
4_exo_H_exo_O_endo_H_1,2_poz	-608.15212	-608.03126	-608.0213	-608.06514
2_exo_H_exo_O_exo_H_1,2_poz	-608.1447	-608.02504	-608.01481	-608.05916
3_exo_H_exo_O_exo_H_1,2_poz	-608.15061	-608.02973	-608.01974	-608.06365
4_exo_H_exo_O_exo_H_1,2_poz	-608.14848	-608.02812	-608.01793	-608.06225
2,3_POZs				
2_endo_H_endo_O_endo_H_2,3_poz	-608.15168	-608.03083	-608.02087	-608.06479
3_endo_H_endo_O_endo_H_2,3_poz	-608.15033	-608.02958	-608.01957	-608.06366
4_endo_H_endo_O_endo_H_2,3_poz	-608.14379	-608.02257	-608.01245	-608.05699

2_endo_H_endo_O_exo_H_2,3_poz	-608.14635	-608.02516	-608.01531	-608.05898
3_endo_H_endo_O_exo_H_2,3_poz	-608.14707	-608.02657	-608.01639	-608.06115
4_endo_H_endo_O_exo_H_2,3_poz	-608.14463	-608.02319	-608.01317	-608.05742
2_endo_H_exo_O_endo_H_2,3_poz	-608.15296	-608.03192	-608.02204	-608.06583
3_endo_H_exo_O_endo_H_2,3_poz	-608.15187	-608.03127	-608.02131	-608.06499
4_endo_H_exo_O_endo_H_2,3_poz	-608.14153	-608.02065	-608.01021	-608.05575
2_endo_H_exo_O_exo_H_2,3_poz	-608.14763	-608.02683	-608.01682	-608.06078
3_endo_H_exo_O_exo_H_2,3_poz	-608.15035	-608.02969	-608.01955	-608.06379
4_endo_H_exo_O_exo_H_2,3_poz	-608.14373	-608.02253	-608.01241	-608.05679
2_exo_H_endo_O_endo_H_2,3_poz	-608.14483	-608.0243	-608.01421	-608.05848
3_exo_H_endo_O_endo_H_2,3_poz	-608.14814	-608.02743	-608.01741	-608.06171
4_exo_H_endo_O_endo_H_2,3_poz	-608.14463	-608.02319	-608.01317	-608.05742
2_exo_H_endo_O_exo_H_2,3_poz				
3_exo_H_endo_O_exo_H_2,3_poz	-608.14568	-608.02504	-608.01493	-608.05925
4_exo_H_endo_O_exo_H_2,3_poz	-608.14321	-608.02183	-608.01178	-608.05619
2_exo_H_exo_O_endo_H_2,3_poz	-608.14743	-608.02674	-608.01669	-608.06075
3_exo_H_exo_O_endo_H_2,3_poz	-608.15079	-608.03003	-608.02005	-608.06418
4_exo_H_exo_O_endo_H_2,3_poz	-608.14373	-608.02253	-608.01241	-608.05679
2_exo_H_exo_O_exo_H_2,3_poz	-608.15177	-608.03062	-608.02072	-608.06433
3_exo_H_exo_O_exo_H_2,3_poz	-608.15061	-608.02973	-608.01974	-608.06365
4_exo_H_exo_O_exo_H_2,3_poz	-608.14279	-608.02138	-608.01129	-608.05589
3,4_POZs				
2_endo_H_endo_O_endo_H_3,4_poz	-608.14599	-608.02453	-608.01452	-608.05877
3_endo_H_endo_O_endo_H_3,4_poz	-608.1497	-608.02912	-608.01912	-608.06335
4_endo_H_endo_O_endo_H_3,4_poz				
2_endo_H_endo_O_exo_H_3,4_poz	-608.14171	-608.02068	-608.01048	-608.0552
3_endo_H_endo_O_exo_H_3,4_poz	-608.14612	-608.02565	-608.01551	-608.05993
4_endo_H_endo_O_exo_H_3,4_poz	-608.14619	-608.02569	-608.01559	-608.06
2_endo_H_exo_O_endo_H_3,4_poz	-608.14481	-608.02349	-608.0133	-608.05853

3_endo_H_exo_O_endo_H_3,4_poz	-608.15229	-608.03154	-608.0216	-608.06566
4_endo_H_exo_O_endo_H_3,4_poz	-608.15206	-608.03128	-608.02133	-608.06531
2_endo_H_exo_O_exo_H_3,4_poz	-608.14164	-608.02051	-608.01029	-608.05522
3_endo_H_exo_O_exo_H_3,4_poz	-608.1512	-608.03047	-608.02045	-608.06448
4_endo_H_exo_O_exo_H_3,4_poz	-608.15212	-608.03126	-608.0213	-608.06514
2_exo_H_endo_O_endo_H_3,4_poz	-608.13648	-608.01585	-608.00541	-608.0507
3_exo_H_endo_O_endo_H_3,4_poz	-608.14571	-608.0257	-608.01543	-608.06022
4_exo_H_endo_O_endo_H_3,4_poz	-608.14583	-608.02576	-608.01549	-608.06027
2_exo_H_endo_O_exo_H_3,4_poz	-608.14171	-608.02068	-608.01048	-608.0552
3_exo_H_endo_O_exo_H_3,4_poz	-608.14327	-608.02326	-608.0129	-608.05775
4_exo_H_endo_O_exo_H_3,4_poz	-608.1424	-608.02251	-608.0121	-608.0572
2_exo_H_exo_O_endo_H_3,4_poz	-608.13585	-608.01523	-608.00482	-608.04991
3_exo_H_exo_O_endo_H_3,4_poz	-608.14832	-608.02811	-608.01793	-608.06249
4_exo_H_exo_O_endo_H_3,4_poz	-608.1487	-608.02839	-608.01821	-608.06264
2_exo_H_exo_O_exo_H_3,4_poz	-608.1415	-608.02046	-608.01019	-608.05524
3_exo_H_exo_O_exo_H_3,4_poz	-608.14814	-608.02786	-608.01762	-608.06214
4_exo_H_exo_O_exo_H_3,4_poz	-608.14848	-608.02812	-608.01793	-608.06225

Dihydroxybenzene_POZs	**Electronic energies and thermochemical properties (a.u.)**			
B3LYP/6-311+G(2df)	E^{el}	$E^{el} + ZPE$	$E^{el} + H^{therm}$	$E^{el} + G^{therm}$
Ozone	-225.4962	-225.48887	-225.48497	-225.51197
Dihydroxybenzene	-382.81625	-382.70797	-382.7002	-382.7386
Ozone + Dihydroxybenzene	-608.31245	-608.19684	-608.18517	-608.25057
1,2_POZs				
2_endo_H_endo_O_endo_H_1,2_poz	-608.34708	-608.22746	-608.21756	-608.26108
3_endo_H_endo_O_endo_H_1,2_poz	-608.34673	-608.22668	-608.21664	-608.26077
4_endo_H_endo_O_endo_H_1,2_poz	-608.34718	-608.2271	-608.21711	-608.26121
2_endo_H_endo_O_exo_H_1,2_poz	-608.34564	-608.22608	-608.21602	-608.25987
3_endo_H_endo_O_exo_H_1,2_poz	-608.34517	-608.22513	-608.21509	-608.25935
4_endo_H_endo_O_exo_H_1,2_poz	-608.34407	-608.22451	-608.21423	-608.25897

2_endo_H_exo_O_endo_H_1,2_poz	-608.35135	-608.23209	-608.22191	-608.26638
3_endo_H_exo_O_endo_H_1,2_poz	-608.34772	-608.22792	-608.21785	-608.26203
4_endo_H_exo_O_endo_H_1,2_poz	-608.35031	-608.23009	-608.22015	-608.26404
2_endo_H_exo_O_exo_H_1,2_poz	-608.35135	-608.23209	-608.22191	-608.26638
3_endo_H_exo_O_exo_H_1,2_poz	-608.34807	-608.228	-608.21799	-608.26203
4_endo_H_exo_O_exo_H_1,2_poz	-608.34732	-608.22753	-608.21737	-608.26172
2_exo_H_endo_O_endo_H_1,2_poz	-608.34564	-608.22608	-608.21602	-608.25987
3_exo_H_endo_O_endo_H_1,2_poz	-608.34466	-608.22472	-608.21456	-608.25902
4_exo_H_endo_O_endo_H_1,2_poz	-608.34498	-608.22493	-608.21487	-608.25911
2_exo_H_endo_O_exo_H_1,2_poz	-608.33646	-608.21748	-608.20714	-608.25171
3_exo_H_endo_O_exo_H_1,2_poz	-608.34365	-608.22362	-608.21353	-608.25775
4_exo_H_endo_O_exo_H_1,2_poz	-608.34148	-608.22207	-608.21166	-608.25673
2_exo_H_exo_O_endo_H_1,2_poz	-608.35135	-608.23209	-608.22191	-608.26639
3_exo_H_exo_O_endo_H_1,2_poz	-608.34772	-608.22792	-608.21785	-608.26203
4_exo_H_exo_O_endo_H_1,2_poz	-608.35065	-608.23034	-608.2204	-608.26415
2_exo_H_exo_O_exo_H_1,2_poz	-608.34218	-608.22302	-608.21285	-608.25697
3_exo_H_exo_O_exo_H_1,2_poz	-608.34847	-608.22824	-608.21825	-608.2621
4_exo_H_exo_O_exo_H_1,2_poz	-608.34732	-608.22746	-608.2173	-608.26153
2,3_POZs				
2_endo_H_endo_O_endo_H_2,3_poz	-608.34735	-608.2271	-608.21714	-608.26109
3_endo_H_endo_O_endo_H_2,3_poz	-608.34673	-608.22668	-608.21664	-608.26076
4_endo_H_endo_O_endo_H_2,3_poz	-608.34105	-608.22052	-608.21035	-608.25496
2_endo_H_endo_O_exo_H_2,3_poz				
3_endo_H_endo_O_exo_H_2,3_poz	-608.34466	-608.22472	-608.21456	-608.25902
4_endo_H_endo_O_exo_H_2,3_poz	-608.34165	-608.22094	-608.21088	-608.25518
2_endo_H_exo_O_endo_H_2,3_poz				
3_endo_H_exo_O_endo_H_2,3_poz	-608.34772	-608.22792	-608.21785	-608.26203
4_endo_H_exo_O_endo_H_2,3_poz	-608.33952	-608.21931	-608.20886	-608.25429

2_endo_H_exo_O_exo_H_2,3_poz	-608.34488	-608.2248	-608.21471	-608.25883
3_endo_H_exo_O_exo_H_2,3_poz	-608.34847	-608.2284	-608.21828	-608.26241
4_endo_H_exo_O_exo_H_2,3_poz				
2_exo_H_endo_O_endo_H_2,3_poz	-608.34136	-608.22147	-608.21136	-608.25558
3_exo_H_endo_O_endo_H_2,3_poz	-608.34517	-608.22513	-608.21509	-608.25935
4_exo_H_endo_O_endo_H_2,3_poz	-608.34165	-608.22094	-608.21088	-608.25518
2_exo_H_endo_O_exo_H_2,3_poz				
3_exo_H_endo_O_exo_H_2,3_poz	-608.34365	-608.22362	-608.21353	-608.25775
4_exo_H_endo_O_exo_H_2,3_poz	-608.34042	-608.2198	-608.2097	-608.25416
2_exo_H_exo_O_endo_H_2,3_poz	-608.34457	-608.22449	-608.21444	-608.25839
3_exo_H_exo_O_endo_H_2,3_poz	-608.34807	-608.228	-608.21799	-608.26203
4_exo_H_exo_O_endo_H_2,3_poz				
2_exo_H_exo_O_exo_H_2,3_poz	-608.34898	-608.22847	-608.21858	-608.26213
3_exo_H_exo_O_exo_H_2,3_poz	-608.34847	-608.22824	-608.21825	-608.2621
4_exo_H_exo_O_exo_H_2,3_poz	-608.34023	-608.21956	-608.20944	-608.25404
3,4_POZs				
2_endo_H_endo_O_endo_H_3,4_poz	-608.34426	-608.2233	-608.21329	-608.25752
3_endo_H_endo_O_endo_H_3,4_poz	-608.34764	-608.22753	-608.21756	-608.2616
4_endo_H_endo_O_endo_H_3,4_poz				
2_endo_H_endo_O_exo_H_3,4_poz	-608.34027	-608.21978	-608.2095	-608.25438
3_endo_H_endo_O_exo_H_3,4_poz	-608.34495	-608.22497	-608.21487	-608.25915
4_endo_H_endo_O_exo_H_3,4_poz	-608.34498	-608.22493	-608.21487	-608.25911
2_endo_H_exo_O_endo_H_3,4_poz	-608.34359	-608.22273	-608.21258	-608.25733
3_endo_H_exo_O_endo_H_3,4_poz	-608.35037	-608.23024	-608.22028	-608.2643
4_endo_H_exo_O_endo_H_3,4_poz	-608.35031	-608.23009	-608.22015	-608.26404
2_endo_H_exo_O_exo_H_3,4_poz	-608.34042	-608.21995	-608.20959	-608.25487
3_endo_H_exo_O_exo_H_3,4_poz	-608.34983	-608.22966	-608.21967	-608.2636
4_endo_H_exo_O_exo_H_3,4_poz	-608.35065	-608.23034	-608.2204	-608.26415
2_exo_H_endo_O_endo_H_3,4_poz	-608.33535	-608.21528	-608.20478	-608.25028

3_exo_H_endo_O_endo_H_3,4_poz	-608.34397	-608.22442	-608.21416	-608.25883
4_exo_H_endo_O_endo_H_3,4_poz				
2_exo_H_endo_O_exo_H_3,4_poz	-608.34027	-608.21978	-608.2095	-608.25438
3_exo_H_endo_O_exo_H_3,4_poz	-608.34241	-608.22289	-608.21254	-608.25734
4_exo_H_endo_O_exo_H_3,4_poz	-608.34148	-608.22207	-608.21166	-608.25673
2_exo_H_exo_O_endo_H_3,4_poz	-608.33467	-608.21463	-608.20405	-608.24975
3_exo_H_exo_O_endo_H_3,4_poz	-608.34667	-608.22709	-608.21685	-608.26152
4_exo_H_exo_O_endo_H_3,4_poz	-608.34732	-608.22753	-608.21737	-608.26172
2_exo_H_exo_O_exo_H_3,4_poz	-608.3405	-608.21997	-608.20967	-608.2547
3_exo_H_exo_O_exo_H_3,4_poz	-608.34712	-608.22741	-608.21716	-608.26167
4_exo_H_exo_O_exo_H_3,4_poz	-608.34732	-608.22746	-608.2173	-608.26153

Hydroxythiophenol POZs

Hydroxythiophenol_POZs B3LYP/6-31G(d)	**Electronic energies and thermochemical properties (a.u.)**			
	E^{el}	$E^{el} + ZPE$	$E^{el} + H^{therm}$	$E^{el} + G^{therm}$
Ozone	-225.40645	-225.39907	-225.39517	-225.4222
Hydroxythiophenol	-705.65503	-705.55073	-705.54275	-705.58216
Ozone + Hydroxythiophenol	-931.06148	-930.9498	-930.93792	-931.00436
1,2_POZs				
2_endo_H_endo_O_endo_H_1,2_poz	-931.09515	-930.9807	-930.97001	-931.01549
3_endo_H_endo_O_endo_H_1,2_poz	-931.09569	-930.98018	-930.96955	-931.01534
4_endo_H_endo_O_endo_H_1,2_poz	-931.09528	-930.97985	-930.96921	-931.01515
5_endo_H_endo_O_endo_H_1,2_poz	-931.09603	-930.98061	-930.96999	-931.01587
6_endo_H_endo_O_endo_H_1,2_poz	-931.09427	-930.97889	-930.96812	-931.01442
2_endo_H_endo_O_exo_H_1,2_poz	-931.09618	-930.98132	-930.97073	-931.0162
3_endo_H_endo_O_exo_H_1,2_poz	-931.09348	-930.97815	-930.9674	-931.0135
4_endo_H_endo_O_exo_H_1,2_poz	-931.09457	-930.97927	-930.96857	-931.01464
5_endo_H_endo_O_exo_H_1,2_poz	-931.09366	-930.9784	-930.96766	-931.01377
6_endo_H_endo_O_exo_H_1,2_poz	-931.09446	-930.97866	-930.96814	-931.01349
2_endo_H_exo_O_endo_H_1,2_poz	-931.09607	-930.98154	-930.97089	-931.01658
3_endo_H_exo_O_endo_H_1,2_poz	-931.09556	-930.98024	-930.96944	-931.01575
4_endo_H_exo_O_endo_H_1,2_poz	-931.09827	-930.98276	-930.97211	-931.01795
5_endo_H_exo_O_endo_H_1,2_poz	-931.09778	-930.98222	-930.97162	-931.01748
6_endo_H_exo_O_endo_H_1,2_poz	-931.09698	-930.98168	-930.97084	-931.01708
2_endo_H_exo_O_exo_H_1,2_poz	-931.10003	-930.98489	-930.97446	-931.01941
3_endo_H_exo_O_exo_H_1,2_poz	-931.09557	-930.98024	-930.96942	-931.01554
4_endo_H_exo_O_exo_H_1,2_poz	-931.09883	-930.98322	-930.97261	-931.01825
5_endo_H_exo_O_exo_H_1,2_poz	-931.09682	-930.98134	-930.97069	-931.0165
6_endo_H_exo_O_exo_H_1,2_poz	-931.09706	-930.98143	-930.97079	-931.01643
2_exo_H_endo_O_endo_H_1,2_poz	-931.09123	-930.97699	-930.96608	-931.01258
3_exo_H_endo_O_endo_H_1,2_poz	-931.09495	-930.97934	-930.96874	-931.01449
4_exo_H_endo_O_endo_H_1,2_poz	-931.09164	-930.97673	-930.96583	-931.01232
5_exo_H_endo_O_endo_H_1,2_poz	-931.09211	-930.97721	-930.96635	-931.01271
6_exo_H_endo_O_endo_H_1,2_poz	-931.09137	-930.97594	-930.96529	-931.01118

2_exo_H_endo_O_exo_H_1,2_poz	-931.09076	-930.97595	-930.96529	-931.01079
3_exo_H_endo_O_exo_H_1,2_poz				
4_exo_H_endo_O_exo_H_1,2_poz	-931.09094	-930.97614	-930.96519	-931.01178
5_exo_H_endo_O_exo_H_1,2_poz	-931.09043	-930.97563	-930.96465	-931.01122
6_exo_H_endo_O_exo_H_1,2_poz	-931.09299	-930.97752	-930.96687	-931.01256
2_exo_H_exo_O_endo_H_1,2_poz	-931.09779	-930.98313	-930.9726	-931.0178
3_exo_H_exo_O_endo_H_1,2_poz	-931.09657	-930.98101	-930.97036	-931.01629
4_exo_H_exo_O_endo_H_1,2_poz	-931.09484	-930.97977	-930.96891	-931.01514
5_exo_H_exo_O_endo_H_1,2_poz	-931.09374	-930.97868	-930.96784	-931.01421
6_exo_H_exo_O_endo_H_1,2_poz	-931.09401	-930.97851	-930.96782	-931.01364
2_exo_H_exo_O_exo_H_1,2_poz	-931.0953	-930.98079	-930.96993	-931.01631
3_exo_H_exo_O_exo_H_1,2_poz	-931.09658	-930.98094	-930.97032	-931.01601
4_exo_H_exo_O_exo_H_1,2_poz	-931.09541	-930.98025	-930.96944	-931.01549
5_exo_H_exo_O_exo_H_1,2_poz	-931.09344	-930.97845	-930.96754	-931.0139
6_exo_H_exo_O_exo_H_1,2_poz	-931.09697	-930.98123	-930.97067	-931.016
2,3_POZs				
2_endo_H_endo_O_endo_H_2,3_poz	-931.10106	-930.98569	-930.97501	-931.02097
3_endo_H_endo_O_endo_H_2,3_poz	-931.1028	-930.98735	-930.97669	-931.0227
4_endo_H_endo_O_endo_H_2,3_poz	-931.10007	-930.98367	-930.97304	-931.01914
5_endo_H_endo_O_endo_H_2,3_poz	-931.101	-930.98462	-930.97407	-931.02003
6_endo_H_endo_O_endo_H_2,3_poz	-931.10556	-930.98886	-930.97842	-931.02413
2_endo_H_endo_O_exo_H_2,3_poz	-931.09921	-930.98385	-930.9732	-931.01904
3_endo_H_endo_O_exo_H_2,3_poz	-931.10049	-930.98505	-930.97438	-931.02039
4_endo_H_endo_O_exo_H_2,3_poz	-931.0971	-930.98099	-930.9702	-931.01686
5_endo_H_endo_O_exo_H_2,3_poz	-931.09874	-930.98253	-930.97187	-931.01831
6_endo_H_endo_O_exo_H_2,3_poz	-931.10328	-930.98667	-930.97622	-931.02198
2_endo_H_exo_O_endo_H_2,3_poz	-931.10312	-930.98747	-930.97689	-931.02262
3_endo_H_exo_O_endo_H_2,3_poz	-931.10339	-930.98787	-930.9772	-931.02341
4_endo_H_exo_O_endo_H_2,3_poz	-931.09955	-930.9834	-930.97264	-931.01894
5_endo_H_exo_O_endo_H_2,3_poz	-931.10169	-930.98551	-930.97488	-931.02098
6_endo_H_exo_O_endo_H_2,3_poz	-931.10513	-930.9883	-930.97785	-931.0237

2_endo_H_exo_O_exo_H_2,3_poz	-931.10083	-930.98535	-930.9747	-931.02065
3_endo_H_exo_O_exo_H_2,3_poz	-931.10175	-930.98627	-930.97562	-931.02158
4_endo_H_exo_O_exo_H_2,3_poz	-931.0974	-930.98143	-930.97056	-931.01715
5_endo_H_exo_O_exo_H_2,3_poz	-931.09934	-930.98309	-930.97242	-931.01891
6_endo_H_exo_O_exo_H_2,3_poz	-931.09584	-930.98007	-930.96905	-931.0161
2_exo_H_endo_O_endo_H_2,3_poz	-931.10086	-930.98496	-930.97451	-931.01984
3_exo_H_endo_O_endo_H_2,3_poz				
4_exo_H_endo_O_endo_H_2,3_poz	-931.10006	-930.98356	-930.973	-931.01892
5_exo_H_endo_O_endo_H_2,3_poz	-931.09766	-930.98175	-930.97095	-931.01744
6_exo_H_endo_O_endo_H_2,3_poz	-931.10556	-930.98886	-930.97842	-931.02413
2_exo_H_endo_O_exo_H_2,3_poz	-931.09753	-930.98201	-930.97133	-931.01747
3_exo_H_endo_O_exo_H_2,3_poz				
4_exo_H_endo_O_exo_H_2,3_poz	-931.09651	-930.98033	-930.96958	-931.01606
5_exo_H_endo_O_exo_H_2,3_poz	-931.09874	-930.98253	-930.97187	-931.01831
6_exo_H_endo_O_exo_H_2,3_poz	-931.09563	-930.97987	-930.9689	-931.01586
2_exo_H_exo_O_endo_H_2,3_poz	-931.10501	-930.98891	-930.97849	-931.02368
3_exo_H_exo_O_endo_H_2,3_poz	-931.1031	-930.98748	-930.97679	-931.02267
4_exo_H_exo_O_endo_H_2,3_poz	-931.09875	-930.98238	-930.97165	-931.0183
5_exo_H_exo_O_endo_H_2,3_poz				
6_exo_H_exo_O_endo_H_2,3_poz	-931.10513	-930.9883	-930.97785	-931.0237
2_exo_H_exo_O_exo_H_2,3_poz	-931.10202	-930.98627	-930.97566	-931.02132
3_exo_H_exo_O_exo_H_2,3_poz	-931.10159	-930.986	-930.97533	-931.02113
4_exo_H_exo_O_exo_H_2,3_poz	-931.096	-930.97973	-930.96896	-931.01555
5_exo_H_exo_O_exo_H_2,3_poz	-931.09934	-930.98309	-930.97242	-931.01891
6_exo_H_exo_O_exo_H_2,3_poz	-931.09584	-930.98007	-930.96905	-931.0161
3,4_POZs				
2_endo_H_endo_O_endo_H_3,4_poz	-931.09901	-930.98266	-930.97202	-931.01807
3_endo_H_endo_O_endo_H_3,4_poz	-931.09962	-930.98433	-930.97365	-931.01975
4_endo_H_endo_O_endo_H_3,4_poz	-931.09944	-930.98411	-930.97345	-931.01948
5_endo_H_endo_O_endo_H_3,4_poz	-931.09929	-930.98294	-930.97237	-931.01834
6_endo_H_endo_O_endo_H_3,4_poz	-931.09695	-930.98062	-930.97008	-931.01603
2_endo_H_endo_O_exo_H_3,4_poz	-931.09645	-930.98034	-930.9695	-931.01618

3_endo_H_endo_O_exo_H_3,4_poz	-931.09845	-930.9833	-930.97253	-931.01888
4_endo_H_endo_O_exo_H_3,4_poz	-931.09877	-930.98354	-930.97281	-931.01904
5_endo_H_endo_O_exo_H_3,4_poz	-931.09846	-930.9823	-930.97159	-931.01792
6_endo_H_endo_O_exo_H_3,4_poz	-931.09715	-930.98121	-930.97039	-931.01744
2_endo_H_exo_O_endo_H_3,4_poz	-931.09672	-930.98063	-930.96985	-931.01622
3_endo_H_exo_O_endo_H_3,4_poz	-931.10041	-930.98519	-930.97444	-931.02078
4_endo_H_exo_O_endo_H_3,4_poz	-931.1005	-930.98526	-930.97451	-931.02087
5_endo_H_exo_O_endo_H_3,4_poz	-931.10088	-930.98468	-930.97411	-931.01982
6_endo_H_exo_O_endo_H_3,4_poz	-931.09787	-930.98173	-930.97116	-931.01722
2_endo_H_exo_O_exo_H_3,4_poz	-931.09885	-930.98274	-930.97195	-931.01827
3_endo_H_exo_O_exo_H_3,4_poz	-931.10165	-930.9863	-930.97564	-931.0217
4_endo_H_exo_O_exo_H_3,4_poz	-931.10151	-930.98612	-930.97547	-931.0215
5_endo_H_exo_O_exo_H_3,4_poz	-931.10088	-930.98468	-930.97411	-931.01982
6_endo_H_exo_O_exo_H_3,4_poz	-931.09693	-930.98059	-930.97	-931.01643
2_exo_H_endo_O_endo_H_3,4_poz	-931.10191	-930.98534	-930.97488	-931.02071
3_exo_H_endo_O_endo_H_3,4_poz	-931.09613	-930.98101	-930.97019	-931.01659
4_exo_H_endo_O_endo_H_3,4_poz	-931.09625	-930.98114	-930.97032	-931.01677
5_exo_H_endo_O_endo_H_3,4_poz	-931.0981	-930.98186	-930.97123	-931.01736
6_exo_H_endo_O_endo_H_3,4_poz	-931.09695	-930.98062	-930.97008	-931.01603
2_exo_H_endo_O_exo_H_3,4_poz	-931.10162	-930.9851	-930.97462	-931.0205
3_exo_H_endo_O_exo_H_3,4_poz	-931.09565	-930.98053	-930.9697	-931.01614
4_exo_H_endo_O_exo_H_3,4_poz	-931.09536	-930.98022	-930.96939	-931.01585
5_exo_H_endo_O_exo_H_3,4_poz	-931.09731	-930.98115	-930.97048	-931.01671
6_exo_H_endo_O_exo_H_3,4_poz				
2_exo_H_exo_O_endo_H_3,4_poz	-931.10174	-930.9851	-930.97462	-931.02059
3_exo_H_exo_O_endo_H_3,4_poz	-931.10058	-930.98526	-930.9745	-931.02065
4_exo_H_exo_O_endo_H_3,4_poz	-931.10047	-930.98507	-930.97435	-931.02038
5_exo_H_exo_O_endo_H_3,4_poz	-931.09694	-930.98073	-930.97001	-931.01654
6_exo_H_exo_O_endo_H_3,4_poz				
2_exo_H_exo_O_exo_H_3,4_poz	-931.10129	-930.9847	-930.9742	-931.02026
3_exo_H_exo_O_exo_H_3,4_poz	-931.10107	-930.98566	-930.97496	-931.02093

4_exo_H_exo_O_exo_H_3,4_poz	-931.10157	-930.98611	-930.97544	-931.02131
5_exo_H_exo_O_exo_H_3,4_poz	-931.09815	-930.98189	-930.97123	-931.01643
6_exo_H_exo_O_exo_H_3,4_poz	-931.09693	-930.98059	-930.96999	-931.01643

Hydroxythiophenol_POZs B3LYP/6-31G(d,p)	**Electronic energies and thermochemical properties (a.u.)**			
	E^{el}	$E^{el} + ZPE$	$E^{el} + H^{therm}$	$E^{el} + G^{therm}$
Ozone	-225.40645	-225.39907	-225.39517	-225.4222
Hydroxythiophenol	-705.67016	-705.56587	-705.55788	-705.59731
Ozone + Hydroxythiophenol	-931.07661	-930.96494	-930.95305	-931.01951
1,2_POZs				
2_endo_H_endo_O_endo_H_1,2_poz	-931.11047	-930.996	-930.98531	-931.03079
3_endo_H_endo_O_endo_H_1,2_poz	-931.11055	-930.99513	-930.98449	-931.03031
4_endo_H_endo_O_endo_H_1,2_poz	-931.11008	-930.99474	-930.98408	-931.03007
5_endo_H_endo_O_endo_H_1,2_poz	-931.11081	-930.99551	-930.98486	-931.03079
6_endo_H_endo_O_endo_H_1,2_poz	-931.10914	-930.99384	-930.98305	-931.02937
2_endo_H_endo_O_exo_H_1,2_poz	-931.11128	-930.99644	-930.98583	-931.03136
3_endo_H_endo_O_exo_H_1,2_poz	-931.10845	-930.99319	-930.98243	-931.02854
4_endo_H_endo_O_exo_H_1,2_poz	-931.10947	-930.99426	-930.98354	-931.02965
5_endo_H_endo_O_exo_H_1,2_poz	-931.10855	-930.99338	-930.98262	-931.02877
6_endo_H_endo_O_exo_H_1,2_poz	-931.10955	-930.99379	-930.98326	-931.02861
2_endo_H_exo_O_endo_H_1,2_poz	-931.11148	-930.99691	-930.98625	-931.03211
3_endo_H_exo_O_endo_H_1,2_poz	-931.11048	-930.99522	-930.98441	-931.03077
4_endo_H_exo_O_endo_H_1,2_poz	-931.11309	-930.99766	-930.98699	-931.03287
5_endo_H_exo_O_endo_H_1,2_poz	-931.11262	-930.99714	-930.98653	-931.03242
6_endo_H_exo_O_endo_H_1,2_poz	-931.11184	-930.99663	-930.98577	-931.03208
2_endo_H_exo_O_exo_H_1,2_poz	-931.11514	-931.00003	-930.98958	-931.03457
3_endo_H_exo_O_exo_H_1,2_poz	-931.1105	-930.99524	-930.98441	-931.03055
4_endo_H_exo_O_exo_H_1,2_poz	-931.11372	-930.99818	-930.98757	-931.03322
5_endo_H_exo_O_exo_H_1,2_poz	-931.1117	-930.99631	-930.98564	-931.03149
6_endo_H_exo_O_exo_H_1,2_poz	-931.11209	-930.99649	-930.98585	-931.0315
2_exo_H_endo_O_endo_H_1,2_poz	-931.10654	-930.99234	-930.98141	-931.02815
3_exo_H_endo_O_endo_H_1,2_poz	-931.10982	-930.99428	-930.98367	-931.02945

4_exo_H_endo_O_endo_H_1,2_poz	-931.1065	-930.9917	-930.98078	-931.02733
5_exo_H_endo_O_endo_H_1,2_poz	-931.10699	-930.9922	-930.98131	-931.02774
6_exo_H_endo_O_endo_H_1,2_poz	-931.10631	-930.99096	-930.98028	-931.02623
2_exo_H_endo_O_exo_H_1,2_poz	-931.10593	-930.99116	-930.98048	-931.02606
3_exo_H_endo_O_exo_H_1,2_poz				
4_exo_H_endo_O_exo_H_1,2_poz	-931.10592	-930.99121	-930.98024	-931.02688
5_exo_H_endo_O_exo_H_1,2_poz	-931.1054	-930.99069	-930.97969	-931.02631
6_exo_H_endo_O_exo_H_1,2_poz	-931.10809	-930.99266	-930.98201	-931.02769
2_exo_H_exo_O_endo_H_1,2_poz	-931.11323	-930.99855	-930.98805	-931.03316
3_exo_H_exo_O_endo_H_1,2_poz	-931.11148	-930.99599	-930.98532	-931.0313
4_exo_H_exo_O_endo_H_1,2_poz	-931.10973	-930.99474	-930.98387	-931.03013
5_exo_H_exo_O_endo_H_1,2_poz	-931.10867	-930.99369	-930.98284	-931.02926
6_exo_H_exo_O_endo_H_1,2_poz	-931.10899	-930.99358	-930.98286	-931.02875
2_exo_H_exo_O_exo_H_1,2_poz	-931.11056	-930.99594	-930.98515	-931.03113
3_exo_H_exo_O_exo_H_1,2_poz	-931.11155	-930.99596	-930.98533	-931.03104
4_exo_H_exo_O_exo_H_1,2_poz	-931.11037	-930.9953	-930.98447	-931.03055
5_exo_H_exo_O_exo_H_1,2_poz	-931.1084	-930.9935	-930.98258	-931.02899
6_exo_H_exo_O_exo_H_1,2_poz	-931.11202	-930.99633	-930.98577	-931.03112
2,3_POZs				
2_endo_H_endo_O_endo_H_2,3_poz	-931.11607	-931.00074	-930.99006	-931.03601
3_endo_H_endo_O_endo_H_2,3_poz	-931.11769	-931.00229	-930.99162	-931.03765
4_endo_H_endo_O_endo_H_2,3_poz	-931.11465	-930.99837	-930.98773	-931.03385
5_endo_H_endo_O_endo_H_2,3_poz	-931.11567	-930.99938	-930.98883	-931.03478
6_endo_H_endo_O_endo_H_2,3_poz	-931.12004	-931.00348	-930.99302	-931.03876
2_endo_H_endo_O_exo_H_2,3_poz	-931.11401	-930.99873	-930.98806	-931.03395
3_endo_H_endo_O_exo_H_2,3_poz	-931.11524	-930.99987	-930.98919	-931.03524
4_endo_H_endo_O_exo_H_2,3_poz	-931.11168	-930.99571	-930.98489	-931.03161
5_endo_H_endo_O_exo_H_2,3_poz	-931.11327	-930.99721	-930.98652	-931.033
6_endo_H_endo_O_exo_H_2,3_poz	-931.11778	-931.0013	-930.99083	-931.03663
2_endo_H_exo_O_endo_H_2,3_poz	-931.11813	-931.0025	-930.99193	-931.03763
3_endo_H_exo_O_endo_H_2,3_poz	-931.11827	-931.00281	-930.99213	-931.0384
4_endo_H_exo_O_endo_H_2,3_poz	-931.11406	-930.99803	-930.98727	-931.03355

5_endo_H_exo_O_endo_H_2,3_poz	-931.11642	-931.00035	-930.98972	-931.03576
6_endo_H_exo_O_endo_H_2,3_poz	-931.1196	-931.00289	-930.99243	-931.03831
2_endo_H_exo_O_exo_H_2,3_poz	-931.11567	-931.00024	-930.98958	-931.03556
3_endo_H_exo_O_exo_H_2,3_poz	-931.11655	-931.00113	-930.99047	-931.03646
4_endo_H_exo_O_exo_H_2,3_poz	-931.11197	-930.99612	-930.98524	-931.03186
5_endo_H_exo_O_exo_H_2,3_poz	-931.11386	-930.99774	-930.98706	-931.0336
6_endo_H_exo_O_exo_H_2,3_poz	-931.11058	-930.9949	-930.98389	-931.03092
2_exo_H_endo_O_endo_H_2,3_poz	-931.11575	-930.99993	-930.98947	-931.03484
3_exo_H_endo_O_endo_H_2,3_poz				
4_exo_H_endo_O_endo_H_2,3_poz	-931.11468	-930.99829	-930.98772	-931.03364
5_exo_H_endo_O_endo_H_2,3_poz	-931.11238	-930.99658	-930.98578	-931.03227
6_exo_H_endo_O_endo_H_2,3_poz	-931.12004	-931.00348	-930.99302	-931.03876
2_exo_H_endo_O_exo_H_2,3_poz	-931.1124	-930.99692	-930.98625	-931.03228
3_exo_H_endo_O_exo_H_2,3_poz				
4_exo_H_endo_O_exo_H_2,3_poz	-931.1111	-930.99503	-930.98427	-931.03076
5_exo_H_endo_O_exo_H_2,3_poz	-931.11327	-930.99721	-930.98652	-931.033
6_exo_H_endo_O_exo_H_2,3_poz	-931.11037	-930.99477	-930.98376	-931.03082
2_exo_H_exo_O_endo_H_2,3_poz	-931.11984	-931.00384	-930.99339	-931.03864
3_exo_H_exo_O_endo_H_2,3_poz	-931.11802	-931.00247	-930.99176	-931.03768
4_exo_H_exo_O_endo_H_2,3_poz	-931.11332	-930.99708	-930.98633	-931.03306
5_exo_H_exo_O_endo_H_2,3_poz				
6_exo_H_exo_O_endo_H_2,3_poz	-931.1196	-931.00289	-930.99243	-931.03831
2_exo_H_exo_O_exo_H_2,3_poz	-931.11684	-931.00116	-930.99054	-931.0362
3_exo_H_exo_O_exo_H_2,3_poz	-931.11646	-931.00093	-930.99025	-931.03608
4_exo_H_exo_O_exo_H_2,3_poz	-931.11056	-930.99441	-930.98362	-931.03024
5_exo_H_exo_O_exo_H_2,3_poz	-931.11386	-930.99774	-930.98706	-931.0336
6_exo_H_exo_O_exo_H_2,3_poz	-931.11058	-930.9949	-930.98389	-931.03092
3,4_POZs				
2_endo_H_endo_O_endo_H_3,4_poz	-931.11378	-930.99753	-930.98689	-931.03292
3_endo_H_endo_O_endo_H_3,4_poz	-931.1144	-930.9992	-930.98851	-931.03465
4_endo_H_endo_O_endo_H_3,4_poz	-931.11422	-930.99898	-930.9883	-931.03438

5_endo_H_endo_O_endo_H_3,4_poz	-931.11392	-930.99769	-930.98711	-931.0331
6_endo_H_endo_O_endo_H_3,4_poz	-931.11154	-930.99535	-930.9848	-931.03079
2_endo_H_endo_O_exo_H_3,4_poz	-931.11112	-930.99512	-930.98427	-931.03096
3_endo_H_endo_O_exo_H_3,4_poz	-931.11329	-930.99821	-930.98743	-931.0338
4_endo_H_endo_O_exo_H_3,4_poz	-931.11359	-930.99843	-930.9877	-931.03396
5_endo_H_endo_O_exo_H_3,4_poz	-931.11313	-930.99708	-930.98637	-931.0327
6_endo_H_endo_O_exo_H_3,4_poz	-931.11195	-930.99609	-930.98528	-931.03218
2_endo_H_exo_O_endo_H_3,4_poz	-931.11134	-930.99536	-930.98456	-931.03095
3_endo_H_exo_O_endo_H_3,4_poz	-931.1153	-931.00012	-930.98936	-931.0357
4_endo_H_exo_O_endo_H_3,4_poz	-931.11538	-931.00021	-930.98944	-931.03586
5_endo_H_exo_O_endo_H_3,4_poz	-931.11549	-930.99942	-930.98884	-931.03457
6_endo_H_exo_O_endo_H_3,4_poz	-931.11257	-930.99656	-930.98598	-931.03207
2_endo_H_exo_O_exo_H_3,4_poz	-931.11357	-930.99755	-930.98677	-931.03303
3_endo_H_exo_O_exo_H_3,4_poz	-931.11648	-931.0012	-930.99053	-931.03661
4_endo_H_exo_O_exo_H_3,4_poz	-931.11633	-931.00102	-930.99036	-931.03643
5_endo_H_exo_O_exo_H_3,4_poz	-931.11549	-930.99942	-930.98884	-931.03457
6_endo_H_exo_O_exo_H_3,4_poz	-931.11151	-930.9953	-930.98468	-931.03116
2_exo_H_endo_O_endo_H_3,4_poz	-931.11651	-931.00006	-930.98959	-931.03544
3_exo_H_endo_O_endo_H_3,4_poz	-931.11105	-930.99601	-930.98518	-931.03162
4_exo_H_endo_O_endo_H_3,4_poz	-931.11117	-930.99614	-930.9853	-931.0318
5_exo_H_endo_O_endo_H_3,4_poz	-931.11271	-930.99661	-930.98596	-931.03213
6_exo_H_endo_O_endo_H_3,4_poz	-931.11154	-930.99535	-930.9848	-931.03079
2_exo_H_endo_O_exo_H_3,4_poz	-931.11624	-930.99983	-930.98934	-931.03523
3_exo_H_endo_O_exo_H_3,4_poz	-931.11061	-930.99555	-930.9847	-931.03118
4_exo_H_endo_O_exo_H_3,4_poz	-931.11033	-930.99524	-930.98441	-931.03088
5_exo_H_endo_O_exo_H_3,4_poz	-931.11197	-930.99591	-930.98523	-931.03147
6_exo_H_endo_O_exo_H_3,4_poz				
2_exo_H_exo_O_endo_H_3,4_poz	-931.11633	-930.99981	-930.98931	-931.03531
3_exo_H_exo_O_endo_H_3,4_poz	-931.11551	-931.00022	-930.98946	-931.03561
4_exo_H_exo_O_endo_H_3,4_poz	-931.11541	-931.00006	-930.98933	-931.03538
5_exo_H_exo_O_endo_H_3,4_poz	-931.11158	-930.9955	-930.98476	-931.03132
6_exo_H_exo_O_endo_H_3,4_poz				

2_exo_H_exo_O_exo_H_3,4_poz	-931.11589	-930.9994	-930.98889	-931.03496
3_exo_H_exo_O_exo_H_3,4_poz	-931.11596	-931.00062	-930.9991	-931.03591
4_exo_H_exo_O_exo_H_3,4_poz	-931.11645	-931.00107	-930.99039	-931.03628
5_exo_H_exo_O_exo_H_3,4_poz	-931.11275	-930.99662	-930.98594	-931.03227
6_exo_H_exo_O_exo_H_3,4_poz	-931.11151	-930.9953	-930.98468	-931.03116

Hydroxythiophenol_POZs B3LYP/6-311+G(2df)	**Electronic energies and thermochemical properties (a.u.)**			
	E^{el}	$E^{el} + ZPE$	$E^{el} + H^{therm}$	$E^{el} + G^{therm}$
Ozone	-225.4962	-225.48887	-225.48497	-225.51197
Hydroxythiophenol	-705.78911	-705.68553	-705.67749	-705.71702
Ozone + Hydroxythiophenol	-931.28531	-931.1744	-931.16246	-931.22899
1,2_POZs				
2_endo_H_endo_O_endo_H_1,2_poz	-931.30883	-931.19512	-931.18436	-931.23
3_endo_H_endo_O_endo_H_1,2_poz	-931.30991	-931.19515	-931.18449	-931.23031
4_endo_H_endo_O_endo_H_1,2_poz	-931.31084	-931.19605	-931.18542	-931.23125
5_endo_H_endo_O_endo_H_1,2_poz	-931.3113	-931.19648	-931.18587	-931.23164
6_endo_H_endo_O_endo_H_1,2_poz	-931.30846	-931.19383	-931.18302	-931.22929
2_endo_H_endo_O_exo_H_1,2_poz				
3_endo_H_endo_O_exo_H_1,2_poz	-931.30864	-931.19414	-931.1833	-931.22959
4_endo_H_endo_O_exo_H_1,2_poz	-931.31084	-931.19612	-931.18545	-931.23137
5_endo_H_endo_O_exo_H_1,2_poz	-931.30964	-931.19499	-931.18426	-931.23029
6_endo_H_endo_O_exo_H_1,2_poz	-931.30881	-931.19386	-931.18325	-931.22877
2_endo_H_exo_O_endo_H_1,2_poz	-931.31356	-931.19933	-931.18881	-931.23401
3_endo_H_exo_O_endo_H_1,2_poz				
4_endo_H_exo_O_endo_H_1,2_poz	-931.31346	-931.19859	-931.18795	-931.23371
5_endo_H_exo_O_endo_H_1,2_poz	-931.31297	-931.19809	-931.18748	-931.23328
6_endo_H_exo_O_endo_H_1,2_poz	-931.3111	-931.19649	-931.18567	-931.2318
2_endo_H_exo_O_exo_H_1,2_poz	-931.31338	-931.19903	-931.18853	-931.23359
3_endo_H_exo_O_exo_H_1,2_poz	-931.31098	-931.19626	-931.18546	-931.23149
4_endo_H_exo_O_exo_H_1,2_poz	-931.31462	-931.19963	-931.18905	-931.2346
5_endo_H_exo_O_exo_H_1,2_poz	-931.3126	-931.19776	-931.18711	-931.23288

6_endo_H_exo_O_exo_H_1,2_poz	-931.3114	-931.19653	-931.18587	-931.23148
2_exo_H_endo_O_endo_H_1,2_poz	-931.30638	-931.19269	-931.18184	-931.22788
3_exo_H_endo_O_endo_H_1,2_poz	-931.30966	-931.19481	-931.18419	-931.22989
4_exo_H_endo_O_endo_H_1,2_poz	-931.30762	-931.19335	-931.18244	-931.22888
5_exo_H_endo_O_endo_H_1,2_poz	-931.30789	-931.19357	-931.18271	-931.22901
6_exo_H_endo_O_endo_H_1,2_poz	-931.30603	-931.19127	-931.18061	-931.22637
2_exo_H_endo_O_exo_H_1,2_poz	-931.30545	-931.19175	-931.18079	-931.22735
3_exo_H_endo_O_exo_H_1,2_poz				
4_exo_H_endo_O_exo_H_1,2_poz	-931.30766	-931.19344	-931.18251	-931.22898
5_exo_H_endo_O_exo_H_1,2_poz	-931.30682	-931.19261	-931.18163	-931.22819
6_exo_H_endo_O_exo_H_1,2_poz				
2_exo_H_exo_O_endo_H_1,2_poz	-931.31247	-931.19834	-931.1879	-931.23292
3_exo_H_exo_O_endo_H_1,2_poz	-931.31116	-931.19633	-931.18567	-931.23155
4_exo_H_exo_O_endo_H_1,2_poz	-931.31044	-931.19597	-931.18513	-931.23129
5_exo_H_exo_O_endo_H_1,2_poz	-931.30946	-931.19507	-931.1842	-931.23061
6_exo_H_exo_O_endo_H_1,2_poz	-931.30872	-931.19394	-931.18323	-931.22902
2_exo_H_exo_O_exo_H_1,2_poz	-931.31008	-931.19598	-931.18529	-931.23089
3_exo_H_exo_O_exo_H_1,2_poz	-931.31164	-931.1967	-931.18608	-931.23171
4_exo_H_exo_O_exo_H_1,2_poz	-931.31163	-931.19703	-931.18625	-931.23218
5_exo_H_exo_O_exo_H_1,2_poz	-931.30963	-931.19531	-931.18436	-931.23081
6_exo_H_exo_O_exo_H_1,2_poz	-931.31172	-931.19669	-931.18612	-931.23145
2,3_POZs				
2_endo_H_endo_O_endo_H_2,3_poz	-931.31553	-931.20077	-931.19009	-931.23604
3_endo_H_endo_O_endo_H_2,3_poz	-931.31761	-931.20278	-931.19211	-931.23804
4_endo_H_endo_O_endo_H_2,3_poz	-931.3148	-931.1992	-931.18849	-931.23477
5_endo_H_endo_O_endo_H_2,3_poz	-931.31689	-931.20118	-931.1906	-931.23659
6_endo_H_endo_O_endo_H_2,3_poz	-931.32044	-931.2044	-931.19396	-931.23965
2_endo_H_endo_O_exo_H_2,3_poz	-931.31346	-931.19882	-931.18812	-931.2341
3_endo_H_endo_O_exo_H_2,3_poz	-931.31522	-931.2005	-931.1898	-931.23584
4_endo_H_endo_O_exo_H_2,3_poz	-931.31193	-931.19664	-931.18579	-931.23253
5_endo_H_endo_O_exo_H_2,3_poz	-931.31477	-931.19929	-931.18861	-931.23507
6_endo_H_endo_O_exo_H_2,3_poz	-931.3185	-931.20253	-931.19207	-931.23784

2_endo_H_exo_O_endo_H_2,3_poz	-931.31828	-931.20328	-931.1927	-931.23831
3_endo_H_exo_O_endo_H_2,3_poz	-931.31919	-931.2043	-931.19362	-931.23963
4_endo_H_exo_O_endo_H_2,3_poz	-931.31393	-931.19843	-931.18757	-931.2344
5_endo_H_exo_O_endo_H_2,3_poz	-931.31746	-931.2019	-931.1912	-931.23774
6_endo_H_exo_O_endo_H_2,3_poz				
2_endo_H_exo_O_exo_H_2,3_poz	-931.31594	-931.20113	-931.19049	-931.23628
3_endo_H_exo_O_exo_H_2,3_poz	-931.31749	-931.20269	-931.19202	-931.23793
4_endo_H_exo_O_exo_H_2,3_poz	-931.31163	-931.19655	-931.18559	-931.23264
5_endo_H_exo_O_exo_H_2,3_poz	-931.31567	-931.20009	-931.18944	-931.23565
6_endo_H_exo_O_exo_H_2,3_poz	-931.31243	-931.19717	-931.18623	-931.23305
2_exo_H_endo_O_endo_H_2,3_poz	-931.31633	-931.20107	-931.19062	-931.23596
3_exo_H_endo_O_endo_H_2,3_poz				
4_exo_H_endo_O_endo_H_2,3_poz	-931.31481	-931.19904	-931.18845	-931.2344
5_exo_H_endo_O_endo_H_2,3_poz				
6_exo_H_endo_O_endo_H_2,3_poz	-931.32044	-931.2044	-931.19396	-931.23965
2_exo_H_endo_O_exo_H_2,3_poz	-931.3131	-931.1982	-931.18751	-931.23365
3_exo_H_endo_O_exo_H_2,3_poz				
4_exo_H_endo_O_exo_H_2,3_poz	-931.31142	-931.19605	-931.18525	-931.23184
5_exo_H_endo_O_exo_H_2,3_poz				
6_exo_H_endo_O_exo_H_2,3_poz	-931.31186	-931.19672	-931.18574	-931.2327
2_exo_H_exo_O_endo_H_2,3_poz	-931.3207	-931.20524	-931.19482	-931.23996
3_exo_H_exo_O_endo_H_2,3_poz	-931.31951	-931.20452	-931.19383	-931.2397
4_exo_H_exo_O_endo_H_2,3_poz	-931.31414	-931.19847	-931.18775	-931.23422
5_exo_H_exo_O_endo_H_2,3_poz				
6_exo_H_exo_O_endo_H_2,3_poz	-931.32043	-931.20428	-931.19384	-931.23963
2_exo_H_exo_O_exo_H_2,3_poz	-931.31774	-931.20261	-931.19203	-931.23756
3_exo_H_exo_O_exo_H_2,3_poz	-931.31793	-931.20301	-931.19235	-931.23809
4_exo_H_exo_O_exo_H_2,3_poz				
5_exo_H_exo_O_exo_H_2,3_poz	-931.31567	-931.20009	-931.18944	-931.23565
6_exo_H_exo_O_exo_H_2,3_poz	-931.31243	-931.19717	-931.18623	-931.23305
3,4_POZs				

2_endo_H_endo_O_endo_H_3,4_poz	-931.31419	-931.19858	-931.18791	-931.23401
3_endo_H_endo_O_endo_H_3,4_poz	-931.31535	-931.20062	-931.18997	-931.23596
4_endo_H_endo_O_endo_H_3,4_poz	-931.31514	-931.20041	-931.18976	-931.23574
5_endo_H_endo_O_endo_H_3,4_poz	-931.31273	-931.19913	-931.18853	-931.23455
6_endo_H_endo_O_endo_H_3,4_poz	-931.31234	-931.19675	-931.18619	-931.23216
2_endo_H_endo_O_exo_H_3,4_poz	-931.31169	-931.19648	-931.18551	-931.2327
3_endo_H_endo_O_exo_H_3,4_poz	-931.31436	-931.19976	-931.18897	-931.23533
4_endo_H_endo_O_exo_H_3,4_poz	-931.31449	-931.19991	-931.18912	-931.2355
5_endo_H_endo_O_exo_H_3,4_poz	-931.314	-931.19857	-931.18781	-931.23428
6_endo_H_endo_O_exo_H_3,4_poz	-931.31298	-931.19759	-931.18682	-931.23365
2_endo_H_exo_O_endo_H_3,4_poz	-931.31097	-931.19574	-931.18478	-931.23199
3_endo_H_exo_O_endo_H_3,4_poz	-931.31676	-931.20215	-931.19137	-931.23771
4_endo_H_exo_O_endo_H_3,4_poz	-931.31692	-931.2022	-931.19146	-931.2377
5_endo_H_exo_O_endo_H_3,4_poz	-931.31551	-931.20016	-931.18951	-931.23552
6_endo_H_exo_O_endo_H_3,4_poz	-931.31363	-931.19808	-931.18754	-931.23351
2_endo_H_exo_O_exo_H_3,4_poz	-931.31343	-931.19801	-931.18711	-931.23451
3_endo_H_exo_O_exo_H_3,4_poz	-931.31777	-931.20306	-931.1924	-931.23838
4_endo_H_exo_O_exo_H_3,4_poz	-931.31779	-931.20298	-931.19236	-931.2382
5_endo_H_exo_O_exo_H_3,4_poz	-931.31551	-931.20016	-931.18951	-931.23552
6_endo_H_exo_O_exo_H_3,4_poz	-931.31259	-931.19696	-931.18635	-931.23269
2_exo_H_endo_O_endo_H_3,4_poz	-931.31651	-931.20069	-931.1902	-931.23609
3_exo_H_endo_O_endo_H_3,4_poz	-931.31296	-931.19839	-931.18761	-931.23386
4_exo_H_endo_O_endo_H_3,4_poz	-931.31295	-931.19835	-931.18757	-931.23385
5_exo_H_endo_O_endo_H_3,4_poz	-931.31374	-931.1982	-931.18758	-931.23365
6_exo_H_endo_O_endo_H_3,4_poz	-931.31234	-931.19675	-931.18619	-931.23216
2_exo_H_endo_O_exo_H_3,4_poz	-931.31633	-931.20051	-931.19001	-931.23591
3_exo_H_endo_O_exo_H_3,4_poz	-931.3125	-931.19793	-931.18709	-931.23351
4_exo_H_endo_O_exo_H_3,4_poz	-931.31222	-931.19768	-931.18682	-931.23336
5_exo_H_endo_O_exo_H_3,4_poz	-931.31298	-931.19749	-931.18682	-931.23302
6_exo_H_endo_O_exo_H_3,4_poz				
2_exo_H_exo_O_endo_H_3,4_poz				
3_exo_H_exo_O_endo_H_3,4_poz	-931.31732	-931.20254	-931.1918	-931.23786

4_exo_H_exo_O_endo_H_3,4_poz	-931.31724	-931.2025	-931.19173	-931.2379
5_exo_H_exo_O_endo_H_3,4_poz	-931.31294	-931.1975	-931.18672	-931.23331
6_exo_H_exo_O_endo_H_3,4_poz				
2_exo_H_exo_O_exo_H_3,4_poz	-931.31631	-931.20043	-931.18991	-931.23595
3_exo_H_exo_O_exo_H_3,4_poz	-931.31775	-931.20296	-931.19229	-931.23816
4_exo_H_exo_O_exo_H_3,4_poz	-931.31818	-931.20332	-931.19268	-931.23845
5_exo_H_exo_O_exo_H_3,4_poz				
6_exo_H_exo_O_exo_H_3,4_poz	-931.31259	-931.19696	-931.18635	-931.23269

APPENDIX D Geometrical parameters.

Note: All the bond distances (R_i) are given in angstroms (Å) and all angles sizes (θ) are given in degrees (°).

Ozone

Geometrical parameter	**6-31G(d)**	**6-31G(d,p)**	**6-311+G(2df)**
R_1	1.264	1.264	1.253
R_2	1.264	1.264	1.253
θ	117.919	117.919	118.370

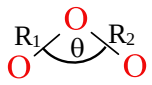

Chlorophenol POZs

B3LYP/6-31G(d)

Geometrical parameter	**Chloro-phenol**	**2-endo-H-exo-O-1,2-poz**	**2-endo-H-exo-O-2,3-poz**	**4-endo-H-exo-O-3,4-poz**
R_1	1.357	1.378	1.353	1.359
R_2	1.403	1.611	1.502	1.349
R_3	1.393	1.493	1.574	1.487
R_4	1.394	1.342	1.492	1.572
R_5	1.398	1.460	1.345	1.495
R_6	1.391	1.340	1.453	1.339
R_7	1.400	1.501	1.348	1.464
R_8		1.445	1.392	1.444
R_9		1.436	1.470	1.428
R_{10}		1.459	1.427	1.471
R_{11}		1.394	1.442	1.396
θ		100.461	100.687	100.932

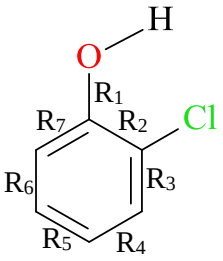

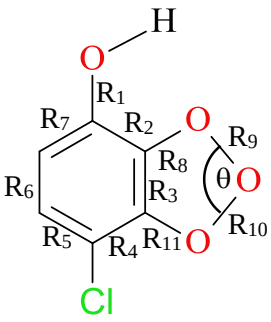

B3LYP/6-31G(d,p)

Geometrical parameter	Chloro-phenol	2-endo-H-exo-O-1,2-poz	2-endo-H-exo-O-2,3-poz	4-endo-H-exo-O-3,4-poz
R_1	1.356	1.376	1.352	1.358
R_2	1.403	1.611	1.502	1.349
R_3	1.392	1.493	1.573	1.487
R_4	1.394	1.342	1.491	1.572
R_5	1.397	1.460	1.345	1.495
R_6	1.391	1.340	1.453	1.338
R_7	1.400	1.501	1.347	1.464
R_8		1.445	1.392	1.444
R_9		1.435	1.470	1.428
R_{10}		1.459	1.427	1.471
R_{11}		1.393	1.442	1.396
θ		100.460	100.698	100.934

B3LYP/6-311+G(2df)

Geometrical parameter	Chloro-phenol	4-exo-H-exo-O-1,2-poz	2-endo-H-exo-O-2,3-poz	4-endo-H-exo-O-3,4-poz
R_1	1.354	1.401	1.350	1.357
R_2	1.397	1.560	1.499	1.341
R_3	1.387	1.489	1.569	1.481
R_4	1.388	1.333	1.486	1.567
R_5	1.392	1.458	1.337	1.490
R_6	1.386	1.332	1.448	1.331
R_7	1.394	1.498	1.339	1.458
R_8		1.426	1.390	1.442
R_9		1.449	1.457	1.421
R_{10}		1.428	1.421	1.459
R_{11}		1.436	1.439	1.394
θ		101.185	100.948	101.120

Dihydroxybenzene POZs

B3LYP/6-31G(d)

Geometrical parameter	Dihydroxy-benzene	2-endo-H-exo-O-endo-H-1,2-poz	2-endo-H-exo-O-endo-H-2,3-poz	3-endo-H-exo-O-endo-H-3,4-poz
R_1	1.367	1.422	1.354	1.361
R_2	1.396	1.599	1.509	1.346
R_3	1.398	1.501	1.571	1.489
R_4	1.398	1.341	1.495	1.577
R_5	1.397	1.462	1.345	1.498
R_6	1.391	1.342	1.456	1.338
R_7	1.401	1.495	1.345	1.465
R_8	1.368	1.415	1.430	1.442
R_9		1.468	1.457	1.449
R_{10}		1.436	1.440	1.449
R_{11}		1.449	1.450	1.442
R_{12}		1.382	1.409	1.401
θ		100.916	100.994	101.211

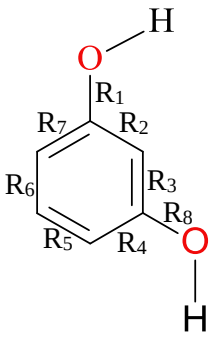

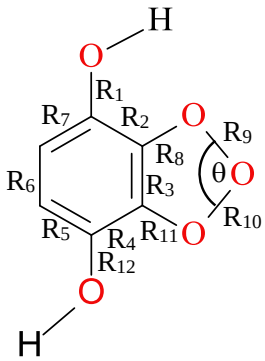

B3LYP/6-31G(d,p)

Geometrical parameter	Dihydroxy-benzene	2-endo-H-exo-O-endo-H-1,2-poz	2-endo-H-exo-O-endo-H-2,3-poz	3-endo-H-exo-O-endo-H-3,4-poz
R_1	1.364	1.421	1.353	1.360
R_2	1.406	1.599	1.509	1.346
R_3	1.390	1.501	1.571	1.489
R_4	1.399	1.341	1.495	1.577
R_5	1.394	1.462	1.344	1.498
R_6	1.397	1.342	1.455	1.338
R_7	1.393	1.496	1.345	1.465
R_8	1.378	1.415	1.430	1.443
R_9		1.468	1.457	1.448
R_{10}		1.436	1.440	1.450
R_{11}		1.449	1.451	1.442
R_{12}		1.381	1.408	1.400
θ		100.908	101.005	101.217

B3LYP/6-311+G(2df)

Geometrical parameter	**Dihydroxy-benzene**	**2-endo-H-exo-O-endo-H-1,2-poz**	**2-exo-H-exo-O-exo-H-2,3-poz**	**3-endo-H-exo-O-exo-H-2,3-poz**	**4-endo-H-exo-O-exo-H-3,4-poz**	**3-endo-H-exo-O-endo-H-3,4-poz**
R_1	1.361	1.378	1.358	1.358	1.359	1.359
R_2	1.398	1.595	1.507	1.494	1.340	1.338
R_3	1.385	1.496	1.563	1.561	1.483	1.485
R_4	1.392	1.333	1.489	1.494	1.560	1.573
R_5	1.388	1.457	1.336	1.336	1.499	1.492
R_6	1.391	1.333	1.452	1.450	1.330	1.331
R_7	1.387	1.496	1.337	1.338	1.459	1.459
R_8	1.376	1.444	1.427	1.436	1.442	1.439
R_9		1.425	1.446	1.433	1.426	1.440
R_{10}		1.454	1.428	1.443	1.452	1.438
R_{11}		1.415	1.438	1.432	1.426	1.438
R_{12}		1.414	1.396	1.401	1.402	1.400
θ		100.703	101.165	100.995	101.072	101.270

Hydroxythiophenol POZs

Note: The numbering and labeling of the geometrical parameters of hydroxythiophenol and its POZs follows the same numbering and labeling as that of the geometrical parameters of dihydroxybenzene and its POZs.

B3LYP/6-31G(d)

Geometrical parameter	**Hydroxy-thiophenol**	**2-endo-H-exo-O-exo-H-1,2-poz**	**2-exo-H-exo-O-endo-H-2,3-poz**	**6-exo-H-endo-O-endo-H-2,3-poz**	**3-endo-H-exo-O-exo-H-3,4-poz**
R_1	1.801	1.860	1.789	1.786	1.780
R_2	1.409	1.596	1.515	1.500	1.345
R_3	1.401	1.498	1.566	1.571	1.496
R_4	1.391	1.341	1.495	1.502	1.574
R_5	1.399	1.460	1.343	1.337	1.497
R_6	1.393	1.342	1.460	1.465	1.339
R_7	1.400	1.499	1.345	1.355	1.470
R_8	1.355	1.433	1.437	1.452	1.440
R_9		1.449	1.454	1.439	1.451
R_{10}		1.447	1.438	1.443	1.446
R_{11}		1.436	1.438	1.445	1.442
R_{12}		1.393	1.393	1.350	1.400
θ		100.915	101.172	101.008	101.202

B3LYP/6-31G(d,p)

Geometrical parameter	Hydroxy-thiophenol	2-endo-H-exo-O-exo-H-1,2-poz	2-exo-H-exo-O-endo-H-2,3-poz	3-endo-H-exo-O-exo-H-3,4-poz
R_1	1.801	1.861	1.789	1.780
R_2	1.409	1.596	1.514	1.345
R_3	1.401	1.498	1.566	1.496
R_4	1.390	1.340	1.495	1.574
R_5	1.399	1.459	1.342	1.497
R_6	1.392	1.342	1.460	1.339
R_7	1.399	1.499	1.345	1.470
R_8	1.354	1.432	1.437	1.440
R_9		1.449	1.455	1.451
R_{10}		1.447	1.438	1.447
R_{11}		1.436	1.438	1.442
R_{12}		1.392	1.392	1.399
θ		100.915	101.178	101.210

B3LYP/6-311+G(2df)

Geometrical parameter	Hydroxy-thiophenol	4-endo-H-exo-O-exo-H-1,2-poz	2-exo-H-exo-O-endo-H-2,3-poz	4-exo-H-exo-O-exo-H-3,4-poz
R_1	1.791	1.847	1.777	1.769
R_2	1.403	1.567	1.511	1.340
R_3	1.394	1.483	1.563	1.487
R_4	1.385	1.341	1.489	1.557
R_5	1.393	1.456	1.335	1.497
R_6	1.386	1.331	1.455	1.331
R_7	1.394	1.495	1.338	1.465
R_8	1.353	1.427	1.434	1.439
R_9		1.447	1.444	1.428
R_{10}		1.426	1.430	1.450
R_{11}		1.442	1.435	1.426
R_{12}		1.358	1.392	1.402
θ		101.461	101.300	101.126

APPENDIX E Mulliken charges.

Note: The table below follows the same numbering of C atoms as in Figure 5 in the text (Results and Discussion section).

	Mulliken charges (e^-)			
C atom no.	**Ozone (terminal O atoms)**	**Chlorophenol**	**Dihydroxybenzene**	**Hydroxythiophenol**
1	-0.131	-0.632	-0.198	1.560
2		0.084	-0.198	-1.150
3		-0.765	0.280	0.373
4		0.872	-0.434	-0.555
5		-0.776	-0.434	-0.161
6		0.249	0.280	-0.636

APPENDIX F Relative electronic energies and thermochemical properties of TSs.

Chlorophenol POZs TS	**Relative Energies and Thermochemical Properties**				
	(kcal/mol)				**(kcal/mol.K)**
B3LYP/6-311+G(2df) level	ΔE^{el}	ΔE^{el} + ZPE	$\Delta H^{‡}$	$\Delta G^{‡}$	$\Delta S^{‡}$
Ozone + Chlorophenol	0.0	0.0	0.0	0.0	0.0000
3_endo_H_exo_O_3,4_poz_ts	0.0	0.1	0.4	8.5	-0.0272
5_exo_H_exo_O_1,2_poz_ts	-0.4	0.2	0.4	8.9	-0.0284
4_exo_H_exo_O_1,2_poz_ts	0.1	0.3	0.5	8.1	-0.0253
4_endo_H_exo_O_3,4_poz_ts	47.5	46.9	47.1	56.8	-0.0326

Dihydroxybenzene POZs TS	**Relative Energies and Thermochemical Properties**				
	(kcal/mol)				**(kcal/mol.K)**
B3LYP/6-311+G(2df) level	ΔE^{el}	ΔE^{el} + ZPE	$\Delta H^{‡}$	$\Delta G^{‡}$	$\Delta S^{‡}$
Ozone + Dihydroxybenzene	0.0	0.0	0.0	0.0	0.0000
3_endo_H_exo_O_endo_H_3,4_poz_ts	-1.3	-0.8	-0.8	8.3	-0.0305
4_endo_H_exo_O_endo_H_1,2_poz_ts	-1.5	-0.3	-0.5	9.5	-0.0337
2_endo_H_exo_O_endo_H_1,2_poz_ts	2.1	2.2	2.3	11.2	-0.0298

Hydroxythiophenol POZs TS **B3LYP/6-311+G(2df) level**	**Relative Energies and Thermochemical Properties**				
	(kcal/mol)				**(kcal/mol.K)**
	ΔE^{el}	$\Delta E^{el} + ZPE$	$\Delta H^{‡}$	$\Delta G^{‡}$	$\Delta S^{‡}$
Ozone + Hydroxythiophenol	0.0	0.0	0.0	0.0	0.0000
3_endo_H_exo_O_endo_H_2,3_poz	-0.1	0.4	0.7	8.6	-0.0265
3_exo_H_exo_O_endo_H_2,3_poz	0.5	0.9	1.0	10.4	-0.0314
2_exo_H_exo_O_endo_H_2,3_poz	1.1	1.2	1.4	10.4	-0.0300
6_exo_H_endo_O_endo_H_2,3_poz	1.6	1.5	2.0	9.4	-0.0246
6_exo_H_exo_O_endo_H_2,3_poz	2.7	2.5	3.1	10.1	-0.0236